SPECTROSCOPIC INVESTIGATIONS ON THE PROPERTIES OF TWO DRUGS: CURCUMIN AND CHLORIN p_6

By

RAJESH KUMAR SAINI

(CHEM03200804001)

Raja Ramanna Center for Advanced Technology,

Indore - 452013, India

A thesis submitted to the
Board of Studies in Chemical Sciences
In partial fulfillment of requirements
For the Degree of

DOCTOR OF PHILOSOPHY
of
HOMI BHABHA NATIONAL INSTITUTE

December, 2013

Homi Bhabha National Institute

Recommendations of the Viva Voce Board

As members of the Viva Voce Board, we certify that we have read the dissertation prepared by **Rajesh Kumar Saini** entitled **"Spectroscopic investigations on the properties of two drugs: Curcumin and Chlorin p_6"** and recommend that it may be accepted as fulfilling the dissertation requirement for the Degree of Doctor of Philosophy.

P. K. Gupta Date: 17.04.14

Chairman – Prof. P. K. Gupta

Kaustuv Das Date: 17/4/14

Guide/ Convener – Asst. Prof. K. Das

S. K. Sarkar Date: 17/4/14

Member 1 – Prof. S. K. Sarkar

Date: 17/4/14

External Examiner – Prof. Anindya Datta

Final Approval and acceptance of this dissertation is contingent upon the candidate's submission of the final copies of the dissertation to HBNI.

I hereby certify that I have read this dissertation prepared under my direction and recommend that it may be accepted as fulfilling the dissertation requirement.

Kaustuv Das

Date: 17th April, 2014 (Guide)

Place: RRCAT, Indore

STATEMENT BY AUTHOR

This dissertation has been submitted in partial fulfillment of requirements for an advanced degree at Homi Bhabha National Institute (HBNI) and is deposited in the Library to be made available to borrowers under rules of the HBNI.

Brief quotations from this dissertation are allowable without special permission, provided that accurate acknowledgement of source is made. Requests for permission for extended quotation from or reproduction of this manuscript in whole or in part may be granted by the Competent Authority of HBNI when in his or her judgment the proposed use of the material is in the interests of scholarship. In all other instances, however, permission must be obtained from the author.

(Rajesh Kumar Saini)

DECLARATION

I, hereby declare that the investigation presented in the thesis has been carried out by me. The work is original and has not been submitted earlier as a whole or in part for a degree / diploma at this or any other Institution / University.

(Rajesh Kumar Saini)

LIST OF PUBLICATIONS

IN JOURNALS:-

[1] "pH dependent reversible aggregation of Chitosan & glycol-Chitosan stabilized silver Nanoparticles", **R. K. Saini**, P. K. Gupta, K. Das, *Chem. Phys. Lett.* **2011**, 511, 326-330.*

[2] "Diffusion of Chlorine p_6 across phosphatidyl choline liposome bilayer probed by second harmonic generation", **R. K. Saini**, A. Dube, P. K. Gupta, K. Das, *J. Phys. Chem. B,* **2012**, *116*, 4199-4205.

[3] "Plasmon-molecular resonance coupling: Chlorine p_6 adsorbed on poly-L-lysine coated silver Nanoparticles", **R. K. Saini**, P. K. Gupta, K. Das, *J. Mol. Struc.* **2012**, 1024, 13-17.*

[4] "Picosecond Spectral Relaxation of Curcumin Excited State in a Binary Solvent Mixture of Toluene and Methanol", **R. K. Saini,** K. Das, *J. Phys. Chem. B*, **2012**, *116*, 10357-10363.

[5] "Picosecond Spectral Relaxation of Curcumin Excited State in toluene-alcohol Mixtures", **R. K. Saini,** K. Das, *J. Lumin.* **2013,** *144*, 169-175.

[6] "Effect of Curcumin on the Diffusion Kinetics of a Hemicyanine Dye, LDS-698 across a Lipid Bilayer Probed by Second Harmonic Spectroscopy", G. K. Varshney, **R. K. Saini**, P. K. Gupta, K. Das, *Langmuir,* **2013**, *29*, 2912-2918.*

[7] "Photophysics of Curcumin Excited State in toluene-Polar Solvent Mixtures: Role of H-bonding Property of the Polar Solvent", **R. K. Saini,** K. Das, *J. Lumin.* **2014**, *145*, 832-837.

[8] *"*Hyper-Rayleigh scattering from gold nanoparticles: Effect of size and shape", K. Das, A. Uppal, **R. K. Saini,** G. K. Varshney, P. Mondal and P. K. Gupta. *Spectrochim. Acta Part A: Molecular and Biomolecular Spectroscopy,* **2014**, *128*, 398–402.*

[9] "A comparative study on the effect of Curcumin and Chlorine p_6 on the diffusion of two organic cations across a negatively charged lipid bilayer probed by second harmonic spectroscopy", **R. K. Saini**, G. K. Varshney, A. Dube, P. K. Gupta, K. Das. (Under revision)

[10] "Surfactant Induced Aggregation Behavior of Merocyanine-540 Adsorbed on Polymer Coated Positively Charged Gold Nanoparticles"**,** A. Uppal, **R. K. Saini**, G. K. Varshney, P. K. Gupta and K. Das**.*** (Manuscript under preparation)

*These papers are not included in thesis.

IN CONFERENCES PROCEEDINGS:-

[1] pH dependent reversible aggregation of Chitosan stabilized silver nanoparticles. **R.K. Saini**, P.K. Gupta, K. Das, 3rd Asia Pacific Symposium on Radiation Chemistry and 10th Biennial Trombay Symposium on Radiation & Photochemistry (APSRC-TSRP-2010), held at Bhabha Atomic Research Centre (BARC), Mumbai, India during September 14-17, 2010.

[2] Plasmon–Molecular resonance coupling: Chlorine p_6 adsorbed on poly-L-lysine coated silver Nanoparticles. **R.K. Saini**, B. Jain, P.K. Gupta, K. Das, DAE-BRNS National Laser Symposium (NLS-19), held at RRCAT, Indore, India during December 1-4, 2010.

[3] Diffusion of Chlorine p_6 across phosphatidyl choline liposome bilayer probed by second harmonic generation. **R.K. Saini**, A. Dube, P.K. Gupta, K. Das, DAE-BRNS Theme Meeting on Emerging Trends in Application of Lasers and Accelerators in Nanomaterials

(ETALAN-2011), held at Bhabha Atomic Research Centre (BARC), Mumbai, India during October 20-21, 2011.

[4] Picosecond Spectral Relaxation of Curcumin Excited State in a Binary Solvent Mixture of Toluene and Methanol. **R.K. Saini,** K. Das, National Symposium on Radiation and Photochemistry (NSRP – 2013) held at Department of Chemistry, NEHU Shillong, Meghalaya, India during March 20-22, 2013.

[5] Diffusion Kinetics of a Hemicyanine Dye, LDS-698 Across a Lipid Bilayer Probed by Second Harmonic Spectroscopy. G.K. Varshney, **R.K. Saini**, P.K. Gupta, K. Das. National Symposium on Radiation and Photochemistry (NSRP – 2013) held at Department of Chemistry, NEHU Shillong, Meghalaya, India during March 20-22, 2013.

(Rajesh Kumar Saini)

Dedicated

To

My Beloved Family

ACKNOWLEDGEMENTS

A journey is always easier when you travel together. I would like to take this opportunity to thank all those who helped me to complete this thesis.

First I want to express my greatest gratitude to my advisor, **Dr. Kaustuv Das**, for his excellent and invaluable guidance and constant encouragement. His extensive knowledge of the field and sincere effort in science has been a great benefit and inspiration for me throughout my research study.

I am extremely thankful to **Prof. P. K. Gupta**, Head, Laser Bio-medical Application and Instrumentation Division (RRCAT, Indore) for his motivating words, advices and helpful suggestions in carrying out the research work.

I am extremely grateful to my doctoral committee member, Prof. S. K. Sarkar, Director Chemistry Group (BARC, Mumbai) for his guidance and motivation.

I am also very thankful to Dr. Alok Dube for his support, scientific discussion, encouragement and specially for providing a lot of Chlorin p_6 (Cp_6) used in my research work.

I am also thankful to other members of LBAID, Dr. Abha Uppal, Beena jain, Dr. Mrinalini Sharma, H.S. Patel, Mahesh Swami, Ravi Shanker Verma, Khageswar Sahu, Dr. Rashmi Shrivastava, Sunita Ahlawat and Dr. Biplab Bose for providing their constant support, useful discussion, encouragement and help in carrying out the research work.

I take this opportunity to thank my colleagues Dr. S. S. Manhas, Arpana Parihar, S. P. Singh, G. K. Varshney, Paromita and S. R. Kintali for their support, help and co-operation.

I am grateful to my friends Vikas Sahu, Sohan, Ravindra, Vishal, Apurav, Deepak, Neelam, Manju, Ashish, Mahesh, Amit, Nagesh, and Dr. B. Ramakrishna for providing their crucial support and good wishes for me. I would also like to acknowledge all my friends for their help during my stay at RRCAT guest house.

I am very much indebted for the heartfelt gratitude of my parents for their warm support, caring and always a source of inspiration towards achieving the goals in my life. Immense love and affection of my brother Ashok have been invaluable in this journey. I am thankful to my dearest wife Priyanka for her patience, support, love and care. My sweetest son Vihaan, a new arrival to the family towards the end of my Ph.D. brought a cheerful atmosphere.

Last but not least, I am thankful to Almighty for all time blessings.

December, 2013

(Rajesh Kumar Saini)

CONTENTS

SYNOPSIS

Curcumin is a naturally occurring yellow-orange pigment derived from the rhizomes of *Curcuma longa* (turmeric). Curcumin shows a wide variety of biological effects which includes antioxidant, antiangiogenic, anticarcinogenic, and wound-healing capacities [1]. Curcumin has a great affinity for biological membranes at neutral pH and has been shown to alter their properties [2-6]. It might thus be tempting to speculate that many of its biological activity may arise from its effect on the membrane structure. In addition, studies have shown that the anticarcinogenic and antibacterial effect of Curcumin is enhanced when combined with light and oxygen [7-9]. Therefore spectroscopic characterization of photoexcited Curcumin and effect of Curcumin on membrane bilayer is a subject of potential interest. This is one of the objectives of the current thesis.

Chlorin p_6 (Cp_6), an amphiphilic Chlorophyll derivative is currently being used for photodynamic treatment of tumors and bacterial infections [10-11]. Cp_6 has three carboxylic acid groups whose protonation and deprotonation plays an important role in controlling the hydrophobic and hydrophilic species of the drug at different pH [12]. The pH dependent acid-base equilibrium of the drug is believed to play an important role in the higher uptake of Cp_6 in tumors where extra-cellular pH can be slightly acidic [10]. Thus, knowledge of the factors governing the dynamics of the diffusion of Cp_6 across membranes may be useful for a better understanding of the cellular uptake of the drug. This is the second objective of this thesis.

The organization of this thesis is as follows:

Chapter 1 provides an introduction to Curcumin and Cp_6.

Chapter 2 describes in detail about the experimental procedures for spectroscopic characterization techniques with a particular emphasis on the Second Harmonic generation (SHG) spectroscopy. SHG spectroscopy has been demonstrated to probe various surfaces and interfaces at length scales of few nanometer [13]. The transport kinetics of a molecule across a lipid bilayer can be monitored by the SHG technique provided it possesses a reasonable hyperpolarizability value at the excitation wavelength. The underlying principles of using SHG spectroscopy to monitor real time molecular diffusion across a bilayer are discussed in this chapter.

Chapter 3 describes the results of the photophysical processes of the medicinal pigment Curcumin in polar-nonpolar solvent mixtures investigated with steady state and picoseconds time resolved fluorescence spectroscopy. Several spectroscopic studies have been carried out to investigate the properties of photo excited Curcumin. It has been predicted that excited-state hydrogen atom transfer (ESHT), and solvation are the two fundamental photophysical processes of the pigment after photoexcitation [14-16]. In nonpolar solvents the ESHT process is dominant and in polar protic solvents, both ESHT and solvation processes are dominant. These processes are typically completed within few picoseconds in neat solvents. The results of the photophysical investigations of the pigment in toluene-polar solvent mixture are presented. The observed trend in the fluorescence properties of the pigment correlated with the polar solvent (like acetonitrile or chloroform) mole-fraction. However when the polar solvent is MeOH which has a strong H-

bonding property, the fluorescence (intensity and lifetime) of the pigment first increases and then decreases with increasing mole-fraction of MeOH. In addition, fluorescence decays of the pigment, taken at the red edge of the emission spectrum started to show measurable rise times the magnitude of which decreased gradually with increasing MeOH mole-fraction. This is attributed to the modulation of the non-radiative rates associated with the excited state intermolecular hydrogen (ESIH) bonding between the pigment and the polar protic solvent. As a consequence the solvation times of the pigment in the binary mixture were observed to slow down considerably (20-40 times) at certain solvent compositions compared to neat MeOH. Additional experiments carried out suggest the existence of at least three species in the excited state. The observed results are rationalized with a scheme where ground state of the pigment exists in free and H-bonded (intermolecular) state. Optical excitation results in a mixture of these species in the excited state and the observed spectral relaxation correspond to the conversion of these two species in to a third species where dipolar solvation and intermolecular H-bonding have been optimized. The effect of replacing MeOH with other alcohols (Ethanol, 1-Propanol, 1-Butanol and 1-Octanol) was also studied. The observed changes in the fluorescence properties of the pigment in toluene-alcohol mixtures depended only modestly upon the nature of the alcohol except 1-Octanol. The observed results suggest that ESIH bonding between the pigment and the polar protic solvent does not depend upon the alkyl chain length of the alcohol but depends upon the viscosity of the medium. In order to investigate how this phenomena depends upon specific H-bonding property of the polar solvent two solvents were chosen which have either H-bond accepting (HBA) or H-bond donating (HBD) property. The solvation time constant of Curcumin increases significantly (and therefore, can be detected with ~40 ps time resolution) when 1,1,1,3,3,3-Hexafluoro-2-Propanol (which have only H-bond donating ability) is used with

toluene. These results suggest that the rate limiting step in the excited state dynamics of the pigment in toluene-polar solvent mixtures might be the formation and reorganization of the intermolecular H-bonding between the keto group of the pigment and the H-bond donating property of the polar solvent.

Chapter 4 describes the diffusion characteristic of the photosensitizer Cp_6 across an egg lecithin membrane investigated by SH spectroscopy. Cp_6 can be hydrophilic at neutral pH and hydrophobic at acidic pH due to protonation/de-protonation of its carboxylic groups. The first and second pK_a of the three carboxylic acid groups have been identified at pH 7.0 and 4.8 respectively. At acidic pH, addition of liposomes to a Cp_6 solution generates an instantaneous rise (<1 second) in the second harmonic (SH) signal of the drug followed by decays whose time constants ranged from ten to hundreds of seconds. The instantaneous rise is attributed to the adsorption of Cp_6 to the outer lipid bilayer and the decay is attributed to the diffusion of the lipophilic species of the drug. At pH 6, the intensity of the generated SH signals on addition of liposome reduced and at physiological pH it was too weak to be detected. The characteristics of the SH signal of the drug changed significantly when liposomes incorporating cholesterol were used at a low temperature. Under these conditions, the SH signal consisted of an instantaneous (< 1s) followed by a slower rise (10-90s) and then it decayed on a much longer time scale. It was also observed that at room temperature, the magnitude of increase of the SH signal from Cp_6 after addition of liposomes at acidic pH were similar irrespective of the lipid head group (negatively charged POPG or zwitterionic POPC). The observed results indicate that adsorption and subsequent transport of the drug across the bilayer is most likely caused by hydrophobic interaction between the drug and bilayer which becomes significant at acidic pH.

Chapter 5 describes the effect of Curcumin and Cp_6 on the transport kinetics of two organic cations Cp_6 across a negatively charged lipid bilayer investigated by the SH technique. The diffusion characteristics of two organic cations, LDS-698 (LDS) and Malachite Green (MG) were observed to be significantly affected in the presence of liposomes containing these two drugs. Although the effect of Curcumin in reducing the diffusion of LDS at neutral pH was observed to be superior to Cp_6, a significant reduction in the average diffusion time of LDS in the presence of Cp_6 indicates definite interactions between the negatively charged drug and negatively charged liposomes which is not detected by static spectroscopy. The quantum of reduction in the average diffusion times of the organic cations by the drugs were observed to depend upon the pH and temperature of the medium as well as the cation type. A comparitive study on the effect of Curcumin and Cp_6 on the diffusion of cations at different pH shows that membrane permeability induced by Curcumin was observed to be dependent upon pH of the medium whereas for Cp_6 it was observed to be independent of the medium pH. This is an interesting finding of the present study.

Finally in **Chapter 6** a summary of the major observations are presented. A brief outline of future investigations that may evolve from the thesis is also provided.

References

[1] B.B. Aggarwal, et. al., In: B.B. Aggarwal, Y.J. Surth (Eds.), Molecular Targets and Therapeutic Uses of Curcumin in Health and Disease, Springer, New York (2007).

[2] H.I. Ingolfsson, R.E. Koeppe, O.S. Andersen, Biochemistry 46 (2007) 10384.

[3] E. Jaruga, S. Salvioli, J. Dobrucki, S. Chrul, J. Bandorowicz-Pikuła, E. Sikora, C. Franceschi, A. Cossarizza, G. Bartosz, FEBS Lett. 433 (1998) 287.

[4] E. Jarugaa, A. Sokala, S. Chrulb, G. Bartosza, Exp. Cell Res. 245 (1998) 303.

[5] W.C. Hung, F.Y. Chen, C.C. Lee, Y. Sun, M.T. Lee, H.W. Huang, Biophys. J. 94 (2008) 4331.

[6] J. Barry, M. Fritz, J.R. Brender, P.E. Smith, D.K. Lee, A. Ramamoorthy, J. Am. Chem. Soc. 131 (2009) 4490.

[7] T. Atsumi, K. Tonosaki, S. Fujisawa, Anticancer Res. 27 (2007) 363.

[8] N.C. Araujo, C.R. Fontana, V.S. Bagnato, M. E. Gerbi, Photomed. Laser Surg. 30 (2012) 393.

[9] A.P. Ribeiro, A.C. Pavarina, L.N. Dovigo, I.L. Brunetti, V.S. Bagnato, C.E. Vergani, C.A.D.S. Costa, Lasers Med. Sci. 28 (2013) 391.

[10] M. Sharma, A. Dube, H. Bansal, P. K. Gupta, Photochem. Photobiol. Sci. 3 (2004) 231.

[11] A. Dube, S. Sharma, P. K. Gupta, Oral Oncol. 42 (2006) 77.

[12] A. Datta, A. Dube, B. Jain, A. Tiwari, P. K. Gupta Photochem. Photobiol. 75 (2002) 488.

[13] K.B. Eisenthal, Chem. Rev. 106 (2006) 1462.

[14] R. Adhikary, P.J. Carlson, T.W. Kee, J. W. Petrich, J. Phys. Chem. B 114 (2010) 2997.

[15] R. Ghosh, J.A. Mondal, D. K. Palit, J. Phys. Chem. B 114 (2010) 12129.

[16] Y. Erez, I. Presiado, R. Gepshtein, D. Huppert, J. Phys. Chem. A 116 (2012) 2039.

LIST OF FIGURES AND SCHEMES

LIST OF TABLES

LIST OF ABBREVIATION

Cp_6	Chlorin p_6
SHG	Second Harmonic Generation
HRS	Hyper-Rayleigh scattering
IHT	Intramolecular hydrogen atom transfer
ESIHT or ESIPT	Excited - State Intramolecular hydrogen atom (or proton) transfer
TCSPC	Time correlated single photon counting system
TRES	Time resolved emission spectra
MG	Malachite green
MeOH	Methanol
MeOH-d_4	Deuterated methanol
MeCN	Acetonitrile
$CHCl_3$	Chloroform
EtOH	Ethanol
PrOH	1-Propanol
BuOH	1-Butanol
OcOH	1-Octanol
DMSO	Dimethyl sulfoxide
HFP	1,1,1,3,3,3-Hexafluoro-2-Propanol
HBD	Hydrogen-bond donating
HBA	Hydrogen-bond accepting

POPG	1-oleoyl-2-palmitoyl-sn-glycero-3-phosphatidylglycerol
POPC	1-oleoyl-2-palmitoyl-sn-glycero-3-phosphocholine

Chapter – 1

In this chapter a brief introduction of Curcumin and Chlorin p_6 are provided with a particular emphasis on some of their biological properties which are relevant to the work presented in this thesis. The chapter is concluded by providing the scope and motivation of the present work.

1.1. Curcumin

Curcumin is a naturally occurring yellow-orange pigment derived from the rhizomes of *Curcuma longa* (turmeric) [1]. Turmeric, cultivated in several tropical parts of Asia, is used as a spice in Indian cooking, a cosmetic agent for skin care and a traditional medicine. The medicinal potential of turmeric has been demonstrated against various diseases such as common cold, fever, skin disease, stomachache, liver disease etc. In addition it also has beneficial effects against wounds and chronic inflammations. Additional interest in the spice was created when epidemiological studies showed 10–50% lower incidence in certain types of cancer among those who consumed the spice regularly [2-3]. About 2–8% of turmeric by weight consists of a naturally occurring yellow-orange pigment known as Curcumin. The biological properties of Curcumin have been reported as early as in 1970s [4-6]. The ability of Curcumin to act as an anticancer agent was demonstrated in mid 1990 [7] and thereafter interest in the biological activity of the pigment has increased significantly.

1.1.1. Chemical structure and keto–enol tautomerism

The chemical structure of Curcumin (Scheme 1.1) consists of two o-methoxyphenolic moieties which are attached symmetrically through two π-conjugated ethylene linkers (α, β-unsaturated β-diketone). Various spectroscopic techniques have been employed to study the structural, photophysical, photobiological and biophysical properties of Curcumin and its derivatives in solution phase [8–22, 28-38, 43-50]. Although several possible isomeric structures of Curcumin are possible, only three of them can be considered as candidates for the ground state of the pigment (Scheme 1.1). Ab-initio computations showed that the trans-diketo form (II) has minimum energy compared to the cis-diketo form (I) [22] making this as the stable isomer of Curcumin. The driving force for the cis to trans isomerization was attributed to the negative charges on the carbonyl groups, which resulted in a strong electrostatic repulsion between the two carbonyl groups. However, NMR and IR spectroscopic investigation of Curcumin in chlorobenzene revealed that the cis-keto structure undergoes a keto-enol rearrangement by transfer of a proton from the CH_2 group to form the enol form (III) which is essentially the major conformer of Curcumin present in a variety of solvents [21-22, 28-32]. This was also supported by theoretical studies which showed that the cis-enol structure is the most stable form of the ground state of Curcumin both in the gas phase and in aqueous solution [33-38]. The large dipole moment (7.7 and 10.8 Debye in the gas and solution phases, respectively) of the cis-enol form leads to the formation of a strong intramolecular hydrogen bond, as well as the extended conjugation of the molecular backbone which makes it more favorable than the diketo form [33-34]. NMR spectroscopic analysis showed that in solution the cis-enol form coexist as two symmetric keto-enol tautomers (III & IV, Scheme 1.1) whose interconvertion involves a rapid intramolecular hydrogen atom transfer (IHT) process [22].

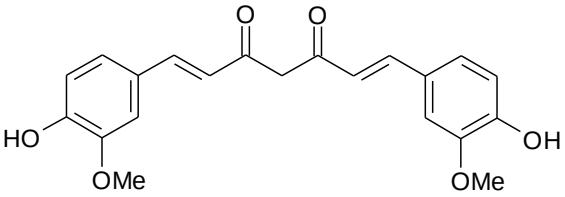

Cis-diketo (I)

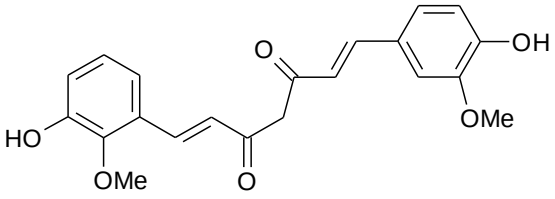

Trans-diketo (II)

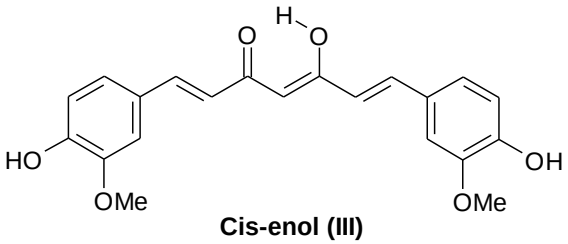

Cis-enol (III)

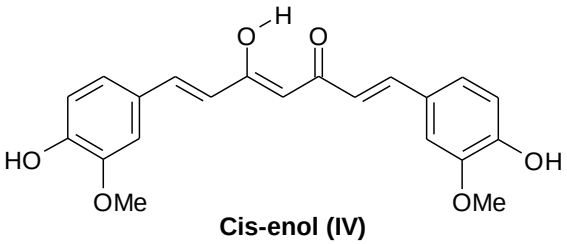

Cis-enol (IV)

Scheme 1.1*: Chemical structures of the cis-diketo, trans-diketo and keto-enol tautomeric forms of Curcumin.*

1.1.2. Excited state photophysical properties

Studies have shown that the anticarcinogenic and antibacterial effect of Curcumin is enhanced when combined with light and oxygen [23-27]. Therefore spectroscopic characterization of Curcumin excited state is a subject of current research interest.

The excited state properties of Curcumin have been investigated in several studies and the obtained results point to the occurrence of two fundamental photophysical processes: excited-state intramolecular hydrogen atom (or proton) transfer, ESIHT (or ESIPT) process, as well as dipolar solvation [9–20]. Photoexcitation of Curcumin from the ground electronic (S_0) state to the first excited singlet (S_1) state is accompanied by a significant change in the dipole moment ($\Delta\mu \sim 6.1$ D) [9] and therefore solvation is expected to play an important role in the excited-state relaxation dynamics of Curcumin. Also, several studies [9, 14-15, 17] have predicted that the ESIHT process in the hydrogen-bonded chelate ring of the cis-enol form (Structures III & IV, Scheme 1.1) plays an important role in the efficient nonradiative deactivation process of the excited state. It is pertinent to note that earlier studies on the ESIPT process occurring in molecules having an asymmetric intramolecular hydrogen-bonded chelate center have shown that this process is ultrafast (in the range of a few hundred femtosecond) [39–42]. Curcumin being a symmetric molecule (with respect to the hydrogen-bonded chelate center, structures III and IV, Scheme 1.1), it is therefore unlikely that the ESIHT process will lead to any change in the excited state absorption and emission profile thereby enabling to monitor the process spectroscopically. Adhikary et al. studied the excited-state photophysics of Curcumin in alcoholic solutions as well as in surfactant micelles using subpicosoecond fluorescence upconversion spectroscopy [17-18]. They reported the presence of two decay components in the excited-state kinetics with the lifetimes of about 12-20 and 100 ps in methanol and ethylene

glycol (EG). Deuteration of the acidic hydrogens of Curcumin had no effect on the shorter lifetime component but significantly affected the longer lifetime component. Therefore they attributed the shorter lifetime component associated to solvation of the S_1 state and longer lifetime to the ESIHT process. Ghosh et al. has also studied the dynamics of the S_1 state in different solvents using time-resolved absorption and fluorescence spectroscopic techniques with subpicosecond time resolution [43]. They have observed that solvation is the major process contributing to the relaxation dynamics of the S_1 state. Solvation dynamics is also influenced by specific hydrogen-bonding interaction between Curcumin and the solvent. In nonpolar solvents nonradiative deactivation of the S_1 state occurs via ultrafast excited-state intramolecular hydrogen transfer (ESIHT) reaction in the six-membered hydrogen-bonded chelate ring of Curcumin. In polar solvents, nonradiative deactivation of the S_1 state occurs as a result of stretching vibration in the intermolecular hydrogen bonds formed in the hydrogen-bonding (both donating and accepting) solvents.

Erez et al. have studied the temperature dependence of nonradiative process of Curcumin in ethanol and 1-propanol by steady-state and time-resolved spectroscopy [44]. They have observed that the trends in nonradiative rate constants (temperature range: 175-250 K) are similar as the dielectric relaxation times of both neat solvents. They attribute the nonradiative process of the pigment to solvent-controlled proton transfer. They have also observed a kinetic isotope effect on the nonradiative process. Based on their results they propose that excited-state proton transfer breaks the hydrogen-bonded planar hexagonal chelate ring of the cis-enol form which, in turn, enhances the nonradiative process driven by the twist angle between the two phenol moieties.

They have also studied the ESIHT reaction occurring between excited Curcumin, a photoacid and acetate, a mild base, by monitoring the fluorescence property of Curcumin in methanol and ethanol solutions [45]. They observed that the steady-state emission intensity as well as the average fluorescence decay time is reduced by a factor of 5 in presence of 1.8 M acetate ions. This large reduction in the fluorescence is attributed to excited-state proton transfer from the acidic groups of Curcumin to the acetate anion.

1.1.3. Biological effects

It has been demonstrated that Curcumin exhibits potential therapeutic application against several chronic diseases including cancer [51-63]. Currently, there are several phase I and phase II ongoing clinical trials on Curcumin for the treatment of variety of cancers and also for Alzheimer's disease [3]. Recent research has shown that Curcumin modulates a number of targets including growth factors, growth factor receptors, transcription factors, cytokines, enzymes and genes regulating cell proliferation and apoptosis [51-63]. Curcumin shows phototoxicity to bacterial systems, which is mediated through the excited states of Curcumin and their subsequent reactions with oxygen [64].

1.1.4. Interaction with biological membranes

Curcumin has a great affinity for biological membranes and has been shown to alter their properties [64-73]. Following an earlier study [64] it has been proposed that Curcumin can regulate the action of membrane proteins indirectly by changing the physical properties of the membrane rather than direct binding to the protein. Subsequently it has been demonstrated that

Curcumin is capable of altering the properties of model and cell membranes [65-68]. Jarugaa et al. have observed that rat thymocyte cells treated with Curcumin exhibit increased membrane permeability [64]. They have also observed that Curcumin significantly affects the bilayer properties in erythrocyte membranes [65].

Subsequently studies have been carried out to investigate the effect of Curcumin on the properties of several model bilayers [66-69]. The interaction of Curcumin with a model bilayer consisting of 1, 2-dioleoyl-sn-glycero-3-phosphocholine (DOPC) lipid has been studied by isothermal titration calorimetry and X-ray lamellar diffraction [66]. Results obtained suggest that Curcumin causes thinning of the bilayer as well as weaken its elastic moduli. Solid-state NMR and differential scanning calorimetry experiments revealed that Curcumin has a strong effect on model membrane structure consisting of DMPC, DHPC and DPPC lipids. Results obtained suggest that the drug inserts deep into the membrane in a trans-bilayer orientation, anchored by hydrogen bonding to the phosphate group of lipids. In addition NMR results also suggested that Curcumin forms higher order oligomeric structures in the membrane that span and likely thin the bilayer [67]. In another study the effect of Curcumin on model multilamellar DPPC and DEPE membranes were studied by a variety of experimental techniques [68]. On the basis of the obtained results it has been suggested that the drug is oriented in the bilayer with its main axis parallel to the acyl chains and interacts with the polar head groups of the lipid in such a way that favors negative curvature of the membrane. Sun et. al., have investigated Curcumin induced changes in the membrane thickness and membrane area of giant unilamellar vesicles made from DOPC. They have observed that the drug binding to the bilayer is a two-step process. Initially Curcumin binds to the interface and then at higher concentrations gradually partitions to the

hydrocarbon region. The presence of Curcumin alters the physical properties of the lipid bilayer, including a decrease of the hydrocarbon thickness and softening of its elastic rigidity [69].

Kunwar et al. have investigated the fraction of Curcumin localized in different sites of phosphatidylcholine (PC) liposomes by monitoring the quenching of Curcumin fluorescence by potassium iodide and acrylamide. The results obtained showed that the distribution of Curcumin in the liposome is pH-dependent. The neutral form of Curcumin predominant at pH 5.0 is preferentially located in the hydrophobic phase, whiles the anionic form of Curcumin predominant at pH 9, is mostly located in the liposomal surface. At pH 7, the drug is non-uniformly distributed into different compartments of the liposomal bilayer [71].

1.2. Chlorin p_6

Photosensitizers which are derived from the plant pigment Chlorophyll-a have received considerable attention because they possess significantly higher absorption in the longer wavelength region (660-800 nm) which is a desirable feature for achieving higher depth of treatment in photodynamic therapy [74]. Various Chlorophyll-a derivatives have been synthesized and evaluated for their photo-therapeutic efficacy. Chlorophyll-a derivatives, on the basis of their chemical nature can be categorized in two classes: hydrophobic such as pheophorbide and its derivatives and amphiphilic such as Chlorin-e_6 and Chlorin p_6 (Cp_6) and their derivatives [75-78]. Cp_6 is an amphiphilic photosensitizer having three ionizable carboxyl groups in the lower periphery of the molecule (Scheme 1.2). The molecule has a strong absorption around 400 nm (called the soret band) and another prominent absorption band around 660 nm (called q-band) and good singlet oxygen generation capacity (singlet oxygen quantum yield ~0.60 in ethanol) [74]. The synthesis and phototoxic property of Cp_6 was reported as early

as in 1986 by Hoober et al [76]. Several studies have been carried out at RRCAT and elsewhere on photophysical, photochemical and photo biological characterization of Cp_6 [76-98]. In-vivo studies carried out in hamster cheek pouch model on efficacy of Cp_6 for photodynamic treatment of tumors led to promising result. Cp_6 showed preferential accumulation in small size tumors (dia < 5 mm), rapid clearance from skin and complete tumor regression after PDT [87, 93]. However, for relatively large tumors its uptake was poor which compromised the PDT efficacy.

1.2.1. Photophysical and photobiological properties: Effect of pH

Cp_6 has three ionizable carboxylic acid groups and consequently neutral and several ionic forms (structures A-D, Scheme 1.2) of Cp_6 are expected to be present depending upon the pH of

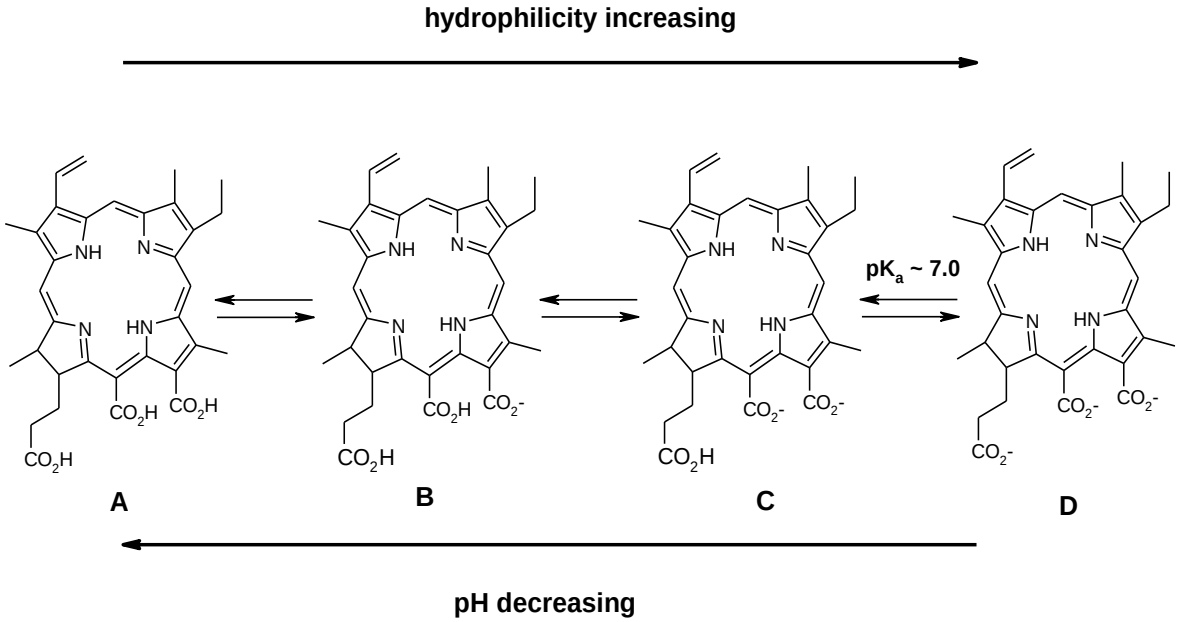

***Scheme 1.2**: Different structures of Chlorin p_6 present in the pH range of 3-8.*

the solution. Steady state and time-resolved fluorescence properties of Cp_6, have been investigated as functions of pH [77]. It has been observed that a decrease in the pH of the medium causes protonation of the ionizable carboxylic acid side chain, leading to an increase in hydrophobicity and consequent aggregation. The pK_a for inter-conversion between structures C and D has been reported to be around 7.0 which is similar to the value observed for the pK_a of the side chain carboxylic groups of other porphyrins [96-97]. This would suggest that an increase in hydrophobicity at low pH would have significant influence on the cellular uptake of Cp_6. The effect of reducing the extracellular pH from 7.4 to 6.0 on the uptake of Cp_6, has therefore been investigated in two mammalian cell lines, human colon (Colo-205) and breast (MCF-7) adenocarcinoma cells [78]. In Colo-205 cells, the uptake of Cp_6 was observed to increase as the pH of the incubation medium decreased. In contrast, no significant variation in uptake was observed for MCF-7 cells. A possible explanation offered to explain this effect was mechanism for drug uptake is cell line dependent. It was proposed that drug uptake in Colo-205 cells occurs mainly through endocytosis whereas in MCF-7 cells the uptake is controlled by diffusion.

An understanding of the photobleaching of the photosensitizer and the resulting photoproducts is essential since these have significant influence on the photodynamic efficacy of the photosensitizer. Therefore the photobleaching process of the drug was studied in neat phosphate buffer, phosphatidylcholine liposomes and in 10% fetal bovine serum [84]. The rate of photobleaching of Chlorin p_6 in neat buffer and liposomes were comparable, but it was three times faster in the serum media. Additional studies indicate that the photobleaching of the drug in these environments may proceed via a type II mechanism.

Subsequently the effect of pH on the binding properties of the drug with various macromolecules has been studied [77, 80-82, 85-86, 90]. The effect of pH on the formation of

complexes of Cp_6 with surfactants has been studied [77, 81, 85]. Ionic surfactants are found to cause aggregation of the drug only at submicellar concentrations. A significant pH effect is observed in the ionic surfactant induced aggregation process as the charge on the drug is controlled by the pH of the medium. The neutral Tx-100 was also observed to induce aggregation of the drug at low surfactant concentrations. The obtained results are rationalized by the interplay of electrostatic and hydrophobic effects between the drug and the surfactants where pH plays a major role. The effect of pH on the binding of Cp_6 with phosphatidylcholine liposomes was also investigated by absorption and emission spectroscopy [80]. Substantial changes in the absorption and emission spectra of the drug were observed when liposomes were added at acidic pH. At higher pH these changes became progressively smaller. Fluorescence quenching studies suggest that at acidic pH (5.0) the drug localizes in the central hydrophobic region of lipid bilayer and for neutral pH (7.0) the drug binds closer to the charged liposome interface. The influence of pH on the binding of the drug with Cremophor EL, a potential drug delivery vehicle has been monitored by fluorescence spectroscopy [82]. Interestingly it has been observed that the hydrophilic species of the drug bound preferentially with the hydrophobic delivery medium. The binding of the drug with serum albumins and lipoprotein have also been studied and it was concluded that hydrophobic interactions are responsible for the binding [86, 90].

In a recent study the effect of silica nanoparticles (SiNPs) having positively charged amino groups on the acid-base ionization equilibrium of Cp_6 in aqueous medium is significantly affected as a result of strong electrostatic binding between the negatively charged drug and SiNP [92]. At neutral pH the spectroscopic signature of the drug bound to SiNPs suggests that the tri-anionic form of the drug remains bound to the positively charged SiNPs. It was concluded that

the interplay of hydrophobic and electrostatic forces in the drug-nanoparticle binding process might affect the relative uptake and photodynamic efficacy of the free drug and the drug-nanoparticle complex in cancer cells. Subsequently studies were carried out on cellular uptake and phototoxicity of the free drug and its complex with SiNP in colon (Colo-205) and oral cancer (Nt8e) cell lines [98]. Phototoxicity measurements showed that the Cp_6-SiNP complex was more effective as compared to free Cp_6. The observed increase in photodynamic activity of Cp_6-SiNP complex was attributed to the enhanced photostability of the Cp_6-SiNP complex.

The binding of the drug with positively charged gold nanorods have also been studied at neutral pH conditions [95]. Absorption, emission and photostability of the drug-nanorod complex were observed to depend critically on the nature of the nanorod coating material. Therefore before exploring the efficacy of the drug-nanorod complex for combined hyperthermia and photodynamic therapy applications a judicious choice of the nanorod coating material is essential.

1.3. Objective and scope of the present thesis

The excited state properties of Curcumin are a subject of current research interest. Solvation dynamics and excited state proton transfer of the pigment are shown to be the major processes occurring in the excited state of the pigment. In nonpolar solvents the major process is the ultrafast excited-state intramolecular hydrogen transfer (ESIHT) reaction occurring in the six-membered hydrogen-bonded chelate ring of Curcumin. Whereas in polar solvents both solvation and excited state proton transfer can occur. Additionally it has been shown that in polar solvents the dynamics of solvation is also influenced by specific hydrogen-bonding interaction between Curcumin and the solvent [38]. In this thesis a significant portion has been devoted to

elucidate the role of polarity and hydrogen bonding properties of polar solvents on the excited state properties of the pigment.

The Chlorophyll a derivative, Cp_6 has three carboxylic acid groups whose protonation and deprotonation plays an important role in controlling the hydrophobic and hydrophilic species of the drug at different pH. The pH dependent acid-base equilibrium of the drug is believed to play an important role in the higher uptake of Cp_6 in tumors where extra-cellular pH can be slightly acidic. Thus, knowledge of the factors governing the dynamics of the diffusion of Cp_6 across membranes may be useful for a better understanding of the cellular uptake of the drug. In addition drug-liposome interactions may also change the properties of a lipid bilayer [96]. Both Curcumin and Cp_6 have great affinity for biological membranes and therefore the effect of these two drugs on bilayer properties is a subject of potential interest. The second part of the thesis work is therefore devoted to investigate the diffusion properties of Cp_6 and the effect of liposomal Curcumin and Cp_6 on the diffusion properties of two organic cations across a lipid bilayer.

The organization of the remaining chapters of this thesis is as follows:

Chapter 2 describes in detail about the spectroscopic characterization techniques used with a particular emphasis on the Second Harmonic spectroscopic technique.

Chapter 3 describes the photophysical studies used to characterize the excited state processes of the medicinal pigment Curcumin in polar-nonpolar solvent mixtures using steady state and picosecond time resolved fluorescence spectroscopic techniques.

Chapter 4 describes the diffusion characteristic of the photosensitizer Cp_6 across an egg lecithin membrane investigated by Second Harmonic spectroscopy.

Chapter 5 describes the effect of Curcumin and Cp_6 on the transport kinetics of two organic cations across a negatively charged lipid bilayer investigated by the SH spectroscopy.

Finally in **Chapter 6** a summary of the major observations are presented. A brief outline of future investigations that may evolve from the thesis is also provided.

1.4. References

[1] B.B. Aggarwal, Y.J. Surh, S. Shishodia (Eds.), *The Molecular Targets and Therapeutic Uses of Curcumin in Health and Disease*, ADVANCES IN EXPERIMENTAL MEDICINE AND BIOLOGY, Springer, New York, 595 (2007)

[2] A. Carter, JNCI News 100 (2008) 616.

[3] B.B. Aggarwal, B. Sung, Trends Pharmacol. Sci. 30 (2008) 85.

[4] V. Lampe, J. Milobedzaka, Ber. Dtsch. Chem. Ges. 41 (1913) 1640.

[5] R.C. Srimal, B.N. Dhawan, J. Pharm. Pharm. 25 (1973) 447.

[6] O.P. Sharma, Biochem. Pharmacol. 25 (1976) 1811.

[7] S. Singh, B. Aggarwal, J. Biol. Chem. 270 (1995) 24995.

[8] A.A. Gorman, I. Hamblett, V.S. Srinivasan, P.D. Wood, Photochem. Photobiol. 59 (1994) 389.

[9] S.M. Khopde, K.I. Priyadarsini, D.K. Palit, T. Mukherjee, Photochem. Photobiol. 72 (2000) 625.

[10] K.I. Priyadarsini, Free Rad. Chem. Biol. 23 (1997) 838.

[11] A. Barik, K.I. Priyadarsini, H. Mohan, Orient. J. Chem. 18 (2002) 427.

[12] K.I. Priyadarsini, D.K. Maity, G.H. Naik, M.S. Kumar, M.K. Unnikrishnan, J.G. Satav, H. Mohan, Free Rad. Chem. Biol. 35 (2003) 475.

[13] K.I. Priyadarsini, J. Photochem. Photobiol. C. 10 (2009) 81.

[14] L. Nardo, R. Paderno, A. Andreoni, M. Masson, T. Haukvik, H.H. Tonnesen, Spectroscopy 22 (2008) 187.

[15] L. Nardo, A. Andreoni, M. Bondani, M. Masson, H.H. Tonnesen, J. Photochem. Photobiol. B: Biol. 97 (2009) 77.

[16] M. Caselli, E. Ferrari, C. Imbriano, F. Pignedoli, M. Saladini, G. Ponterini, J. Photochem. Photobiol. A: Chem. 210 (2010) 115.

[17] R. Adhikary, P. Mukherjee, T.W. Kee, J.W. Petrich, J. Phys. Chem. B 113 (2009) 5255.

[18] R. Adhikary, P. J. Carlson, T.W. Kee, J.W. Petrich, J. Phys. Chem. B 114 (2010) 2997.

[19] T.A. Dahl, P. Bilski, K.J. Reszka, C.F. Chignell, Photochem. Photobiol. 59 (1994) 290.

[20] C.F. Chignell, P. Bilski, K.J. Reszka, A.G. Motten, R.H. Sik, T.A. Dahl, Photochem. Photobiol. 59 (1994) 295.

[21] Y.M. Sun, R.X. Wang, S.L. Yuan, X.J. Lin, C.B. Liu, Chinese J. Chem. 22 (2004) 827.

[22] K.J. Balasubramanian, Agric. Food Chem. 54 (2006) 3512.

[23] T. Atsumi, K. Tonosaki, S. Fujisawa, S Anticancer Res. 27 (2007) 363.

[24] E. M. Bruzell, E. Morisbak, H. H. Tønnesen, Photochem. Photobiol. Sci. 4 (2005) 523.

[25] H. Koon, A. W. Leung, K. K. Yue, N. K. Mak, J. Environ. Pathol. Toxicol. Oncol. 125 (2006) 205.

[26] N. C. Araújo, C. R. Fontana, V. S. Bagnato, M. E. Gerbi, Photomed. Laser Surg. 30 (2012) 393.

[27] A. P. Ribeiro, A. C. Pavarina, L. N. Dovigo et. al. Lasers Med. Sci. 28 (2013) 391.

[28] L.R. Barclay, M.R. Vinquist, K. Mukai, H. Goto, Y. Hashimoto, A. Tokunaga, H. Uno, Org. Lett. 2 (2000) 2841.

[29] F. Payton, P. Sandusky, W.L. Alworth, J. Nat. Prod. (2007) 143.

[30] P.J. Roughley, D.A. Whiting, J. Chem. Soc., Perkin Trans. I 20 (1973) 2379.

[31] H.W.D. Matthes, B. Luu, G. Ourisson, Photochemistry 170 (1980) 425.

[32] U. Pedersen, P.B. Rasmussen, S.O. Lawesson, Liebigs Ann. Chem. 8 (1985) 1557.

[33] P.H. Bong, Bull. Korean Chem. Soc. 21 (2000) 81.

[34] L. Shen, H.F. Ji, Spectrochim. Acta, Part A 67 (2007) 619.

[35] L. Shen, H.Y. Zhang, H.F. Ji, Org. Lett. 7 (2005) 243.

[36] L. Kong, K.I. Priyadarsini, H.Y. Zhang, J. Mol. Struct. THEOCHEM 688 (2004) 111.

[37] Y.M. Sun, H.Y. Zhang, D.Z. Chen, C.B. Liu, Org. Lett. 4 (2002) 2909.

[38] J.S. Wright, J. Mol. Struct. THEOCHEM 591 (2002) 207.

[39] T. Elsaesser, In: J. Manz, L. Wo¨ste, (Eds.), Femtosecond Chemistry, VCH-Verlag, Weinheim, Germany, 2 (1995) pp 563.

[40] T. Elsaesser, W. Kaiser, Chem. Phys. Lett. 128 (1986) 231.

[41] F. Laermer, T. Elsaesser, W. Kaiser, Chem. Phys. Lett. 148 (1988) 119.

[42] W. Frey, F. Laermer, T. Elsaesser, J. Phys. Chem. 95 (1991) 10391.

[43] R. Ghosh, J.A. Mondal, D.K. Palit, J. Phys. Chem. B 114 (2010) 12129.

[44] Y. Erez, I. Presiado, R. Gepshtein, D. Huppert, J. Phys. Chem. A 115 (2011) 10962.

[45] Y. Erez, I. Presiado, R. Gepshtein, D. Huppert, J. Phys. Chem. A 116 (2012) 2039.

[46] M.H.M. Leung, H. Colangelo, T.W. Kee, Langmuir 24 (2008) 5672.

[47] M.H.M. Leung, T.W. Kee, Langmuir 25 (2009) 5773.

[48] Z. Wang, M.H.M. Leung, T.W. Kee, D.S. English, Langmuir 26 (2010) 5520.

[49] D. Ke, X. Wang, Q. Yang, Y. Niu, S. Chai, Z. Chen, X. An, W. Shen, Langmuir 27 (2011) 14112.

[50] C. Ghatak, V.G. Rao, S. Mandal, S. Ghosh, N. Sarkar, J. Phys. Chem. B 116 (2012) 3369.

[51] B.B. Aggarwal, A. Kumar, A.C. Bharti, Anticancer Res. 23 (2003) 363–398.

[52] P. Anand, S.G. Thomas, A.B. Kunnumakkara, et al., Biochem. Pharmacol. 76 (2008) 1590.

[53] R.A. Sharma, A.J. Gescher, W.P. Steward, Eur. J. Cancer 41 (2005) 1955.

[54] P. Anand, A.B. Kunnumakkara, R.A. Newman, B.B. Aggarwal, Mol. Pharm. Rev. 4 (2007) 807.

[55] A.L. Cheng, C.H. Hsu, J.K. Lin, M.M. Hsu, Y.F. Ho, T.S. Shen, J.Y. Ko, J.T. Lin, B.R. Lin, M.S. Wu, H.S. Yu, S.H. Jee, G.S. Chen, T.M. Chen, C.A. Chen, M.K. Lai, Y.S. Pu, M.H. Pan, Y.J. Wang, C.C. Tsai, C.Y. Hsieh, Anticancer Res. 21 (2001) 2895.

[56] H. Hatcher, R. Planalp, J. Cho, F.M. Torti, S.V. Torti, Cell. Mol. Life Sci. 65 (2008) 1631.

[57] L. Pari, D. Tewas, J. Eckel, Physiol. Biochem. 114 (2008) 127.

[58] P. Mecocci, E. Mariani, M.C. Polidori, K. Hensley, D.A. Butterfield, Cent. Nerv. Syst. Agents Med. Chem. 8 (2008) 48.

[59] N. Kaludercic, M.L. Lindsey, B. Tavazzi, G. Lazzrino, N. Palocci, Card. Vasc. Drug Rev. 26 (2008) 24.

[60] A. Goel, A.B. Kunnamakkara, B.B. Aggarwal, Bichem. Pharmacol. 75 (2008) 787.

[61] N. Khan, F. Afaq, H. Mukhtar, Antioxid. Redox Signal. 10 (2008) 476.

[62] J.G. Bilmen, S.Z. Khan, M.U.H. Javed, F. Michelangeli, Eur. J. Biochem. 268 (2001) 6318.

[63] H.I. Ingolfsson, R.E. Koeppe, O.S. Andersen, Biochemistry 46 (2007) 10384.

[64] E. Jaruga, S. Salvioli, J. Dobrucki, S. Chrul, J. Bandorowicz-Pikuła, E. Sikora, C. Franceschi, A. Cossarizza, G. Bartosz, FEBS Lett. 433 (1998) 287.

[65] E. Jarugaa, A. Sokala, S. Chrulb, G. Bartosza, Exp. Cell Res. 245 (1998) 303.

[66] W.C. Hung, F.Y. Chen, C.C. Lee, Y. Sun, M.T. Lee, H.W. Huang, Biophys. J. 94 (2008) 4331.

[67] J. Barry, M. Fritz, J.R. Brender, P.E. Smith, D.K. Lee, A. Ramamoorthy, J. Am. Chem. Soc. 131 (2009) 4490.

[68] A. Perez-Lara, A. Ausili, F.J. Aranda, A. Godos, A. Torrecillas, S. Corbalan-Garcia, J.C. Gomez-Fernandez, J. Phys. Chem. B 114 (2010) 9778.

[69] Y. Sun, C.C. Lee, W.C. Hung, F.Y. Chen, M.T. Lee, H.W. Huang, Biophys. J. 95 (2008) 2318.

[70] G. Began, E. Sudharshan, K. Udaya Sankar, A.G. Appu Rao, J. Agric. Food Chem. 47 (1999) 4992.

[71] A. Kunwar, A. Barik, R. Pandey, K.I. Priyadarsini, Biochim. Biophys.Acta 1760 (2006) 1513.

[72] E.S. Nyman, P.H. Hynninen, J. Photochem Photobiol B. Biol. 73 (2004) 1.

[73] H. You, H.E. Yoon, J.H. Yoon, H. Ko, Y.C. Kim, Bioorg Med Chem. 19 (2011) 5383.

[74] A. Juzeniene, Photodiagnosis Photodyn Ther. 6 (2009) 94.

[75] E. Zenkevich, E. Sagun, V. Knyukshto, A. Shulga, A. Mironov, O. Efremova, R. Bonnett, S.P. Songca, M. Kassem, J. Photochem. Photobiol. B., 33 (1996) 171.

[76] J.K. Hoober, T.W. Sery, N. Yamamoto, Photochem. Photobiol. 48 (1988) 579.

[77] A. Datta, A. Dube, B. Jain, A. Tiwari, P.K. Gupta, Photochem. Photobiol, 75 (2002) 488.

[78] M. Sharma, A. Dube, H. Bansal, P.K. Gupta, Photochem. Photobiol. Sci. 3 (2004) 231.

[79] P.P. Mishra, J. Bhatnagar, A. Datta, Chem. Phys. Lett. 386 (2004) 158.

[80] K. Das, B. Jain, A. Dube, P.K. Gupta, Chem. Phys. Lett. 401 (2005) 185.

[81] T.K. Mukherjee, P.P. Mishra, A. Datta, Chem. Phys. Lett. 407 (2005) 119.

[82] S. Patel, A. Datta, Chem. Phys. Lett. 413 (2005) 31.

[83] P.P. Mishra, J. Bhatnagar, A. Datta, J. Phys. Chem. B 109 (2005) 24225.

[84] K. Das, A. Dube, P. K. Gupta, Dyes and Pigments 64 (2005) 201.

[85] P.P. Mishra, R. Adhikary, P. Lahiri, A. Datta, Photochem. Photobio. Sci. 5 (2006) 741.

[86] P.P. Mishra, S. Patel, A. Datta, J. Phys. Chem. B 110 (2006) 21238.

[87] A. Dube, S. Sharma, P.K. Gupta, Oral Oncol 42 (2006) 77.

[88] M. Sharma, A. Dube, K. Das, P.K. Gupta, ISRAPS Bulletin 18 (2006) 39.

[89] B. Jain, A. Dube, K. Das, P.K. Gupta, Chem. Phys. Lett. 426 (2006) 163.

[90] S. Patel, A. Datta, J. Phys. Chem. B 111 (2007) 10557.

[91] S. Patel, A. Datta, Photochem. Photobio. 85 (2009) 725.

[92] B. Jain, A. Uppal, P.K. Gupta, K. Das, Photochem. Photobiol. 85 (2009) 927.

[93] A. Dube, S. Sharma, P.K. Gupta. Oral Oncol. 47 (2011) 467.

[94] R.K. Saini, P.K. Gupta, K. Das, J. Mol. Struc. 1024 (2012) 13.

[95] B. Jain, A. Uppal, P.K. Gupta, K. Das, J. Mol. Struc. 1032 (2013) 23.

[96] B. Cunderlıkova, L. Gangeskat, J. Moan, J. Photochem. Photobiol. B Biol. 53 (1999) 81.

[97] B. Cunderlıkova, E.G. Bjorklund, E.O. Pettersen, J. Moan, Photochem. Photobiol. 74 (2001) 246.

[98] A. Uppal, B. Jain, M.K. Swami, H.S. Patel, A. Dube, P.K. Gupta, K. Das, BioNanoScience (In press).

[99] C. Peetla, A. Stine, V. Labhasetwar, Mol. Pharma. 6 (2009) 1264.

Chapter – 2

Instrumentation and Methods

In this chapter we present preparation and characterization details of liposomes, details of the spectroscopic characterization techniques used with a particular emphasis on Second Harmonic (SH) spectroscopic technique. Sample preparation details are given in individual chapters (3-5).

2.1. Preparation of unilamellar liposomes

The lipids POPG and POPC were obtained from Sigma and were used as received. Two methods were used for liposome preparation:

(A) Rotary evaporation method:-

A 0.1M stock solution of phospholipids was formed in Chloroform. Then 980 µL of Chloroform and 200 µL of Methanol were added to a 50 ml round bottom flask containing 20 µL of phospholipid stock solution and mixed well. After mixing, ~ 7 mL buffer were slowly added to round bottom flask by a pipette to avoid mixing of the aqueous and organic phase. The mixture was then rotated in a rotary evaporator under vacuum till complete evaporation of the organic solvents as evidenced by the lack of bubble formation. This method allows unilamellar liposomes to be prepared in a very short time [1]. The final lipid concentration obtained by this method was ~0.3 mM.

(B) Thin film method:-

For experiments requiring a higher lipid concentration the thin film method was used. In this method around 200 µL of 0.1M of phospholipid stock solution in Chloroform was taken in a round bottom flask and the solvent was evaporated for 8-10 hours in a rotary evaporator using a vacuum pump. The lipid film produced was then dispersed in 10 ml of buffer solution with sonication to produce liposomes [2]. The final lipid concentration prepared in this way was ~2.0 mM.

Liposomes produced by above methods are then passed several times through cellulose-acetate membranes (pore size: 100 or 200 nm) to reduce their polydispersity. The prepared liposomes are then stored in a refrigerator for further use and discarded when they are over a week old.

2.2. Size & Zeta potential measurements of liposomes

The average size of the liposomes suspended in aqueous buffer medium was measured by the dynamic light scattering technique using a Brookhaven 90Plus particle size analyzer. The instrument can measure the size of particles in the range from ~1 nm to 6 µm with an accuracy of ± 5%. It uses a 35 mW diode laser as the light source and the scattered signal is collected at 90º. The sample volume required is ~2 ml. With this system the average diameter of the particles as well as their polydispersity can be measured. The instrument is also fitted with the ZetaPlus unit which is used to measure the zeta potential (a measure of the surface charge) of the liposomes. The instrument can measure zeta potential (range ± 150 mV) of nanoparticles having sizes ranging from 10 nm to 30 µm with an accuracy of ± 2%.

2.3. Principles of absorption and emission spectroscopy

The processes responsible for absorption and fluorescence of fluorophores can be illustrated by a Jablonski diagram (Figure 2.1). The diagram illustrates the electronic states of molecules and the transitions between them. The ground state, first and second electronic states are represented by S_0, S_1 and S_2 respectively. The transitions between the electronic states are indicated as vertical lines. The excitation of the molecules from ground state to excited states is very fast and completed within 10^{-15}s without change in the nuclear coordinates of the molecule (Franck-Condon principle). If molecule is excited to some higher vibrational level of either S_1 or S_2 electronic state, the molecules rapidly relax to the lowest vibrational level of S_1 by internal conversion process and this process completed within 10^{-12} second or less. The internal conversion process is generally complete prior to emission process. The molecules can also relax from the higher vibrational level to the lowest vibrational level via vibrational relaxation process by energy loss to other molecules present in the medium through collisions. This process is completed within 10^{-10} to 10^{-12} second. Fluorescence is observed when molecules return from lowest vibrational state of S_1 electronic state to S_0 electronic state by emission of a photon. The rate of such transition is ~10^{-8} second. The wavelength of the emitted photon is dependent on the energy gap between S_0 and S_1.

The molecules in the singlet excited state S_1 can also undergo a spin conversion to the first triplet state T_1 by intersystem crossing (rate ~10^{-9} second). The probability of the intersystem crossing increases if the vibrational levels of two states overlap. The radiative emission from triplet excited state T_1 to ground state S_0 is known as phosphorescence. It is a spin forbidden process and the energy of the emitted photon is generally shifted to longer wavelength

(lower energy) as compared to the fluorescence. The triplet state has a long lifetime and rate of such transition is slow (milliseconds to seconds) [3-5].

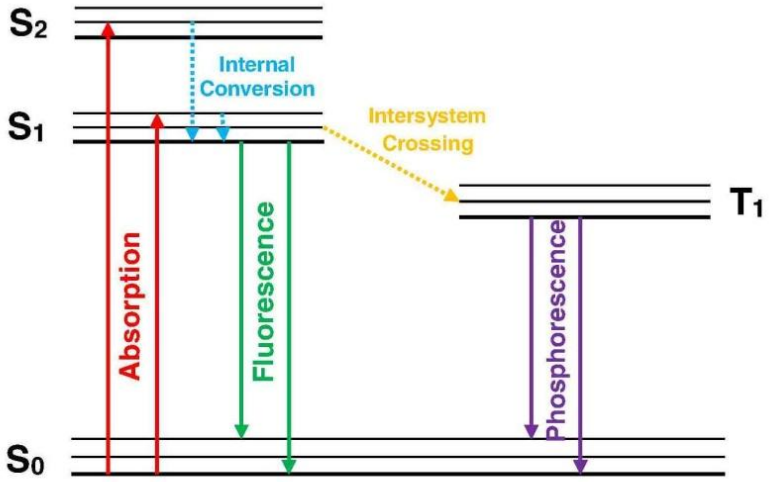

Figure 2.1*: Jablonski diagram of transitions between different electronic energy levels.*

2.3.1 UV-Visible absorption spectroscopy

The steady state absorption spectra were measured using a UV–VIS absorption spectrometer model Cintra 20 (GBC Scientific Equipments Ltd.). It is a dual beam direct ratio recording system having Czerny-Turner style monochromator with holographic grating and variable slit widths and the detector is a photomultiplier tube. Automatic lamp peaking and wavelength calibration is done on power up. The excitation sources are 35 W tungsten–halogen lamp and 30 W deuterium lamp which change automatically at selected wavelength. The wavelength range of the instrument is 190 - 900 nm with variable spectral band pass (0.2 nm to 5 nm in steps of 0.1 nm) having a wavelength accuracy of ± 0.2 nm. The photometric linearity of the instrument is better than 1% up to an absorbance value of 3.

2.3.2. Steady-State Fluorescence spectroscopy

The steady state emission measurements were carried out using a Spex Fluorolog 2 fluorimeter. It has a 450W Xenon lamp as the excitation source. The excitation light is passed through a monochromator (focal length: 20 cm) and focused on the sample placed in the sample chamber at spot size of ~2 mm by ~6 mm. For all fluorescence measurements the emission was collected at right angle geometry. The emitted fluorescence after passing through a double monochromator (focal length: 20 cm each), was collected by a PMT (Hamamatsu R955) which is sensitive from 250 to 850 nm.

2.4. Fluorescence Lifetime Measurements

The time resolved fluorescence measurements were done using the time correlated single photon counting (TCSPC) technique [3, 6-7]. This technique is based on the concept that after an excitation event, the temporal probability distribution of emission of a single photon yields the actual intensity against time distribution of all the emitted photons. In the experiment this probability distribution is constructed by sampling a single photon emission, following a large number of excitation events.

A schematic diagram of a TCSPC system operating in the forward mode is presented in Figure 2.2. A short laser pulse excites the fluorescent sample at a high repetition rate. The fluorescence emitted by the sample is detected by the detector (MCP-PMT). A reference photodiode (PD) triggered by the excitation laser pulse is usually used to start the time-to-amplitude converter (TAC). The role of TAC is to measure the delay time between the excitation pulse and the pulse produced from the MCP by the emitted photon. After being started by the reference PD the TAC charges a capacitor with constant current and generates a linear voltage

ramp, which increases with time. As soon as the output of the MCP reaches the TAC further charging of the capacitor is stopped. The output of the TAC is now a voltage which is proportional to the time delay between the excitation event and the emission event. This voltage is converted to a numerical value by an analog-to-digital converter (ADC) and stored in a multi-channel analyzer (MCA) at a particular channel number. The sample is repeatedly excited by the laser pulse, and the corresponding fluorescence photons are detected, and the TAC output for each absorption-emission event is sent to the MCA which generates a histogram. This histogram corresponds to the emission decay profile of the sample which is convoluted with the instrument response function (IRF) of the TCSPC system. The IRF is the intrinsic or dead time taken by the TCSPC system which limits the time resolution of the system. The IRF is generally recorded by detecting the scattered light from a non-fluorescent scattering sample. The intrinsic emission decay kinetics is then deconvoluted from the IRF using an iterative technique [3, 6-7].

One important constraint in the method is that two photons from the same light pulse must not reach the sample detector. The errors introduced by multiple photons reaching the detector are called pile up errors. In order to avoid pile-up errors, the average count rate at the detector must be 1 to 5% of the excitation rate. Low excitation pulse energy and low sample concentration are also recommended to ignore pile-up errors [6-7].

The emission lifetimes of the fluorophores were recorded by using a TCSPC system called Lifespec-RED manufactured by Edinburgh Instruments. The excitation source was the second harmonic output of the tunable femto second laser (Coherent Model Verdi pumped by Coherent Model Mira) having pulses of ~150 fs duration. A pulse picker (Coherent model 9200) was used to select pulses at 3.8 MHz repetition rate. The fluorescence was collected at right angles to excitation. Proper optical filters were used to avoid the scattered excitation light

reaching to the detector. The instrument response function (IRF) of the system with a Hamamatsu microchannel plate PMT (R3809U-50) was ~50ps. The fluorescence decays were deconvoluted from the IRF using the iterative software based on global least squares analysis algorithm provided by the manufacturer. The goodness of the fit was judged by the reduced chi-square values and visual inspection of the plots of weighted residuals.

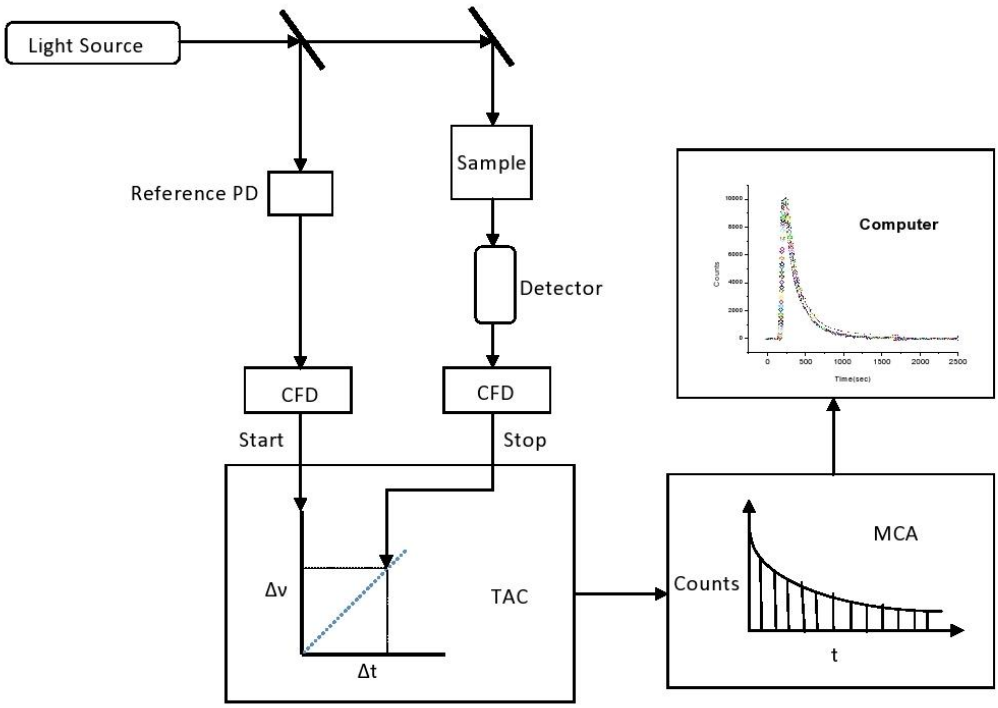

***Figure 2.2**: Schematic diagram of a TCSPC system*

2.5. Solvation Dynamics measurements

Chemical reaction rates in the solution phase are strongly affected by both general and specific interaction between the solute (reactants/intermediates/products) and solvent molecule.

It is therefore important to study and understand how the solvent molecules interacts with solute molecules in order to gain insight about the reaction dynamics. Fluorescence spectroscopy offers a way to study the solvent relaxation dynamics around a solute provided the solute is fluorescent. This is usually accomplished by constructing and analyzing the time dependent fluorescence spectrum of the solute [8-20]. Photoexcitation of certain solute molecules from ground state to excited state ($S_0 \rightarrow S_1$) may lead to a significant change in the dipole moment of the solute. The orientation of the surrounding solvent molecules then starts to rearrange around the newly created dipole. As a result the excited state energy of the solute molecule starts to relax and its fluorescence spectrum starts to shift towards lower energy (or, longer wavelength) with increasing time (Figure 2.3). This relaxation process and the corresponding dynamics of solvation can be monitored by constructing time dependent emission spectrum of the solute using the time resolved fluorescence spectroscopic technique.

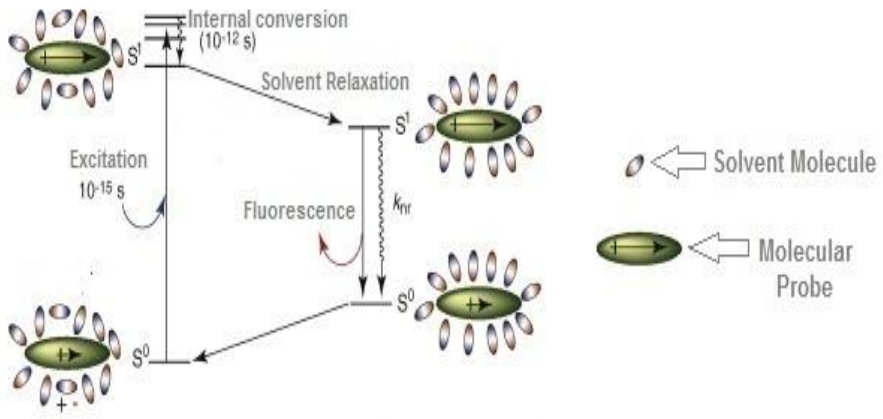

Figure 2.3*: Schematic diagram of dipolar solvation of a polar solute after optical excitation.*

The excited state relaxation process of the solute molecules are expressed by a solvent correlation function C(t), defined as [9]

$$C(t) = \frac{\nu(t) - \nu(\infty)}{\nu(0) - \nu(\infty)} \qquad (2.1)$$

Where ν(0), ν(t), and ν(∞) denote the peak frequency of the fluorescence spectra of the solute at time zero, t, and infinity respectively.

Measurement of time resolved emission spectra (TRES) is the most general and precise way to quantitatively describe the solvation function, C(t). The TRES were generated from a set of fluorescence decays taken at different wavelengths (covering the whole emission band of the solute molecule). The fluorescence decays are then fitted with multi-exponential function to obtain the fitted curve *D*(λ,t).

$$D(\lambda, t) = \sum_i a_i\ (\lambda) e^{-\frac{t}{\tau_i(\lambda)}} \qquad (2.2)$$

Where *a*(λ) and τ(λ) are the pre-exponential factor and time constant at a particular wavelength λ. The TRES spectra, S(λ,t) are constructed using the fitted curve, *D*(λ,t), after their normalization with respect to the steady state fluorescence spectrum, $S_0(\lambda)$ as [9-15]

$$S(\lambda, t) = D(\lambda, t) \frac{S_0(\lambda)}{\int_0^\infty D(\lambda, t) dt} \qquad (2.3)$$

After conversion from a wavelength representation to one linear in energy i.e. frequency, the TRES data are fitted by the empirical "log-normal function" [14], which represents a broad, asymmetric electronic emission band and defined as

$$g(\nu) = g_0 \exp\left[- \ln(2) \left(\frac{\ln\left[1 + 2b(\nu - \nu_p)/\Delta\right]}{b} \right)^2 \right] \qquad (2.4)$$

where g_0, ν_p, b and Δ are the peak height, peak frequency, asymmetric parameter, and width parameter, respectively. Once the TRES data have been fitted by the log-normal function,

the corresponding peak frequencies are used to construct C(t). The constructed C(t) is then fitted with exponential function

$$C(t) = \sum_i \alpha_i exp^{-t/\tau_s^i} \qquad (2.5)$$

to extract the solvation time constants. In this work we have observed that the decay of C(t) can be fitted satisfactorily with single or double exponential components. The average solvation time constant is then obtained using the relation, $<\tau_s> = a_1\tau_{1s} + a_2\tau_{2s}$, where a_1 and a_2 are the relative contribution of the solvation time τ_{1s} and τ_{2s}, respectively.

2.6. Second Harmonic Generation (SHG)

2.6.1. Introduction

Optical second harmonic generation (SHG) is the nonlinear conversion process by which two photons of frequency ω are converted to a single photon of frequency 2ω (Figure 2.4),

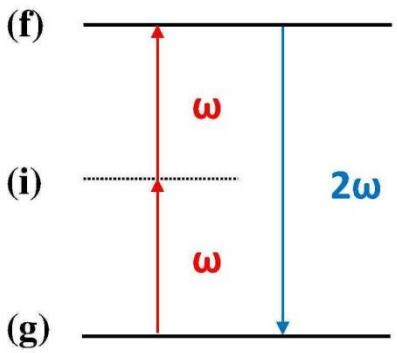

Figure 2.4*: Energy–level digram illustrating SHG. The electronic energy states (g) and (f) corresponds to the ground and excited state and (i) corresponds to the virtual state.*

which, in the electric dipole approximation, requires a noncentrosymmetric medium. Therefore an interface between two dissimilar centrosymmetric media is capable of generating SHG since it is noncentrosymmetric. Since only the first few atomic or molecular monolayers on either side of the interface participate in this symmetry breaking, the SHG process can be used as a highly surface-selective optical probe of interfacial phenomena [21].

2.6.2. Symmetry requirements

The interaction of weak light field with matter is dominated by linear process. However when the light field becomes very intense, non-linear process such as second and third harmonic generation becomes experimentally observable. Shortly after the invention of the optical laser in 1961, source of intense light became available and optical second harmonic generation was observed in a quartz crystal [22].

For weak light field, the induced polarization P(t), linearly depends upon the electric field strength.

$$P(t) = \chi^{(1)} E_{\omega}(t) \qquad (2.6)$$

Where $\chi^{(1)}$ is linear susceptibility and E_{ω}(t) is incident electric field.

But in case of intense light field, the optical response can be described by expressing the polarization P(t) as a power series in the field strength E_{ω}(t) as [23]:

$$P(t) = \chi^{(1)} E_{\omega}(t) + \chi^{(2)} E_{\omega}(t)\, E_{\omega}(t) + \chi^{(3)} E_{\omega}(t)\, E_{\omega}(t)\, E_{\omega}(t) + \ldots \qquad (2.7)$$

$$P(t) = P^{(1)}(t) + P^{(2)}(t) + P^{(3)}(t) + \ldots \qquad (2.8)$$

Where $\chi^{(2)}$ and $\chi^{(3)}$ is known as the second and third-order nonlinear susceptibility respectively.

The induced second order polarization $P^{(2)}$(t) can be expressed as [24-27],

$$P^{(2)}(t) = \chi^{(2)} E_{\omega}(t)\, E_{\omega}(t) \qquad (2.9)$$

Where $E_{\omega}(t)$ is incident electric field and $\chi^{(2)}$ is the second order nonlinear susceptibility of the non linear medium. A rigorous expression for eq. (2.9) where $P^{(2)}(t)$ and $E_{\omega}(t)$ are expressed as vectors and $\chi^{(2)}$ as a tensor is

$$P_i^{(2)}(t) = \sum_{j,k} \chi_{i,j,k}^{(2)}\, E_{\omega}^{j}(t)\, E_{\omega}^{k}(t) \qquad (2.10)$$

Where *i*, *j*, *k* are the three normal coordinates of laboratory system. For a medium having inversion symmetry, the reflection along that plane will not change the sign or magnitude of $\chi^{(2)}$. However, an inversion operation on the electric field $E_{\omega}(t)$ reverses both the sign of the electric field and that of the second order polarization $P^{(2)}(t)$.

Therefore the Eq. 2.9 is transformed as:

$$-P^{(2)}(t) = \chi^{(2)}\big(-E_{\omega}(t)\big)\big(-E_{\omega}(t)\big) \qquad (2.11)$$

Combining Eq. 2.9 with Eq. 2.11, we get $P^{(2)}(t) = -P^{(2)}(t)$, and therefore, $P^{(2)}(t)$ must be zero. Thus, the solution for $\chi^{(2)}$ must be zero. This means that SHG is not allowed in a centrosymmetric medium. However, at an interface between two different bulk media, where inversion symmetry is no longer conserved, $P^{(2)}(t)$ is not necessarily equal to $-P^{(2)}(t)$ on performing an inversion operation. Therefore $\chi^{(2)}$ at interface is not necessarily to be zero, suggesting that SHG from interfaces is allowed.

2.6.3. SHG from centrosymmetric structures

The net coherent second harmonic (SH) field in a bulk medium (which is centrosymmetric) is zero. This is due to the fact that in bulk medium, for every molecule oriented in one direction, there is a neighboring one oriented in opposite direction and located at a

distance that is much less than the coherence length of the process. The nonlinear polarizations induced in these oppositely oriented molecules by the intense incident light are of opposite phase with respect to each other and therefore they cancel. As a consequence, the net polarization is zero and coherent SH light is not generated in the bulk medium. In contrast, incoherent SHG (also called hyper-Rayleigh scattering, HRS) is possible in bulk centrosymmetric medium. This has been attributed to the fluctuation in molecular density and molecular orientation in isotropic bulk solution which can disrupt the phase cancellation and generate incoherent SHG or HRS. SHG has also been observed in individual large non-centrosymmetric molecule in randomly oriented suspension in bulk solution [28-29].

Although SHG is forbidden in centrosymmetric media, microscopic centrosymmetric particles suspended in a liquid medium can generate SHG [30]. We explain this by considering a bare microsphere of diameter L. We note that opposite positions of the microscopic particle surface has oppositely oriented surface structures and the generated second harmonic (SH) electric field will have opposite phases. The total SH field is:

$$E_{2\omega} \propto \beta^{(2)} \mathrm{E}_{\omega} \mathrm{E}_{\omega} \left(1 - \mathrm{e}^{-\mathrm{i}\Delta\vec{\mathrm{k}}.\vec{\mathrm{L}}}\right) \qquad (2.12)$$

Where $\beta^{(2)}$ is the second-order polarizability of the microsphere and $\Delta\vec{\mathrm{k}}$ is scattering vector:

$$\Delta\vec{k} = \vec{k}_{2\omega} - 2\vec{k}_{\omega} \qquad (2.13)$$

Here $\vec{k}_{2\omega}$ and $\vec{k}_{\omega}$ are the light propagation vectors for the second harmonic light at 2ω and the fundamental light ω respectively. The amplitude of the scattering vector is defined as:

$$\Delta k = \frac{4\pi(n_{\omega} - n_{2\omega})}{\lambda_{\omega}} = \frac{4\pi\Delta n}{\lambda_{\omega}} \qquad (2.14)$$

Therefore it follows that if the separation length L between the oppositely oriented molecules is much less than wavelength of fundamental light, then $\Delta\vec{\mathrm{k}}.\vec{\mathrm{L}} \ll \lambda$ and consequently

$E_{2\omega} = 0$. On the other hand, if separation length L is comparable to the wavelength of fundamental light, then $E_{2\omega} \neq 0$. Therefore although the particle is centrosymmetric depending upon its diameter and wavelength of incident radiation it can generate SHG. For the case when $\Delta\vec{k}.\vec{L} \sim \pi$, $E_{2\omega}$ will be maximum.

2.6.4. SHG: A tool to monitor bilayer transport of molecules

The adsorption and transport kinetics of molecules and ions across a lipid bilayer can be monitored by using the SHG spectroscopic technique [29-36]. The reason for this is that SHG will occur from molecules that are located only in the bilayer region. In addition, the molecule of interest should have a reasonable hyperpolarizability at the wavelength of fundamental radiation. If the size of the liposomes is of the order of the wavelength of the fundamental (~ 800 nm) radiation, the SH field generated from the molecules adsorbed on the outer lipid bilayer can add coherently to generate a non-zero SH field (Figure 2.5). In contrast, due to their random orientation molecules present in the bulk water will not generate SHG but they can still generate incoherent SH by HRS as discussed before. It is pertient to note that due to its coherent nature SH generated from molecules adsorbed on the outer surface of the liposome will be significantly higher than the incoherent HRS generated from molecules present in the bulk medium. When dye molecules diffuse across the lipid bilayer, and get absorbed to the inner surface of the liposome, the adsorbed molecules on the inner and outer surface of the lipid bilayer are oppositely oriented. Since the oppositely oriented molecules are separated by the bilayer thickness (~ 5 nm) which is expected to be much less than the coherence length of the SHG process, the SHG generated from the oppositely oriented molecules will cancel each other. Thus

the resulting SH field generated from the molecules adsorbed on the liposome surface will be proportional to the population difference between the outer and inner surface. Therefore, the diffusion process can be monitored in real time by monitoring the SHG signal subsequent to the addition of molecules to the liposomes. Eisenthal's group at Columbia University was the first to demonstarte the use of SHG to monitor the diffusion of an organic cation Malachite green (MG), across a bilayer [31]. They have studied the diffusion process of MG across a negatively charged phospholipid bilayer under different conditions [31-35].

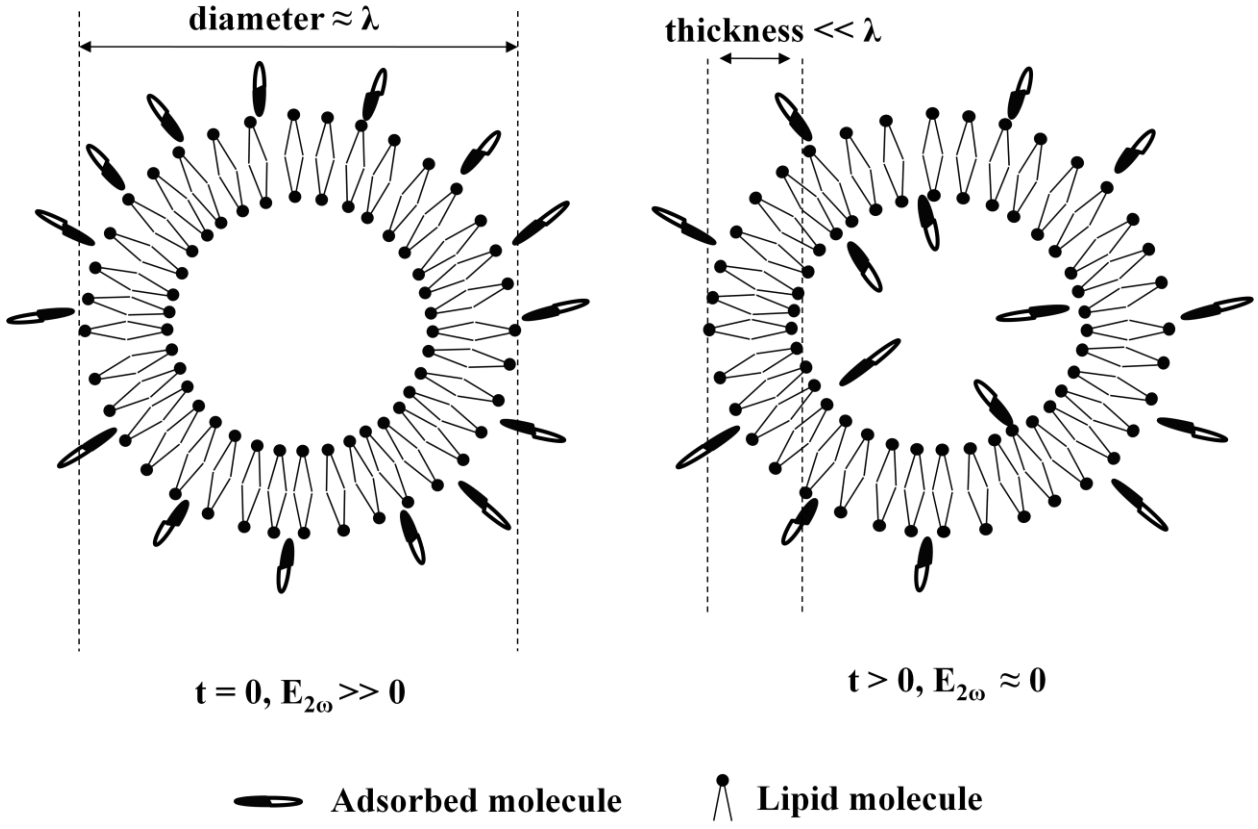

Figure 2.5*: SH generated from molecular adsorption on a liposome. Initially when molecules are adsorbed at the outer surface the SH signal is maximum. As the molecules diffuse through the lipid bilayer, and adsorb onto the inner surface the SHG signal becomes minimum.*

2.6.5. Experimental setup

The schematic of the experimental setup used to montior the diffusion process by the SH technique is shown in Figure 2.6. The fundamental radiation was the quasi-CW output (tunable from 780 to 850 nm) of a Ti-Saphhire (Coherent Mira) laser pumped by a green (532 nm, Coherent Verdi 5W) laser. The average laser power used in the experiments varied between 450 to 650 mW and the pulse width was ~150 fs. The polarization of the laser was fixed in the vertical plane by using a half wave plate (HWP). The laser beam was focused into the sample by a convex lens having a focal length of 10 cm. The generated SH light was detected using a Edinburgh Instruments TCSPC system (Model LifeSpec Red). A band pass filter was placed before the monochromator of the TCSPC system to reject the fundamental. The wavelength resolution of the monochromator was 2 nm. The generated SH light was detected at right angles with respect to the fundamental (800 nm) by a cooled Hamamatsu MCP-PMT using single photon counting technique. A typical SH intensity-time profile of a hemicyanine dye, LDS-698 is shown in Figure 2.7. The SH signal from buffer alone is negligible and after addition of the dye the signal increased modestly due to HRS from the dye. A significant increase in the SH signal intensity was observed after addition of POPG liposomes which occurs due to electrostatic adsorption of the dye on the outer surface of the liposome. As time progresses the SH signal starts to decay signifying diffusion of the dye from inner to outer bilayer. The diffusion time constants can be extracted by exponential fitting of the SH intensity data following liposome addition.

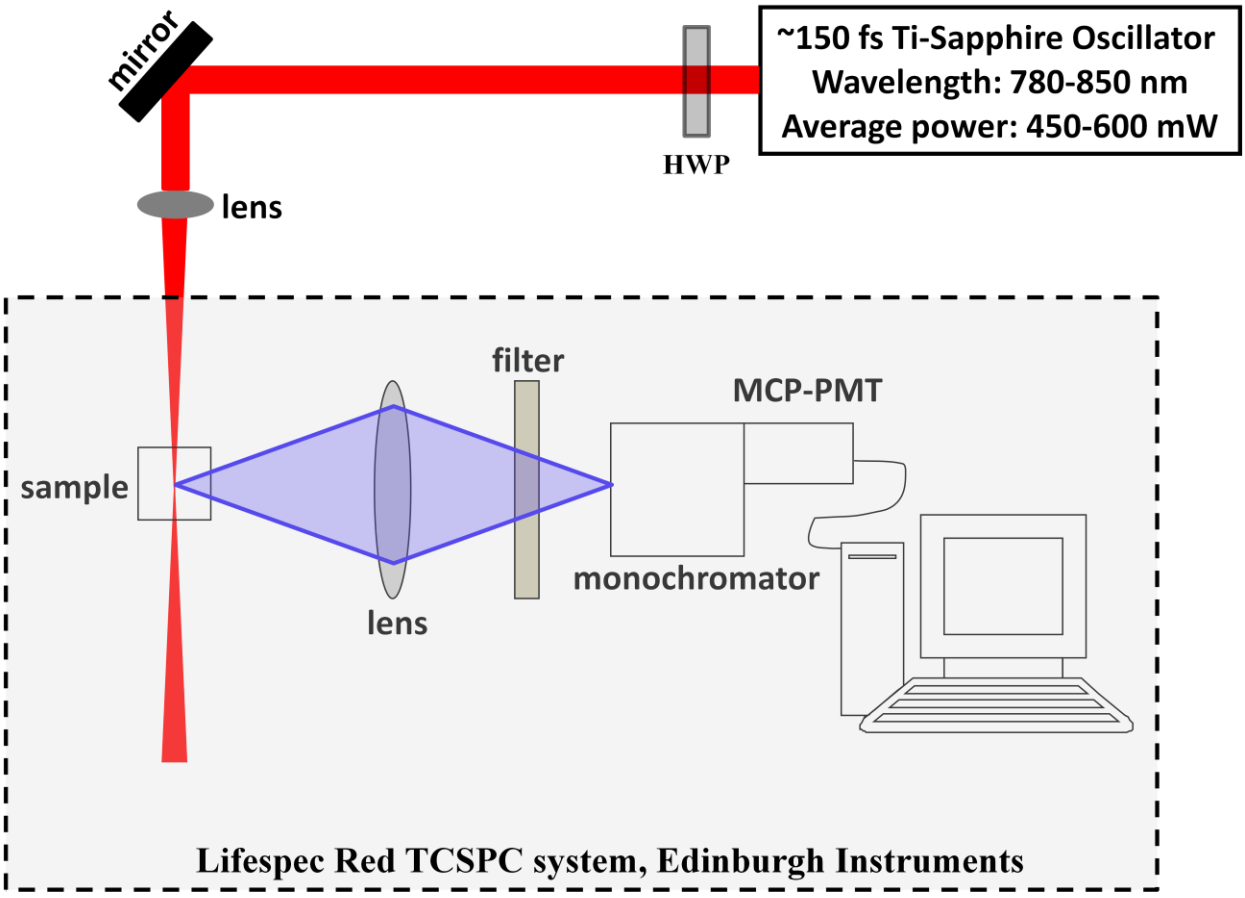

***Figure 2.6**: Schematic of the experimental set up used to measure HRS and SH signals.*

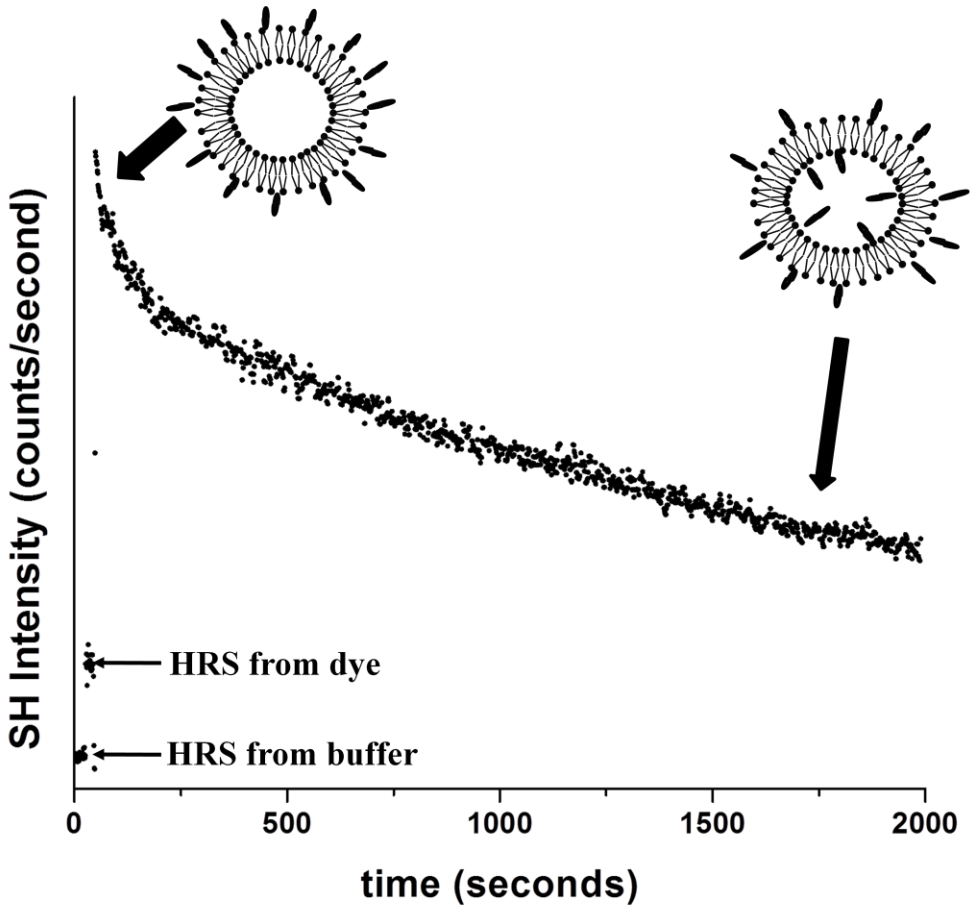

Figure 2.7*: A typical SH decay showing how the molecular diffusion across a bilayer can be monitored in real time.*

2.7. Reference

[1] A. Moscho, O. Orwar, D.T. Chiu, B.P. Modi, R.N. Zare, Proc. Natl. Acad. 93 (1996) 11443.

[2] P.G. Tardi, N.L. Boman, P.R. Cullis, J. of Drug Targeting 4 (1996) 129.

[3] J.R. Lackowicz, *Principles of fluorescence spectroscopy*, 3rd ed., Springer, New York, 2006.

[4] K.K. Rohatgi-Mukherjee, *Fundamentals of Photochemistry*, Wiley Eastern Ltd, India, 1986.

[5] M. Sauer, J. Hofkens, J. Enderlein, *Handbook of Fluorescence Spectroscopy and Imaging*, WILEY-VCH Verlag GmbH & Co. KGaA, Weinheim, 2011.

[6] W. Becker, *Advanced time correlated single photon counting technique*, Springer, New York, 2005.

[7] D.V. O'Connor, D. Phillips, *Time Correlatated Single Photon Counting*, Academic, New York, 1984.

[8] K. Bhattacharyya, B. Bagchi, J. Phys. Chem. *A* 104 (2000) 10603.

[9] E.W. Castner, G.R. Fleming, B. Bagchi, M. Maroncelli, J. Chem. Phys. 89 (1988) 3519.

[10] R.S. Fee, M. Maroncelli, Chem. Phys. 183 (1994) 235.

[11] R.S. Fee, J.A. Milsom, M. Maroncelli, J. Phys. Chem. 95 (1991) 5170.

[12] K. Hara, H. Kuwabara, O. Kajimoto, J. Phys. Chem. A 105 (2001) 7174.

[13] M. Maroncelli, J. Mol. Liq. 57 (1993) 1.

[14] M. Maroncelli, G.R. Fleming, J. Chem. Phys. 86 (1987) 6221.

[15] M. Maroncelli, J. Macinnis, G.R. Fleming, Science 243 (1989) 1674.

[16] N. Nandi, K. Bhattacharyya, B. Bagchi, Chem. Rev. 100 (2000) 2013.

[17] E.R. Riter, D.M. Willard, N.E. Levinger, J. Phys. Chem. B 102 (1998) 2705.

[18] N. Sarkar, A. Datta, S. Das, K. Bhattacharyya, J. Phys. Chem. 100 (1996) 15483.

[19] P. Sen, S. Mukherjee, A. Halder, K. Bhattacharyya, Chem. Phys. Lett. 385 (2004) 357.

[20] D.M. Willard, R.E. Riter, N.E. Levinger, J. Am. Chem. Soc. 120 (1998) 4151.

[21] Y.R. Shen, *The principles of Nonlinear Optics*, Wiley, New York, 1984.

[22] P.A. Franken, A.E. Hill, C.W. Peters, G. Weinreich, Phys. Rev. Lett. 7 (1961) 118.

[23] Y.R. Shen, Nature, 337 (1989) 519.

[24] Y.R. Shen and F. de Martini, in: V.M. Agronovich and D.L. Mills (Eds.), Surface Polaritons, North-Holland, 1982, pp. 629.

[25] T.F. Heinz, Ph.D Dissertation, University of California, Berkeley, 1982.

[26] J.E. Sipe and G.I. Stegman, in: V.M. Agronovich and D.L. Mills (Eds), Surface Polaritons, North-Holland, 1982 pp. 661.

[27] M. Fukui and G.I. Stegman, in: A.D. Boardman (Eds), Electromagnetic Surface Modes, John Wiley & Sons, 1982 pp. 725.

[28] E. Hendrickx, K. Clays, A. Persoons, Acc. Chem. Res. 31 (1998) 675.

[29] K.B. Eisenthal, Chem. Rev. 106 (2006) 1462.

[30] H. Wang, E.C.Y. Yan, E. Borguet, K.B. Eisenthal, Chem. Phys. Lett. 259 (1996) 15.

[31] A. Srivastava, K.B. Eisenthal, Chem. Phys. Lett. 292 (1998) 345.

[32] E.C.Y. Yan, K.B. Eisenthal, Biophys. J. 79 (2000) 898.

[33] X.M. Shang, Y. Liu, E. Yan, K.B. Eisenthal, J. Phys. Chem. B 105 (2001) 12816.

[34] Y. Liu, E.C.Y. Yan, K.B. Eisenthal, Biophys. J. 80 (2001) 1004.

[35] J. Liu, X.M. Shang, R. Pompano, K.B. Eisenthal, Faraday Discussions 129 (2005) 291.

[36] J. Liu, M. Subir, K. Nguyen, K.B. Eisenthal, J. Phys. Chem. B 112 (2008) 15263.

Chapter – 3

Photophysical studies of Curcumin excited state in toluene-polar solvent mixtures

3.1. Introduction

Curcumin, which exhibits a wide variety of biological and photochemical properties [1-10] is currently the subject of a large number of spectroscopic investigations. Several studies have focused on the photophysical properties of the excited states of Curcumin [11-29] and have predicted about the occurrence of two fundamental photophysical processes in the excited state, namely the excited-state hydrogen atom (or proton) transfer (ESHT), and solvation [12-29].

In a recent study by Palit and co-workers [26] subpicosecond time-resolved fluorescence and absorption spectroscopic techniques are used to study the dynamics of the excited singlet (S_1) state of Curcumin in a wide variety of neat solvents. In nonpolar solvents because of the presence of six-membered hydrogen-bonded chelate ring of the cis-enol form (Scheme 3.1) the ESHT process is expected to be primarily intramolecular in nature and based on previous studies [31-36] it should be completed within a few hundreds of femtoseconds. However in polar protic solvents, like methanol (MeOH), there will be significant perturbation of intramolecular H bond as solvent molecules will compete to form intermolecular H bond with Curcumin. As a result specific solvent effects such as H bond reorganization between Curcumin and solvent will affect the relaxation of the S_1 state of Curcumin in these solvents and indeed it has been observed [26]. In neat solvents this relaxation is typically completed within few picoseconds. In this chapter we present the result of our studies on Curcumin excited state behavior in a binary solvent mixture consisting of toluene and different polar solvents.

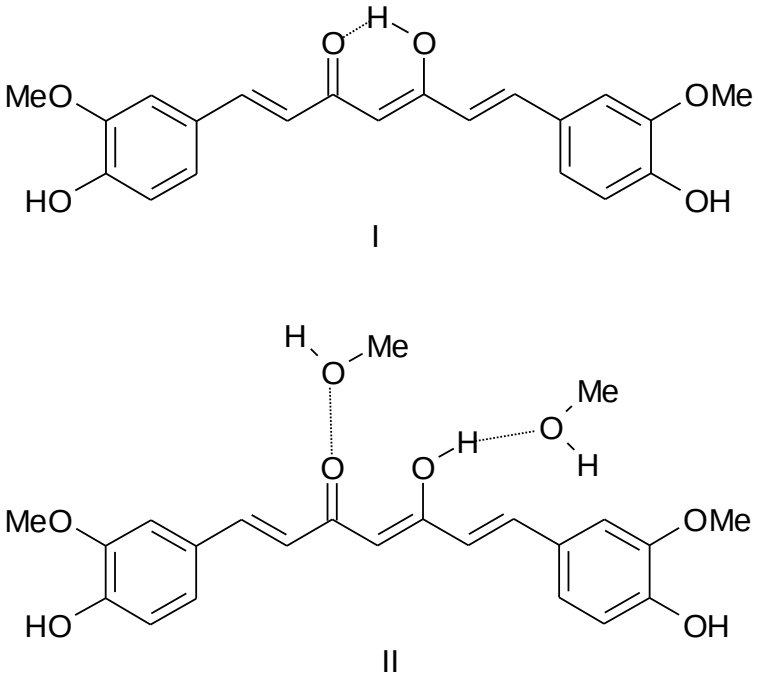

Scheme 3.1*: Likely structures of Curcumin in non hydrogen bonding (top) and hydrogen bonding (bottom) solvents showing the intra molecular and inter molecular hydrogen bonds. MeOH is arbitrarily chosen as an example of a hydrogen bonding solvent. The bottom picture is oversimplified in the sense that only two solvent molecules are shown and the phenolic OH groups are excluded from hydrogen bonding with the solvent.*

3.2. Materials & Methods

Curcumin (Sigma product no. C7727) was further purified by TLC according to a reported method [39]. Deuterated methanol (MeOH-d_4) from Across Chemicals (99 atom % D; product no. A 0305352) was used as received. For the experiments on Curcumin in MeOH-d_4, Curcumin was allowed to equilibrate in the deuterated solvent for 48 h (as reported earlier [24-

25]) to ensure complete exchange of the enolic hydrogen with deuterium. Toluene, Ethanol, 1-Propanol, 1-Butanol, 1-Octanol, DMSO and HFP were all spectroscopic grades (purity > 99%) and were used as received.

For all spectroscopic measurements the optical density of Curcumin (1 cm optical path) were kept typically ~0.2-0.3 at the maximum, which corresponds to micro-molar concentrations of the drug. All the experiments were performed at room temperature. Fluorescence quantum yield of the pigment were calculated with respect to its value reported in toluene [12-15] after proper correction for the slight variation in the absorption spectra in different solvent mixtures.

For the time-resolved fluorescence experiments the acquisition time window had a width of ~2.5 ns with 2048 channels, corresponding to 1.22 ps per channel. All the Curcumin solutions were excited by vertically polarized light at 420 nm, and the emission was detected at magic angle over the whole band after rejecting the excitation light by an appropriate filter. To obtain the time-dependent spectra of Curcumin in toluene-polar solvent mixtures, fluorescence decays were taken at 10-nm intervals with a resolution of 4 nm, having 10K counts in the peak channel. The fluorescence traces were fitted to a single or multi exponential function after de-convolution by the iterative re-convolution method using FAST software supplied by the manufacturer of the TCSPC system. The average lifetimes were calculated using the relation: $\tau_{av} = \sum a_i \tau_i$; where a_i and τ_i are the pre-exponential and lifetime values. The radiative (k_r) and nonradiative (k_{nr}) rates are calculated from the fluorescence quantum yield (Φ_f) and average lifetime (τ_{av}) as: $k_r = \Phi_f / \tau_{av}$ and $k_{nr} = (1/ \tau_{av}) - k_r$.

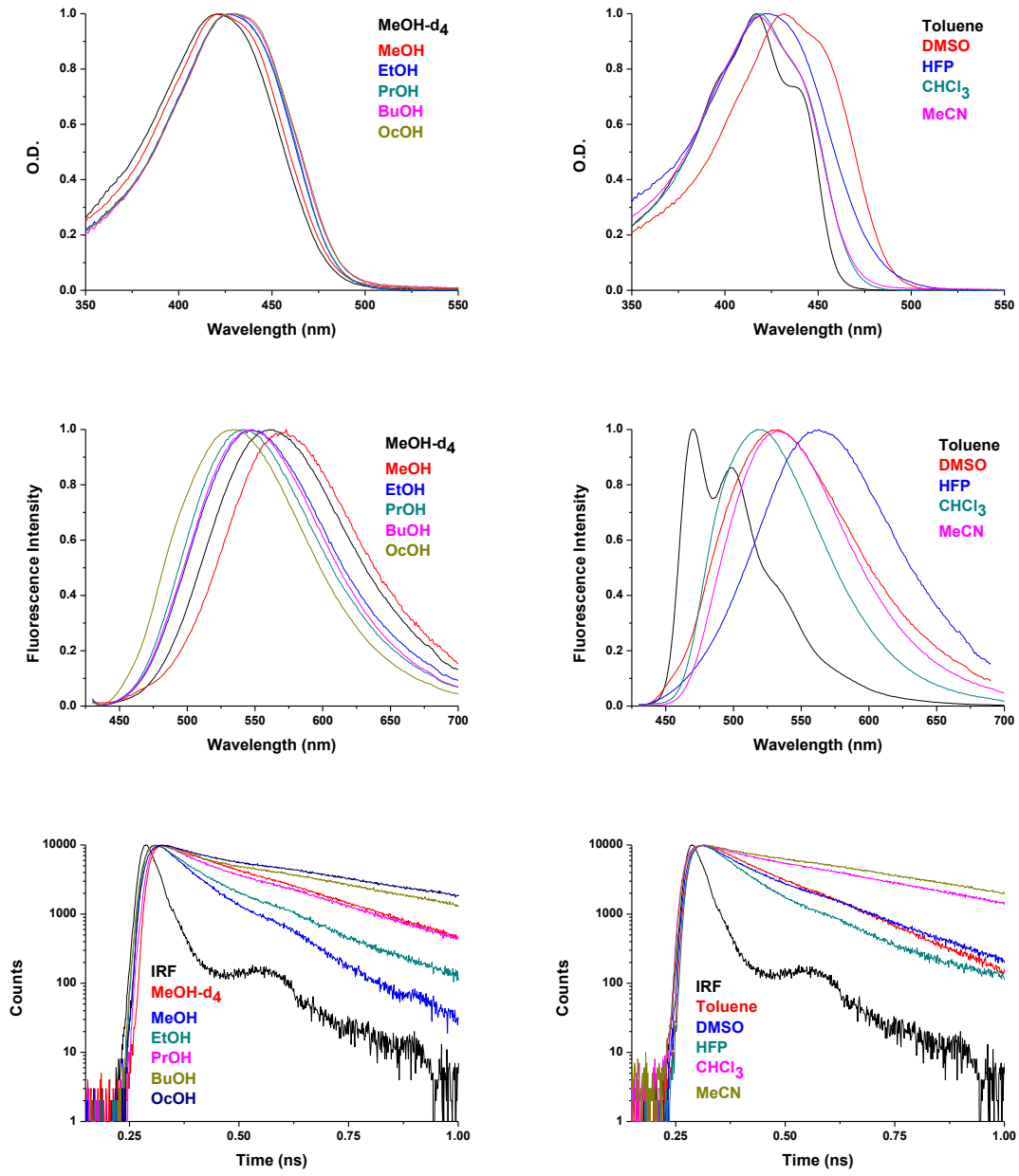

Figure 3.1*: Normalized absorption (top), emission (middle) and fluorescence decays (bottom) of Curcumin in some alcoholic solvents (left panel) and in different non–alcoholic solvents (right panel) used in this work.*

Table 3.1: Photophysical parameters of Curcumin and Kamlet-Taft (K-T) parameters[a] of some solvents

Solvent	K-T parameters			Abs (cm^{-1})	Em (cm^{-1})	Stokes shift (cm^{-1})	Φ^b	a_1	τ_1 (ps)	τ_2 (ps)	τ_{avg} (ps)[b]
	π*	α	β								
Toluene	0.54	0.00	0.11	23964	21739	2225	0.067	0.08	34	140	130
MeOH	0.60	0.93	0.62	23663	17825	5838	0.025	0.30	24	90	70
MeOH-d_4				23842	17825	6017	0.050	0.18	83	235	170
EtOH	0.54	0.86	0.75	23427	18248	5179	0.050	0.24	86	258	127
PrOH	0.52	0.84	0.90	23368	18484	4884	0.090	0.20	58	229	195
BuOH	0.47	0.84	0.84	23427	18281	4746	0.120	0.11	53	372	337
OcOH	0.40	0.77	0.81	23368	18761	4607	0.165	0.13	92	472	423
$CHCl_3$	0.58	0.44	0	23842	19607	4235	0.080	0.08	42	338	314
MeCN	0.75	0.19	0.62	23902	19157	4745	0.080	0.05	32	408	389
DMSO	1.00	0.00	0.76	23200	18450	4750	0.050	0.15	39	147	161
HFP	0.65	1.96	0.00	23665	17545	6120	0.038	0.89	84	533	133

[a]Source: http://www.stenutz.eu/chem/solv26.php

[b]The errors in the values are estimated to be about ~10%

3.3. Results

Figure 3.1 show the normalized absorption (top panel) normalized emission (middle panel) and fluorescence decay curves (bottom panel) of Curcumin in the nonpolar solvent

toluene, and in different polar solvents. Compared to toluene, in all the polar solvents used in this study the vibronic structure in absorption and emission spectra are lost suggesting significant solute-solvent interaction in the ground and excited state. The photophysical parameters of Curcumin in these solvents as well as the solvent Kamlet-Taft (KT) parameters are provided in Table 3.1. For the alcohol solvents, as expected, increasing alkyl chain length decreases the polarity parameter (π^*) of the solvent. In addition, with an increase in the alkyl chain length, the H-bond donating (HBD) property (α) decreases while the H-bond accepting (HBA) property (β) does not show any definite trend. As the polarity of the alcohol solvents decreases (from Methanol to Octanol) the Stokes shift decreases and the corresponding average lifetime increases (Table 3.1). In the Kamlet-Taft scale, while the polarity of MeCN and $CHCl_3$ are comparable to that of MeOH, the former is primarily a HBA and the latter, a HBD solvent (Table 3.1). In Kamlet-Taft scale DMSO and HFP have stronger HBA and HBD property respectively compared to MeCN and $CHCl_3$.

The photophysical properties of Curcumin were studied in different types of toluene–polar solvent mixtures. In a binary mixture of toluene and MeOH (MeOH-d_4) the steady state fluorescence spectra of the pigment shows an interesting behavior (Figure 3.2). The vibrational structure present in the fluorescence spectra of the pigment in toluene remains more or less unchanged as MeOH (MeOH-d_4) mole-fraction is increased to 0.01. After that the spectral shape starts to get broad accompanied by a red sift and an increase in fluorescence intensity till MeOH (MeOH-d_4) mole-fraction of 0.14 (0.40). The fluorescence intensity then drops down significantly as the mole-fraction of the polar protic solvent approaches unity. The variation in fluorescence lifetime follows similar pattern (Table 3.2 and Figure 3.3). Corresponding changes in the absorption spectra of the pigment however were insignificant (data not shown). In order to

find out which properties of the solvent (e.g. polarity, H-bonding ability) are responsible for this kind of changes, the polar protic solvent MeOH is replaced with other polar but aprotic solvents

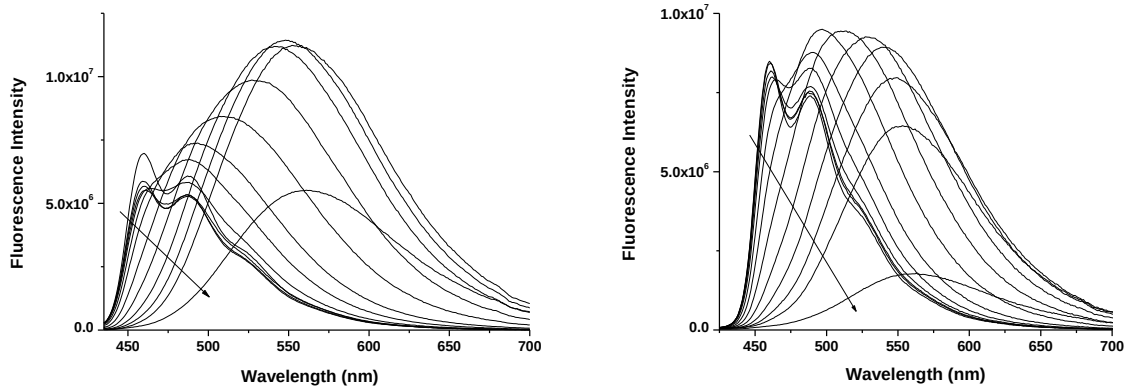

***Figure 3.2**: Evolution of Curcumin fluorescence in binary solvent mixtures of toluene-MeOH (left) and toluene-MeOH-d_4 (right). The arrows indicate increase in the MeOH/ MeOH-d_4 mole-fraction from 0 to 1 (λ_{ex} = 420 nm).*

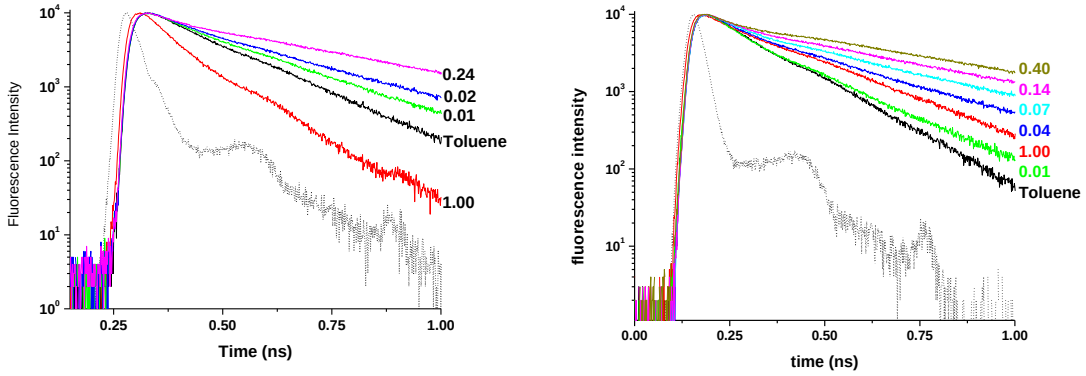

***Figure 3.3**: Fluorescence decays (λ_{ex} = 420 nm) of Curcumin in binary solvent mixtures of Toluene-MeOH (left) and Toluene-MeOH-d_4 (right). The numbers corresponds to the alcohol mole-fraction. The instrument response function is shown as black dotted line.*

such as chloroform ($CHCl_3$) and acetonitrile (MeCN). When MeOH is replaced by $CHCl_3$, the fluorescence properties of the pigment correlated with the mole-fraction of $CHCl_3$, however when MeOH is replaced with MeCN, the fluorescence properties does not exactly correlate

Table 3.2: Lifetime parameters of Curcumin in toluene-MeOH and toluene-MeOH (d_4) solvent mixtures

MeOH mole fraction	τ_1 (ps)	a_1	τ_2 (ps)	a_2	τ_{av} (ps)	MeOH (d_4) mole fraction	τ_1 (ps)	a_1	τ_2 (ps)	a_2	τ_{av} (ps)
0.0013	38	0.12	152	0.88	138	0.0013	84	0.37	159	0.63	131
0.0025	40	0.14	159	0.86	142	0.0025	88	0.39	176	0.61	142
0.0050	44	0.15	173	0.85	154	0.0050	87	0.47	186	0.53	140
0.0100	53	0.18	202	0.82	175	0.0100	92	0.49	225	0.51	160
0.0200	55	0.18	245	0.82	211	0.0200	105	0.45	302	0.55	213
0.0388	55	0.16	297	0.84	258	0.0388	109	0.36	369	0.64	275
0.0747	49	0.13	341	0.87	303	0.0747	105	0.26	444	0.74	356
0.1390	44	0.11	367	0.89	331	0.1390	94	0.18	515	0.82	439
0.2442	36	0.10	361	0.90	329	0.2440	69	0.11	536	0.89	485
0.3925	32	0.10	326	0.90	300	0.3923	56	0.08	540	0.92	501
0.5637	26	0.11	268	0.89	241	0.5635	43	0.06	499	0.94	472

with the mole-fraction of MeCN, instead it resembles the pattern seen with MeOH (Figure 3.4). The variation in fluorescence lifetime follows similar pattern (data not shown). The effect of replacing MeOH with other linear alcohols on the fluorescence behavior of the pigment in toluene-alcohol mixtures were investigated next. The steady state fluorescence spectra of the pigment in these toluene-alcohol mixtures are shown in Figure 3.5. The observed changes in the

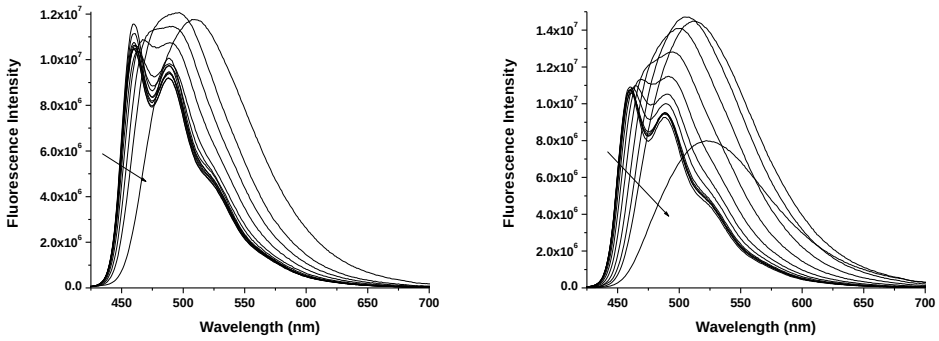

Figure 3.4*: Evolution of Curcumin fluorescence in binary solvent mixtures of toluene-$CHCl_3$ (left) and toluene-MeCN (right). The arrows indicate increase in the polar solvent mole-fraction from 0 to 1 (λ_{ex} = 420 nm).*

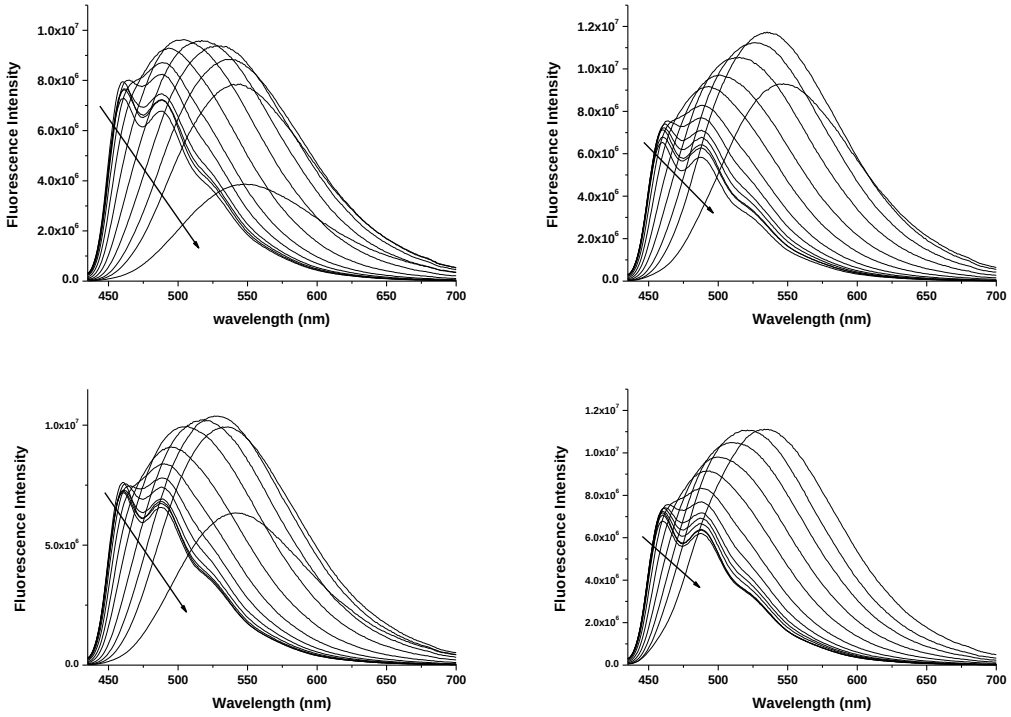

Figure 3.5*: Evolution of Curcumin fluorescence in binary solvent mixtures of toluene-EtOH (top left), toluene-PrOH (bottom left), toluene-BuOH (top right) and toluene-OcOH (bottom right). The arrows indicate increase in the alcohol mole-fraction from zero to unity.*

fluorescence spectra of the pigment in these toluene-alcohol mixtures are similar to that observed in toluene-MeOH mixture. However for toluene-Octanol mixture, the fluorescence intensity was observed to increase steadily as the mole-fraction of Octanol (OcOH) approaches unity.

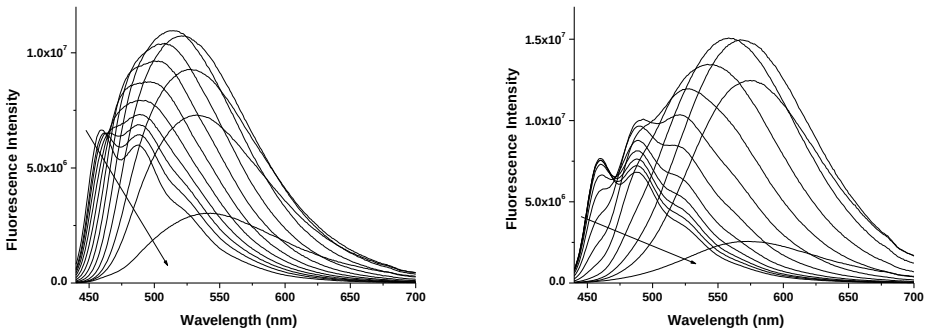

Figure 3.6*: Evolution of Curcumin fluorescence in binary solvent mixtures of toluene-DMSO (left) and toluene-HFP (right). The arrows indicate increase in the polar solvent mole-fraction from zero to unity.*

Finally, MeOH was replaced by two polar solvents, DMSO (only HBA property) and HFP (only HBD property), to investigate the aspect of H-bonding property of the polar solvent. Changes in the steady state fluorescence spectra of the pigment in DMSO-toluene and HFP-toluene solvent mixtures with increasing mole-fractions of the polar solvent (Figure 3.6) are similar to that observed in toluene-MeOH mixture. Corresponding fluorescence lifetime decays (Table 3.3) also shows similar behavior to that observed in toluene-MeOH mixture.

The *relative* changes of the photophysical parameters (fluorescence quantum yield, average fluorescence lifetime, radiative and non-radiative rates) of the pigment in toluene-MeOH and toluene-MeOH-d_4 mixtures with varying mole-fractions of the polar solvent are given in Figure

Table 3.3: Lifetime parameters of Curcumin in DMSO-toluene and HFP-toluene solvent mixtures

DMSO mole-fraction	τ_1 (ps)	a_1	τ_2 (ps)	a_2	τ_3 (ps)	a_3	τ_{av} (ps)
0.0007	134	0.82	301	0.18	0	0	164
0.0014	141	0.7	314	0.3	0	0	193
0.0029	142	0.56	312	0.44	0	0	217
0.0057	149	0.43	329	0.57	0	0	252
0.0114	141	0.26	342	0.74	0	0	290
0.0225	37	0.05	286	0.76	763	0.19	364
0.0441	38	0.04	320	0.73	862	0.23	433
0.0845	41	0.04	357	0.71	1303	0.25	581
0.1558	42	0.04	360	0.71	1201	0.25	558
0.2696	42	0.05	320	0.76	884	0.19	413
0.4247	44	0.07	266	0.77	571	0.16	299
HFP mole-fraction	**τ_1 (ps)**	**a_1**	**τ_2 (ps)**	**a_2**	**τ_3 (ps)**	**a_3**	**τ_{av} (ps)**
0.0005	122	0.83	324	0.17			141
0.0010	125	0.78	371	0.22			156
0.0019	122	0.67	387	0.33			179
0.0039	122	0.53	413	0.47			209
0.0077	128	0.38	446	0.62			259
0.0153	148	0.28	572	0.72			325
0.0301	169	0.23	592	0.77			453
0.0585	180	0.19	681	0.81			495
0.1105	145	0.11	690	0.89			586
0.1991	95	0.06	617	0.94			630
0.3320	65	0.05	476	0.95			586

3.7. For comparison, changes observed with toluene-$CHCl_3$ and toluene-MeCN was also plotted. The trends are clearly different for the alcoholic and non-alcoholic solvents. While the non-radiative rates pass through a minimum, the radiative rates remain more or less unchanged for the alcoholic solvents. Figure 3.7 further shows that the observed trends are different for MeOH

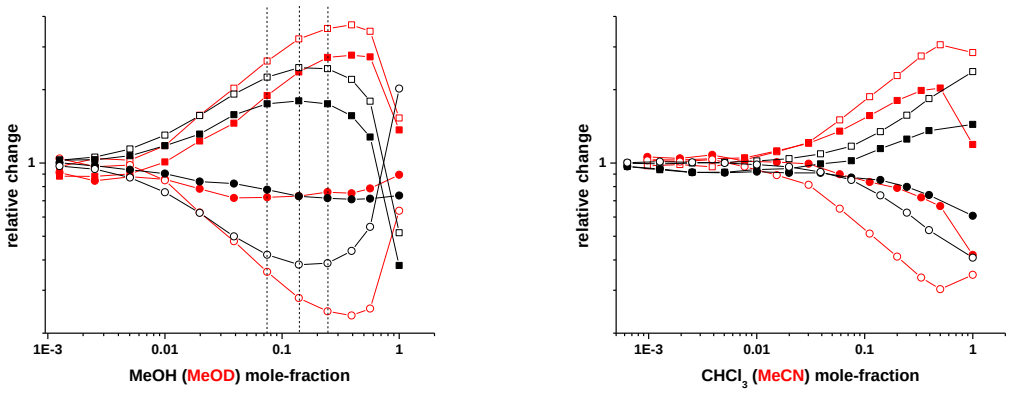

Figure 3.7*: Left: Relative changes in the emission quantum yield (solid squares), average lifetime (hollow squares), radiative (solid circles) & nonradiative (hollow circles) rates of Curcumin with increasing mole-fractions of MeOH (black) and MeOH-d_4 (red). The vertical dashed lines indicate alcohol mole-fractions where time dependent spectra were constructed. Right: Relative changes in the emission quantum yield (solid squares), average lifetime (hollow squares), radiative (solid circles) & nonradiative (hollow circles) rates of Curcumin with increasing mole-fractions of $CHCl_3$ (black) and MeCN (red). For clarity, the parameters were normalized with respect to that in toluene and the Y-axis is represented in the logarithmic scale.*

and MeOH-d_4. The maxima (or minima) of the photophysical parameters of the pigment shifts to a higher mole-fraction (0.40 compared to 0.14) when the deuterated solvent is used. Corresponding changes in the radiative and non-radiative rates of the pigment in the five toluene-

alcohol solvent mixtures with varying mole-fractions of the alcohol solvent are compared in Figure 3.8 (left panel). The radiative rates remain more or less unchanged while the changes in the non-radiative rates depend upon the alcohol used. As the alkyl chain length (of the alcohol) decreases the minima observed in the non-radiative rates starts to be more prominent. The variation in the radiative and non-radiative rates of the pigment in toluene-DMSO and toluene-HFP are similar to that observed in toluene-MeOH mixture (Figure 3.8, right panel).

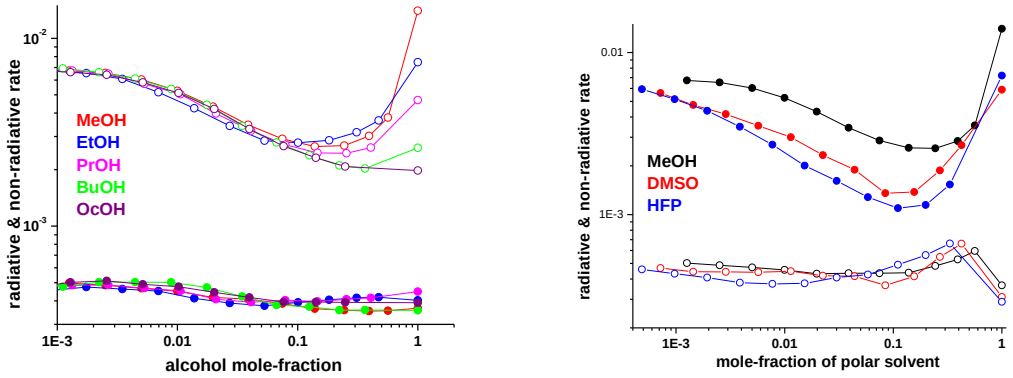

Figure 3.8*: Left: Changes in the radiative (solid circles) & nonradiative (hollow circles) rates of Curcumin with increasing mole-fractions of different alcohol solvents used in this study; Right: Changes in the radiative (solid circles) & nonradiative (hollow circles) rates of Curcumin with increasing mole-fractions of MeOH, DMSO and HFP. The radiative and nonradiative rates are scaled with a factor of* 10^{12}.

Using our TCSPC system we could observe distinct rise times when fluorescence decays were taken at the red edge of the emission spectrum (Figure 3.9) of the pigment, at certain MeOH (or MeOH-d_4) mole-fractions. For example, at MeOH mole-fraction of 0.04 no rise time is observed but increasing the mole-fraction to 0.07 results in the appearance of a ~140 ps rise time. *Further, the magnitude of the observed rise times depends upon the mole-fraction of MeOH*. As the

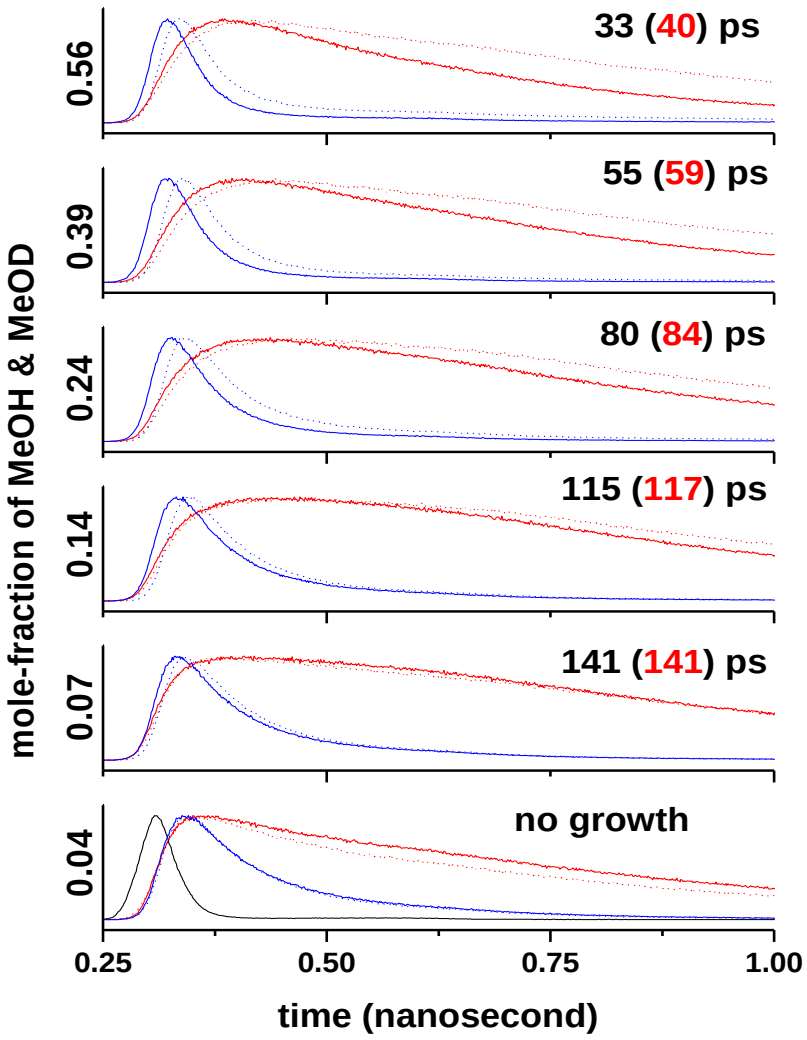

***Figure 3.9**: Fluorescence decays taken at the blue (blue line) and red (red line) edges of Curcumin fluorescence spectra at different MeOH (solid lines) and MeOH-d_4 (dotted lines) mole-fractions. The rise times obtained (black: MeOH; red: MeOH-d_4) are also shown against each mole-fraction. For comparison, the instrument response function is shown at the bottom panel.*

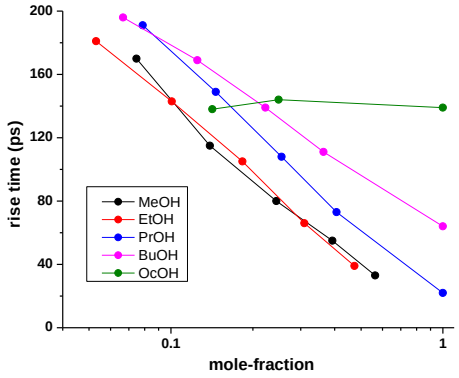

***Figure 3.10**: Variation of fluorescence rise times of Curcumin (taken at the red edge of the emission spectrum) with different alcohol mole-fractions.*

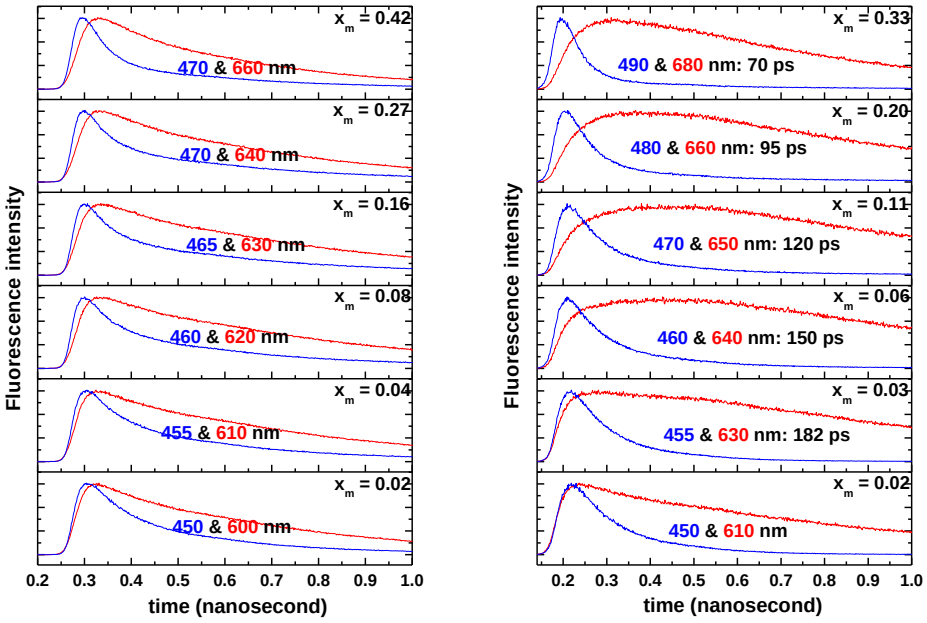

***Figure 3.11**: Fluorescence decays taken at the blue (blue line) and red (red line) edges of Curcumin fluorescence spectra at different DMSO (left) and HFP (right) mole-fractions (x_m). For comparison, the instrument response function is shown at the bottom graph in the left panel. The emission wavelengths and corresponding rise times were also shown.*

MeOH mole-fraction is increased, the magnitude of the rise time decreases and at 0.57 mole-fractions this becomes ~30 ps. Unlike photophysical parameters (Figure 3.7), the observed rise times did not show any significant isotope effect. When MeOH is replaced by $CHCl_3$ and MeCN no rise times could be observed suggesting that spectral relaxation is too fast to be detected by ~40 ps time resolution of our set up. When MeOH is replaced by other alcohols, distinct rise times could still be observed. Figure 3.10 shows the alcohol mole-fraction dependent rise times in different toluene-alcohol mixtures. The observed rise time decreases with increasing alcohol mole-fraction: this trend continues till 1-butanol, however for 1-octanol this trend disappears, the observed rise times are more or less similar. Figure 3.11 shows how the rise times depend upon the nature of the hydrogen bonding property (HBA or HBD) of the polar solvent. Red edge decays shows distinct rise times in the presence of HFP (only HBD) but not for DMSO (only HBA). The magnitude of the rise times in toluene-HFP mixture was also observed to depend upon the mole-fraction of HFP similar to that observed in the toluene-MeOH mixture.

In general, the signature of excited state solvation is manifested as a growth in the kinetics at the red edge of emission spectrum. The dynamics of solvation are quantified by the decay of the solvent response function C(t):

$$C(t) = \frac{\nu(t) - \nu(\infty)}{\nu(0) - \nu(\infty)}$$

Where ν(0), ν(t), and ν(∞) denote the peak frequency of the fluorescence spectra at time zero, t, and infinity respectively. The "zero time" emission spectrum has been approximated using the emission spectrum of Curcumin in a non polar solvent, n-hexane, according to an earlier method [40]. Determination of ν(∞)and ν(t) (peak frequencies of the steady-state and time resolved fluorescence spectra) were carried out according to an earlier method [41] using steady state emission spectrum and fitting parameters from wavelength resolved decay traces. Owing to the

limited time resolution of our setup we have constructed C(t) at three different alcohol mole-fraction of 0.07, 0.14 and 0.24, where the observed rise times are of the order of 100 ps. The decays of C(t) at these mole-fractions are shown in Figure 3.12. The decays can be satisfactorily

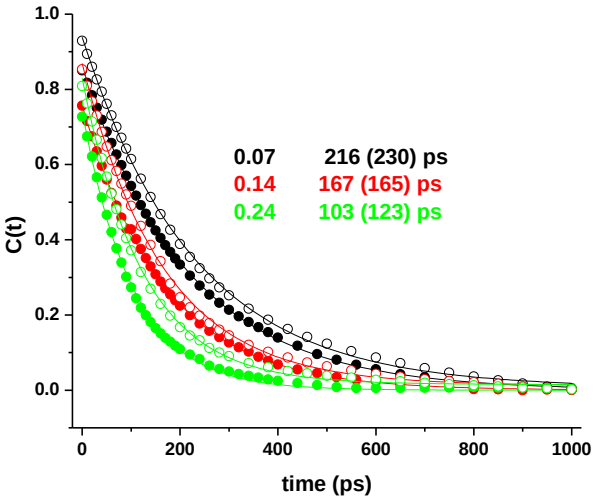

***Figure 3.12**: Decay of solvation response function C(t) at different MeOH (solid) and MeOH-d_4 (hollow) mole fractions (black: 0.07, red: 0.14 and green: 0.24). The raw data are given as points and the fits are given as lines. The time constants given in parenthesis correspond to those in MeOH-d_4.*

fitted with a single exponential function with solvation times ranging from 100-200 ps (~20-40 times slower that observed in neat MeOH or MeOH-d_4 [24-26]). *A ~three fold increase in alcohol mole-fraction results in a ~two fold decrease in solvation time.* It is important to note here that owing to our limited time resolution we are missing the initial (10-30%) solvation dynamics. Figure 3.13 shows the variation in solvation time constants for the various toluene-alcohol mixtures with varying alcohol mole fractions. Finally in Figure 3.14 the solvation time

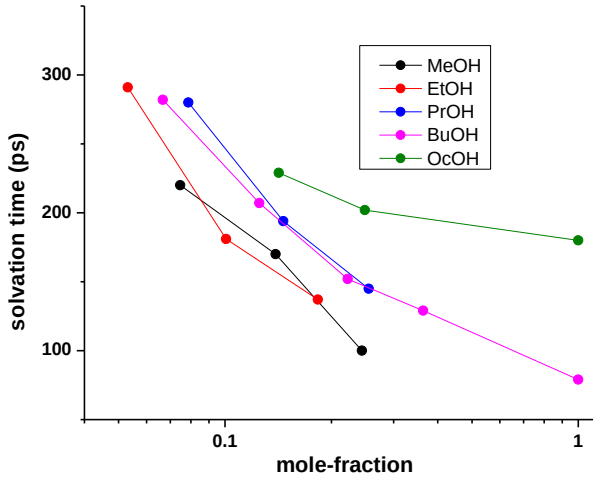

***Figure 3.13**: Variation of solvation time constants with different alcohol mole-fractions.*

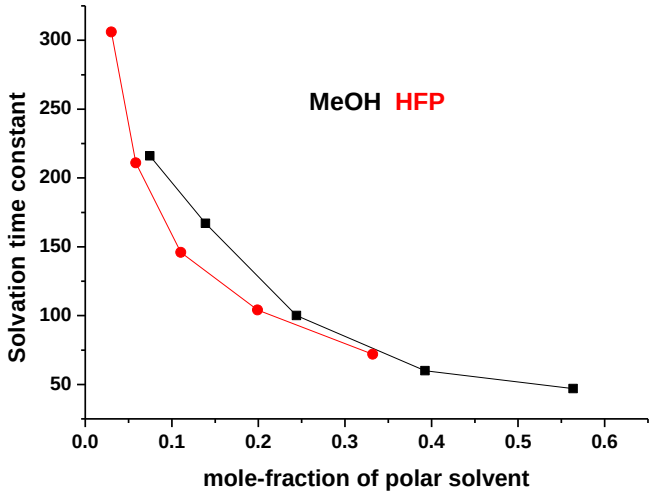

***Figure 3.14**: Variation of solvation time constants with different MeOH and HFP mole-fraction.*

constants for MeOH-toluene and HFP-toluene are plotted against the mole-fraction of the polar solvent. Corresponding solvation time constants with their respective amplitudes are shown in

Table 3.4. The observed curves show similar trends although the onset and offset of solvation time constants are different for MeOH and HFP.

Table 3.4: Solvation time constants and corresponding amplitudes of Curcumin in different MeOH & HFP mole-fractions[a]

MeOH mole-fraction	$\tau_{solvation}$ (ps) (amplitude)	HFP mole-fraction	$\tau_{solvation}$ (ps) (amplitude)
0.07	216 (0.86)	0.03	306 (0.82)
0.14	167 (0.76)	0.06	211(0.80)
0.24	100 (0.74)	0.11	146 (0.70)
0.40	60 (0.76)	0.20	104 (0.63)
0.56	47 (0.7)	0.33	72 (0.55)

[a]The errors in these values are estimated to be about ~10%

3.4. Discussion

As reported earlier [12-15], the absorption and the fluorescence spectra of Curcumin were observed to exhibit significant solvent effect. Compared to toluene, in all the polar solvents used in this study the vibronic structure in absorption and emission spectra are lost suggesting significant solute-solvent interaction in the ground and excited state (Figure 3.1). Although photo-excitation of Curcumin to the S_1 state leads to a large change in dipole moment, ($\Delta\mu \approx 6.1$ D) [12-15], the larger solvatochromic red shift observed in MeOH (and MeOH-d_4) has been explained by the effect of both polarity and hydrogen-bonding ability of the solvent on the excited state of Curcumin. The stokes shift of Curcumin in the neat alcohols (Table 3.1) increases with increasing polarity; this is due to the increasing red shift of the emission maxima. This behavior is consistent with the fact that the excited state is more polar and hence polar solvents will decrease its energy by solvation. The low quantum yield and the low lifetime of the

pigment in polar protic solvents have been attributed to radiation less decay channel associated with the fully solvated ESPT state of the pigment [12-15]. However it has been observed earlier that in polar solvents like acetonitrile or chloroform (whose ability to form H-bond is significantly lower than alcohol solvents like methanol) the quantum yield and lifetime of the pigment increases substantially [12-15]. This indicates that the photophysical properties of the pigment in polar solvents may depend critically on the intermolecular H-bonding properties of the polar solvent.

The fluorescence properties of the pigment in binary solvent mixtures containing MeOH or MeOH-d_4 are significantly different than mixtures containing $CHCl_3$ or MeCN (Figure 3.7) which arises primarily due to the modulation of the non-radiative rates of the pigment. Compared to $CHCl_3$ and MeCN, intermolecular H(D)-bonding is expected to be stronger in MeOH (MeOH-d_4). Since the ESPT process in Curcumin has been predicted to be non-radiative in nature, the significant changes observed in the non-radiative rates shows that excited state *intermolecular* H-bonding between the pigment and the polar protic solvent MeOH (or MeOH-d_4) is significantly perturbed in the presence of toluene. Comparing the Kamlet-Taft parameters of the polar solvents (Table 3.1) it can be argued that *both* H(D)-bond accepting and H(D)-bond donating properties are responsible for this behavior. In neat MeOH (or MeOH-d_4), this intermolecular H(D) bond is likely to involve one Curcumin molecule with "several" MeOH (or MeOH-d_4) molecules consisting of a H(D) bonding network. A simplified picture involving only two solvent molecules is shown in Scheme 3.1. The decay of the excited state is expected to depend upon the "strength" of this network. In the Kamlet-Taft scale, the polarity of toluene is comparable to methanol but its H-bonding ability (both donating and accepting) are much lesser (Table 3.1). Therefore we propose that the observed fluorescence properties of Curcumin in

toluene-alcohol mixtures (which also show a significant isotope effect) depend upon the modulation of the intermolecular H(D) bonding network (between MeOH or MeOH-d_4 molecules) by toluene. In order to further investigate the aspect of H-bonding on the spectral relaxation, we have chosen solvents which have *only* HBA or HBD property (DMSO and HFP respectively). It is pertinent to have a close look at Figure 3.6 which reveals that evolution of the spectral shape is significantly different for DMSO and HFP. The vibrational features are more prominent in HFP and less prominent in DMSO suggesting that intermolecular H-bonding is stronger in HBA solvent DMSO. It is therefore relevant to examine the intermolecular H-bonding (IHB) positions in the pigment. There are four positions, two each for the phenolic OH group and one each for the keto and the enol group (Scheme 3.2). Solvents which have only

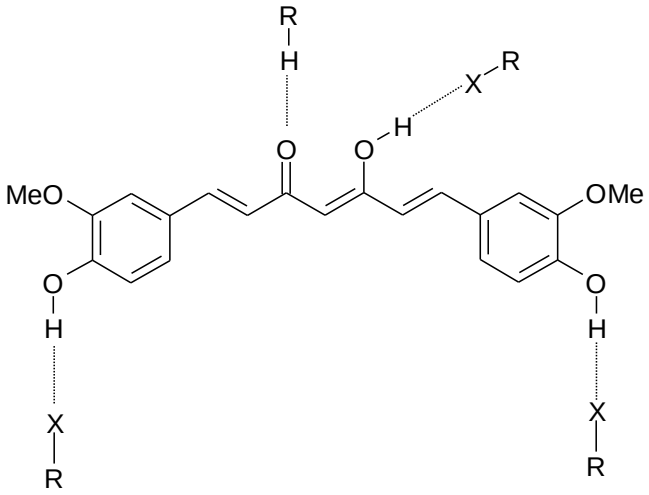

Scheme 3.2*: Likely structures of Curcumin in polar H-bonding solvents showing the intra-molecular and inter-molecular hydrogen bonds. RX (or RH) denotes solvents having only H-bond accepting (or H-bond donating) property.*

HBA property (DMSO) is likely to form IHB with the phenolic OH and the enol groups and solvents which have only HBD property (HFP) is likely to form IHB with the keto group while

alcohol solvents which have both HBA and HBD property is likely to form IHB with all the four groups.

In an earlier study it was observed that the hydrogen belonging to the keto-enol group is the most acidic in the ground state of the pigment [42]. Later, it was shown that luminescence of Curcumin in methanol and ethanol is severely affected by acetate, a mild base, due to ESPT [29-30]. This arises because the pigment becomes a much stronger acid in the excited state, and the proton transfer was shown to involve both phenolic and keto-enolic hydrogens. Therefore it is logical to assume that IHB interactions involving the polar solvent and the phenol and keto-enol part of the pigment, which are stronger in the excited state plays a significant role in the solvation dynamics.

In addition to ESPT, solvation is another major photophysical process of the pigment in the excited state [24-25, 26, 29-30]. The average solvation time of Curcumin in neat methanol was earlier observed to be ~4-7 ps [24-26]. The slow rise times (and consequently slow solvation times) of the pigment observed *only* in toluene-alcohol and toluene-HFP mixture and their dependence on alcohol/HFP mole-fraction (Figures 3.9-3.12) implies that specific H-bonding interactions between excited Curcumin and alcohol/HFP is getting affected in the presence of toluene. The role of toluene thus seems to be critical in controlling the *strength and reorganization of the H-bonding network between the pigment and the H-bonding solvent in the excited state.* It is pertinent to note at this point that the vibronic features in the absorption spectra of Curcumin start to smear out at MeOH mole-fractions of 0.4 and above (data not shown). However, the emission spectrum (Figure 3.2) starts to lose the vibronic features much earlier (0.02 for MeOH). This indicates that specific H bonding interaction between Curcumin and the polar H bonding solvent cannot be ruled out in the ground state, but is definitely stronger

in the excited state. The driving force behind this is obviously the electron localization around the keto and enolic oxygen (due to a large change in the dipole moment) of the pigment after photo excitation. However, another important factor is the *local concentration* of the polar H-bonding solvent around the solute which will depend on its mole-fraction. This, in turn, is expected to affect events like:

i) breakage of the intra molecular H bond

ii) formation of the inter molecular H bond with the alcohol solvent, and

iii) solvation of the excited state

in addition to other events after photoexcitation of the pigment. Based upon the results obtained so far the likely sequence of events after photoexcitation of the pigment can be summarized as follows: photoexcitation of Curcumin leads to formation of species I (Scheme 3.3) which is the

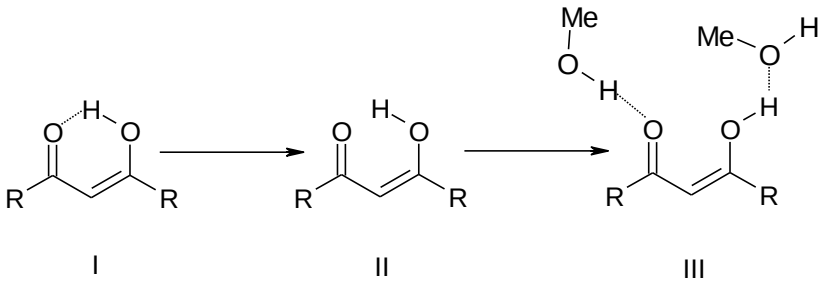

Scheme 3.3*: Likely structures of Curcumin excited state in toluene-polar H-bonding solvent mixtures. For simplicity only the keto-enol part of the molecule is shown and the rest is depicted as R. MeOH is taken as a representative of a polar H-bonding solvent.*

six membered H bonded chelate ring of the cis-enol form (a majority in the ground state as suggested by the ground state absorption spectrum). Species I gets converted into species II in which the intramolecular H bond is broken and its energy decreases continuously (by solvent reorganization as well as intermolecular H bond formation) and finally gets converted into

species III where intermolecular H bond reorganization between the pigment and alcohol solvent have been optimized. It is important to note that the probability of species I & II decaying directly to the ground state can not be ruled out.

Solvation dynamics experiments show that with increasing alcohol mole-fraction the solvation time of the pigment decreases. This is expected because with increasing alcohol mole-fraction, the local concentration of the protic solvent around the pigment will also increase resulting in faster H-bond reorganization and dipolar solvation. This trend however is not observed in the case of toluene-OcOH mixture where the observed fluorescence rise times and solvation times are more or less similar. Although the polarity and H-bond donating ability (α) of OcOH are smaller, its H-bond accepting ability (β) is certainly comparable with the other alcohols, being significantly higher than MeOH. It is therefore difficult to ascertain the individual effects of polarity, H bond donating and H bond accepting property on the excited state spectra relaxation of the pigment from the present study. It is important at this point to consider another property of the solvent, viscosity, which is expected to influence the relaxation process. It is known that the diffusive component of the solvation depends on the shear viscosity of the solvent. For example, a ~6 times increase in the viscosity results in a ~20 times increase of the average solvation time of Coumarin-153 using MeOH and 1-pentanol as the solvent. It is therefore likely that the observed relaxation of the pigment in the various toluene-alcohol mixtures will be affected by the viscosity of the alcohol solvents, especially in OcOH, whose viscosity are ~14 times higher than MeOH.

It is interesting to note that no significant isotope effect was observed in the spectral relaxation, except that observed in the fluorescence properties (Figure 3.7) with changing solvent composition.

Since no spectral relaxation of the pigment in toluene-DMSO mixture could be observed (with 40 ps time resolution) it can be speculated that interaction between the acidic hydrogens of Curcumin and the HBA solvent DMSO is much stronger in the excited state. It is important to note that there is an isosbestic point observed in the absorption spectra of the pigment in toluene-DMSO mixture suggesting the presence of two species. However attempts to resolve the spectral signatures of the individual species (by exciting at the blue and red edge of the absorption spectra) produced similar fluorescence properties, in addition, no rise times were observed when decays are monitored at the red edge of the fluorescence spectra. These results suggests that interconversion between the two species is faster than the time resolution used in this study.

However, when the solvent has only HBD property (in this case, HFP), the most likely place for IHB involves the keto group of the pigment which is likely to acquire sufficient electron charge after photo-excitation. The observation of slow solvation dynamics in toluene-HFP mixture suggests that this process is slower, the formation and reorganization of the H-bond along with redistribution of HFP molecules occurs in hundreds of picoseconds. The observed slow spectral relaxation in tolune-MeOH can, then, be interpreted as formation of IHB between the keto oxygen and MeOH which becomes the rate limiting step. It may be noted that ultrafast experiments showed that average solvation time of the pigment is faster in neat DMSO (~2 ps) than in neat MeOH (~7 ps). This together with the fact that emission spectra of the pigment at similar DMSO or HFP mole-fractions shows least vibrational structure for DMSO suggests that IHB between the acidic hydrogens of the pigment and DMSO is stronger, and hence the relaxation is also expected to be faster.

3.5. Conclusion

In conclusion, the results reported here shows that ESHT reactions of Curcumin excited state in binary solvent mixtures of toluene-polar solvent depends critically upon the H-bonding property of the polar solvent. This is attributed to the modulation of the non-radiative rates associated with the excited state intermolecular H bonding between the pigment and the polar protic solvent. As a consequence the solvation times of the pigment in the binary mixture were observed to slow down significantly at certain polar solvent mole-fractions. The observed results are rationalized with a scheme where ground state of the pigment exists in free and H-bonded (intermolecular) state. Optical excitation results in a mixture of these species in the excited state and the observed spectral relaxation correspond to the conversion of these two species in to a third species where dipolar solvation and intermolecular H-bonding have been optimized. The spectral relaxation, due to dipolar solvation and IHB reorganization, also depends critically on the H-bonding property of the polar solvent. Polar solvents having either HBD or both HBA and HBD were able to cause the spectral relaxation of the pigment in the binary mixture significantly slower. The observed results indicate that the rate limiting step in the excited state dynamics of the pigment in toluene-polar solvent mixtures might be the formation and reorganization of the intermolecular H-bonding between the keto group of the pigment and the H-bond donating property of the polar solvent.

3.6. References

[1] B.B. Aggarwal, C. Sundaram, N. Malini, H. Ichikawa, In: B.B. Aggarwal, Y.J. Surth, (Eds.), Molecular Targets and Therapeutic uses of curcumin in health and disease, Springer, New York, 2007.

[2] A.J. Ruby, G. Kuttan, K.D. Babu, K.N. Rajasekharan, R. Kuttan, Cancer Lett. 94 (1995) 79.

[3] R.C. Lantz, G.J. Chen, A.M. Solyom, S.D. Jolad, B. N. Timmermann, Phytomedicine 12 (2005) 445.

[4] B.B. Aggarwal, A. Kumar, A.C. Bharti, Anticancer Res. 23 (2003) 363.

[5] A. Goel, A.B. Kannumakkara, B.B. Aggarwal, Biochem. Pharamacol. 75 (2008) 787.

[6] M. Shi, Q. Cai, L. Yao, Y. Mao, Y. Ming, G. Ouyang, Cell Biol. Int. 30 (2006) 221.

[7] Y. Surh, J. Food Chem. Toxicol. 40 (2002) 1091.

[8] H. Hatcher, R. Planalp, J. Cho, F.M. Torti, S.V. Torti, Cell. Mol. Life Sci. 65 (2008) 1631.

[9] S.V. Jovanovic, S. Steenken, C.W. Boone, M.G. Simic, J. Am. Chem. Soc. 121 (1999) 9677.

[10] R.A. Sharma, A.J. Gescher, W.P. Steward, Eur. J. Cancer 41 (2005) 1955.

[11] A.A. Gorman, I. Hamblett, V.S. Srinivasan, P.D. Wood, Photochem. Photobiol. 59 (1994) 389.

[12] K.I. Priyadarsini, Free Rad. Chem. Biol. 23 (1997) 838.

[13] S.M. Khopde, K.I. Priyadarsini, D.K. Palit, T. Mukherjee, Photochem. Photobiol. 72 (2000) 625.

[14] K.I. Priyadarsini, D.K. Maity, G.H. Naik, M.S. Kumar, M.K. Unnikrishnan, J.G. Satav, H. Mohan, Free Rad. Biol. Med. 35 (2003) 475.

[15] K.I. Priyadarsini, J. Photochem. Photobiol. C. 10 (2009) 81.

[16] L. Nardo, R. Paderno, A. Andreoni, M. Masson, T. Haukvik, H.H. Tonnesen, Spectroscopy 22 (2008) 187.

[17] L. Nardo, A. Andreoni, M. Bondani, M. Masson, H.H. Tonnesen, J. Photochem. Photobiol. B: Biol. 97 (2009) 77.

[18] M. Caselli, E. Ferrari, C. Imbriano, F. Pignedoli, M. Saladini, G.J. Ponterini, Photochem. Photobiol. A: Chem. 210 (2010) 115.

[19] A. Mukerjee, T.J. Sørensen, A.P. Ranjan, S. Raut, I. Gryczynski, J.K. Vishwanatha, Z. Gryczynski, J. Phys. Chem. B 114 (2010) 12679.

[20] A. Pe´rez-Lara, A. Ausili, F.J. Aranda, A. Godos, A. Torrecillas, S.C. Garcı´a, J.C. Go´mez-Ferna´ndez, J. Phys. Chem. B 114 (2010) 9778.

[21] M.H.M. Leung, H. Colangelo, T.W. Kee, Langmuir 24 (2008) 5672.

[22] M.H.M. Leung, T.W. Kee, Langmuir 25 (2009) 5773.

[23] Z. Wang, M.H.M. Leung, T.W. Kee, D.S. English, Langmuir 26 (2010) 5520.

[24] R. Adhikary, P. Mukherjee, T.W. Kee, J.W. Petrich, J. Phys. Chem. B 113 (2009) 5255.

[25] R. Adhikary, P.J. Carlson, T.W. Kee, J.W. Petrich, J. Phys. Chem. B 114 (2010) 2997.

[26] R. Ghosh, J.A. Mondal, D.K. Palit, J. Phys. Chem. B 114 (2010) 12129.

[27] D. Ke, X. Wang, Q. Yang, Y. Niu, S. Chai, Z. Chen, X. An, W. Shen, Langmuir 27 (2011) 14112.

[28] C. Ghatak, V.G. Rao, S. Mandal, S. Ghosh, N. Sarkar, J. Phys. Chem. B 116 (2012) 3369.

[29] Y. Erez, I. Presiado, R. Gepshtein, D. Huppert, J. Phys. Chem. A 115 (2011) 10962.

[30] Y. Erez, I. Presiado, R. Gepshtein, D. Huppert, J. Phys. Chem. A 116 (2012) 2039.

[31] T. Elsaesser, In: J. Manz, L. Wo¨ste (Eds.), Femtosecond Chemistry, VCH-Verlag, Weinheim, Germany, 2 (1995) pp 563.

[32] B.J. Schwartz, L.A. Peteanu, C.B. Harris, J. Phys. Chem. 96 (1992) 3591.

[33] Th. Arthen-Engeland, T. Bultmann, N.P. Ernsting, M.A. Rodriguez, W. Thiel, Chem. Phys. 163 (1992) 43.

[34] S. Lochbrunner, A.J. Wurzer, E. Riedle, J. Phys. Chem. A 107 (2003) 10580.

[35] S. Lochbrunner, A. Szeghalmi, K. Stock, M. Schmitt, J. Chem. Phys. 122 (2005) 244315.

[36] S. Takeuchi, T. Tahara, Proc. Natl. Acad. Sci. 104 (2007) 5285.

[37] A.S.R. Koti, M.M.G. Krishna, N. Periasamy, J. Phys. Chem. A 105 (2001) 1767.

[38] A. S. R. Koti, N. Periasamy, J. Chem. Phys., 115 (2001) 7094.

[39] L. Peret-Almeida, A.P.F. Cherubino, R.J. Alves, L. Dufosse, M.B.A. Gloria, Food Research International 38 (2005) 1039.

[40] R.S. Fee, M. Maroncelli, Chem. Phys. 183 (1994) 235.

[41] M. Maroncelli, G.R. Fleming, J. Chem. Phys. 86 (1987) 6221.

[42] M. Bernabe-Pineda, M.T. Ramirez-Silva, M. Romero-Romo, E. Gonzalez-Vergara, A. Rojas-Hernandez, Spectrochim. Acta Part A 60 (2004) 1091.

[43] C. Reichardt, Chem. Rev. 94 (1994) 2319.

Chapter – 4

Diffusion of Chlorin p_6 across phosphatidyl choline liposome bilayer probed by second harmonic generation

4.1. Introduction

Chlorin p_6 (Cp_6), a porphyrin based photosensitizer (Scheme 4.1) has three ionizable carboxylic acid side chains whose protonation and deprotonation plays an important role in controlling the hydrophobic and hydrophilic species of the drug at different pH [1]. It has been previously shown that a change in pH from physiological to acidic results in formation of Cp_6 species with less charge and higher lipophilicity due to protonation of the carboxylic side chains [1]. Cp_6 has three ionizable carboxylic acid groups and consequently neutral and several ionic forms (A-D, Scheme 4.1) of Cp_6 generated by acid-base equilibrium are expected to be present in the pH range 3-8 as shown in Scheme 4.1. This property is believed to play an important role in the higher uptake of Cp_6 in tumors where extra-cellular pH can be slightly acidic [2-4]. Indeed it has been observed that lowering the pH of the medium from physiological to slightly acidic leads to an increase in the cellular uptake of Cp_6 in certain cancer cells [5]. It has also been demonstrated that the binding of Cp_6 to lipid bilayer depends on the pH of the medium [6]. Thus, knowledge of the factors governing the dynamics of the diffusion of Cp_6 across membranes may be useful for a better understanding of the cellular uptake of the drug.

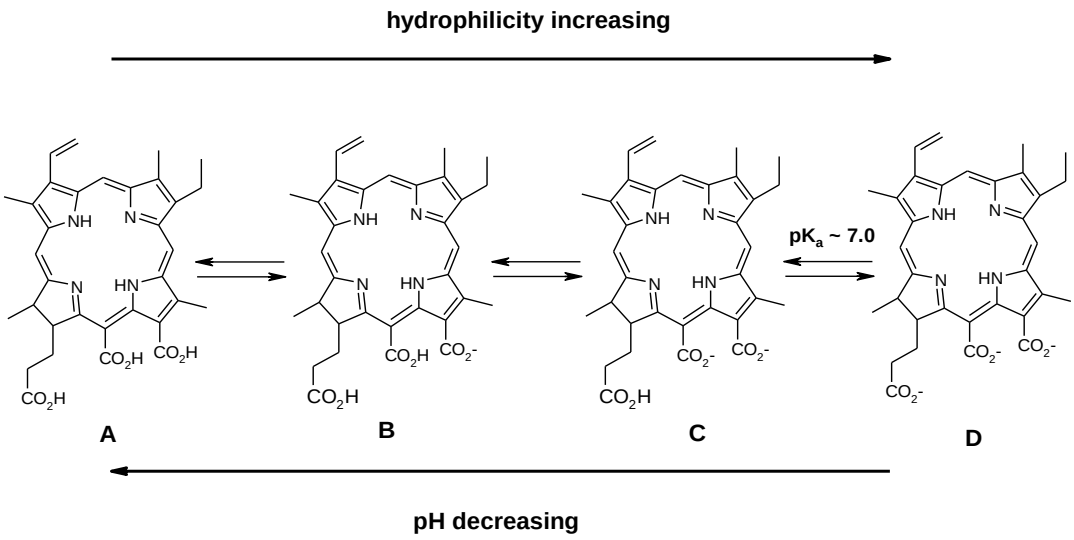

Scheme 4.1: *Different structures of Chlorin p_6 present in the pH range of 3-8*

To study the adsorption and transport of molecules across the lipid bilayers a variety of methods like NMR [7-11], EPR [12], absorption [13-14] and fluorescence spectroscopy [15-23] have been used. For example, by use of fluorescence spectroscopy it could be shown that where the diffusion of deuteroporphyrin, (a dicarboxylic porphyrin) is rapid [19-21] a disulfonated phthalocyanine is retained in the outer monolayer only [22]. Recently, the membrane diffusion properties of different chlorin derivatives were also monitored by ^{1}H NMR spectroscopy [11]. However NMR investigation of kinetics is restricted to observation of slow processes (100s of hours) only and the amount of drug used for these studies were a concern. It is pertinent to note that the success of these spectroscopic techniques requires that the molecules adsorbed on the surface of the liposomes should show different signature than those in bulk solution.

The adsorption and transport kinetics of dye molecules and ions across a lipid bilayer can also be monitored by the second harmonic generation (SHG) technique [24-30]. It is important to note here that for the adsorption and subsequent diffusion across a negatively charged lipid bilayer, it is necessary that molecule should have some net positive charge. Therefore diffusion

of Malachite green (MG), a positively charged organic dye which could easily get adsorbed on negatively charged liposomes could be monitored by the SH signal generated [25-30]. When the molecule of interest and liposome have similar charge, adsorption and subsequently transport across the lipid bilayer is more difficult. However, if by changing some external stimuli, like pH, the lipophilic character of the molecule are enhanced it is expected to bind to the liposome irrespective of the charge and then the transport process may be measured by the SHG method. We have therefore explored the use of the SHG method to investigate the transport of the drug Cp_6 across liposomes made from egg lecithin at different pH. Further, the effect of temperature and cholesterol in this diffusion process has also been investigated.

4.2. Materials and Methods

Cp_6 was prepared and purified according to the procedure described in reference [1]. The presence of an absorption band at ~400 nm [1], which is in resonance with the second-harmonic frequency of the fundamental laser input (800 nm) leads to a resonance enhancement of the SH signal. POPC (the major phospholipid present in Egg lecithin) from dried egg yolk (Sigma; Product No. P-5394) and cholesterol (Titan Biotech, India; Product No. 305) were used as received. Unilamellar liposomes with and without 50 mol % cholesterol were prepared by the method described in reference [31]. Liposomes were prepared in 100 mM buffer solutions having pH values 3, 4, 5, 6 and 7.4. For acidic pH (3, 4 and 5) solutions sodium citrate buffer was used and for other pH phosphate buffer was used. The size and the zeta potential of the liposomes were measured by a Brookhaven Instrument (90 Plus size and zeta potential analyzer). The average size and the zeta potential of the prepared liposomes are given in Table 4.1.

Table 4.1: Size & Zeta potential of PC liposomes

pH	Effective Diameter	Polydispersity	Zeta potential
7.4	102 ± 20 nm	0.22 ± 0.02	-45.7 mV
6.0	90 ± 18 nm	0.23 ± 0.02	-36.0 mV
5.0	83 ± 15 nm	0.25 ± 0.03	-28.0 mV
4.0	95 ± 25 nm	0.27 ± 0.02	-21.5 mV
3.0	87 ± 19 nm	0.28 ± 0.03	-16.0 mV

For HRS and SH experiments the laser wavelength was centered at 800 nm and the average laser power was 500 mW. For HRS and SH experiments signal was averaged for two and one seconds respectively. We have observed that at neutral pH (where Cp_6 exists as monomer) the HRS signal of 10 μM Cp_6 is measurable with our experimental conditions.

Therefore, for HRS measurements, the concentration of Cp_6 was kept at 10 μM and the signal was corrected from the HRS response of the buffer and the changes in absorption of Cp_6 at 400 nm due to a change in the pH. It is important to mention here that Cp_6 does not fluoresce at 400 nm [1]. The sample in the cuvette was constantly stirred during the measurement using a magnetic stirrer. Sample temperature was controlled by a Neslab circulating water chiller. SH experiments were done as follows: First the signal from 2 mL of buffer was recorded followed by addition of 3μM Cp_6 (unless otherwise specified) and finally 50 μL (0.2 mM) of liposome solution was added. The SH signal from the 3μM Cp_6 solution alone, (which arises due to the HRS of water and Cp_6) is insignificant and the signal on addition of 50 μL of liposome to 2 mL of buffer also was not significant. The final ratio of Cp_6: lipid was 0.6. The SH signal were fitted exponentially to extract the decay constants.

4.3. Results

Figure 4.1 shows the absorption spectra of Cp_6 at different pH, (7.4, 5.0 and 3.0) in the presence and in the absence of egg-PC liposomes. The absorption spectra of Cp_6 exhibit a strong Soret band near 400 nm and a weaker Q band between 600 and 700 nm, which is similar to other porphyrin derivatives [32-33]. On decreasing the pH the Soret band undergoes a red shift from 401 nm at pH 7.4 to 407 nm at pH 3.0. A broadening in the Q band, accompanied by the development of a new band around 674 nm is observed. This band becomes most prominent at pH 3.0. At this pH, the absorption spectra show two prominent peaks at 640 and 675 nm. These results are consistent with previous studies [1,6]. Addition of egg-PC liposome at pH 5.0 and 3.0 increases the intensity of the soret band significantly and the broad Q band becomes a single band at 672 nm. In comparison, the effect of addition of liposome at pH 7.4 on the absorption spectra of the drug is insignificant.

The pK_a of inter-conversion between two the anionic forms C and D (Scheme I) of the drug has been estimated to be around pH ~7.0 by fluorescence measurements [1]. However the determination of the other pK_a values of the carboxylic groups is difficult by fluorescence measurements as aggregation of drug occurs at acidic pH and consequently the fluorescence intensity decreases significantly. It is interesting to note that the aggregates of Cp_6 formed at pH 3.0 are shown to be noncentrosymmetric in nature [34]. Since we have observed a measurable HRS signal from 10 μM Cp_6 at pH 7.4, it might be possible to monitor the pH dependent aggregation of Cp_6 by hyper-Rayleigh scattering (HRS) method [35]. HRS is a technique that has been used to monitor the aggregation processes of organic molecules in solution [37].

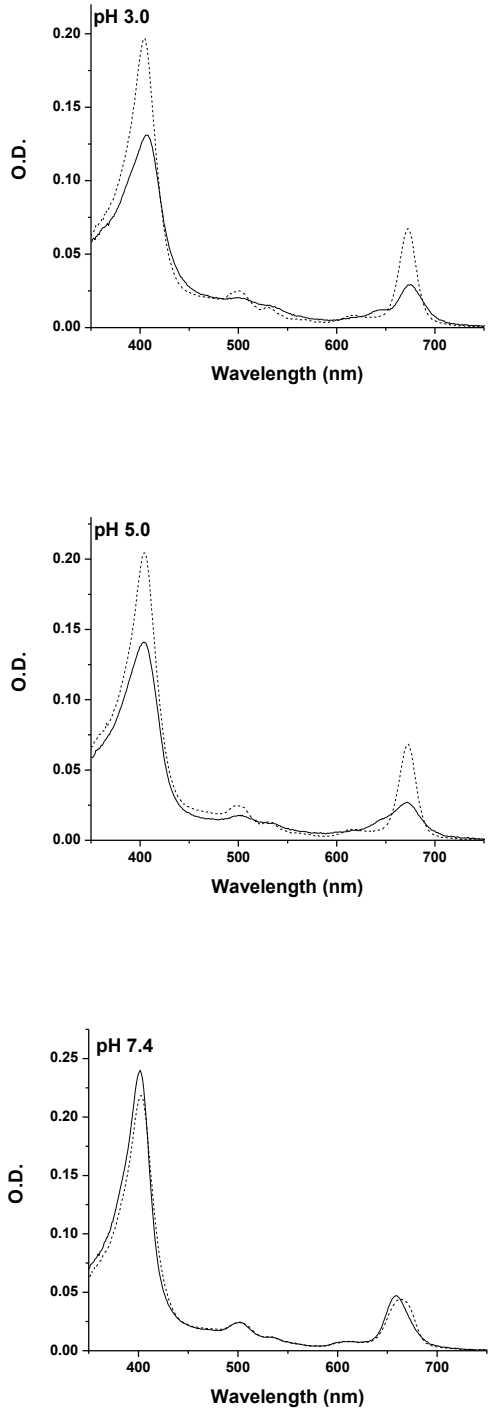

Figure 4.1: *Absorption spectra of 3 μM Cp_6 at pH 3.0 (top), at pH 5.0 (middle) and at pH 7.4 (bottom) in the absence (solid line) and presence (dashed line) of PC liposomes.*

The change in the HRS intensity of Cp_6 with pH is shown in Figure 4.2. The HRS intensity [36] increases with decrease in pH and this is attributed to the formation of non centrosymmetric aggregates of Cp_6. The sigmoidal increase of the HRS intensity has a point of inflection at a pH value of 4.8 ± 0.4.

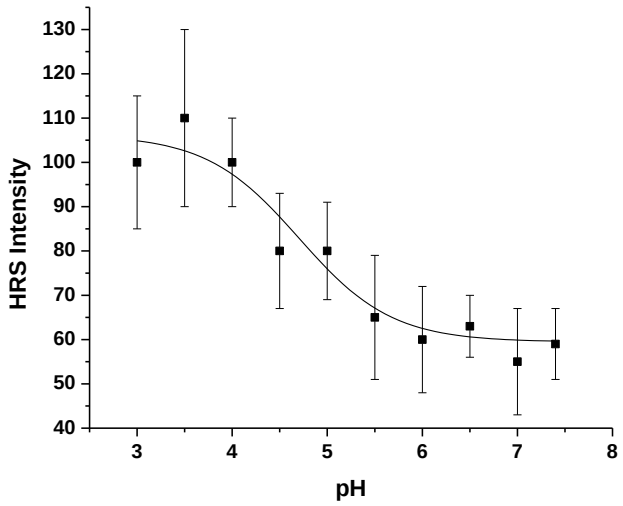

Figure 4.2: *HRS intensity of 10 μM Cp$_6$ at different pH. The inflexion point is at 4.8 ± 0.4.*

Figure 4.3 shows the time profiles of the second harmonic (SH) signals obtained on irradiation of a buffer solution containing Cp_6 and egg-PC liposomes at different pH using 800 nm femtosecond laser. No significant SH signal was observed from buffer alone as well as buffer containing Cp_6 (3 μM). On addition of 50 μL of egg-PC liposome (drug:lipid ratio 0.6) the intensity of the SH signal increased considerably for lower pH values. The initial increase in the SH signal (which corresponds to the adsorption of the drug to the outer lipid bilayer [25]) is completed within the time resolution of our experiment (~ 1s). Subsequently, the intensity of the SH signal decreased with increasing time and for time greater than 500s it was comparable to the

SH intensity obtained before addition of the liposomes. The maximum rise in the intensity of the SH signal (on addition of liposomes to the Cp_6 solution) occurred for a pH range of 3-5. For pH

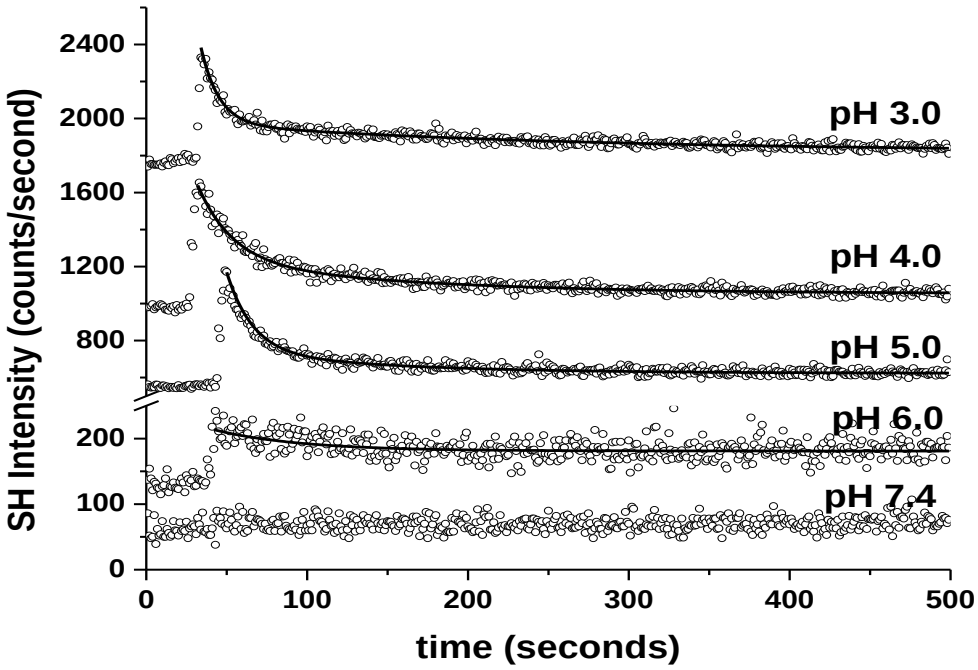

Figure 4.3: *Decay curves at different pH of SHG signal upon addition of PC liposome solution (50 μL in 2 mL) into 3 μM Cp_6 solution. The curves are shifted vertically for clarity.*

6, the increase in the intensity of the SH signal on addition of egg-PC liposome was significantly lower and at physiological pH it was almost negligible. The decay curves at pH 3, 4, 5 and 6 were fitted exponentially and the time constants obtained are listed in Table 4.2. At lower pH, the decay of SH intensity could be fitted satisfactorily to a bi-exponential function. The faster time constant were observed to be around tens of seconds. Its value was relatively constant for pH 3, 4 and 5 (11, 19 and 17 seconds respectively) but increased to ~ 50s for pH 6. For pH 3, 4 and 5, in addition to the fast component of 10-20 second the SH decay had a slower component

whose relative contribution was higher than the faster component. The time constant for this slower component were observed to be of the order of hundreds of seconds (Table 4.2). At pH 6.0 the signal level does not decay to baseline during the 500 second time window and thus the relative contribution of the slower time constant could not be ascertained.

The transport of Cp_6 is also expected to depend upon the fluidity of the lipid bilayer which in turn depends upon the amount of cholesterol present in the bilayer and/or the temperature of the system. Therefore we have investigated the dependence of SHG signal on temperature and on the cholesterol content in egg-PC liposomes. Figures 4.4 shows the measured changes in the SH intensity upon addition of egg-PC liposomes as a function of temperature and cholesterol content at pH 3, 4 and 5.0. For other pH (6 and 7.4) the SH signal was too low to be analyzed with the present setup.

It was observed that at room temperature, addition of 50 mol % cholesterol increases both the time constants for the slower and faster decay of Cp_6 by a factor of 2 to 3 at pH 3 and 4 (Figure 4.4). In addition, the relative contribution of the faster decay increases two-fold at pH 3. For pH 5 although the time constant of the faster decay increases by a factor of 2, the time constant for the slower decay remains more or less unchanged but its relative amplitude increases. A decrease in the temperature from 25^0 to 3^0C, causes the decay of the SH signal at pH 3 and 4 to be considerably slower. However at pH 5, the lowering of temperature results, an instantaneous rise which is then followed by a further slower rise followed by a slow decay of the SH signal (Figure 4.4). In order to estimate the time constants from the decay of the SH signal, it was recorded in a longer (1000s) time window. The SH signal could be fitted with a rise time of ~30s followed by a bi-exponential decay of ~180s and a long component whose time constant can not be correctly estimated at this time window.

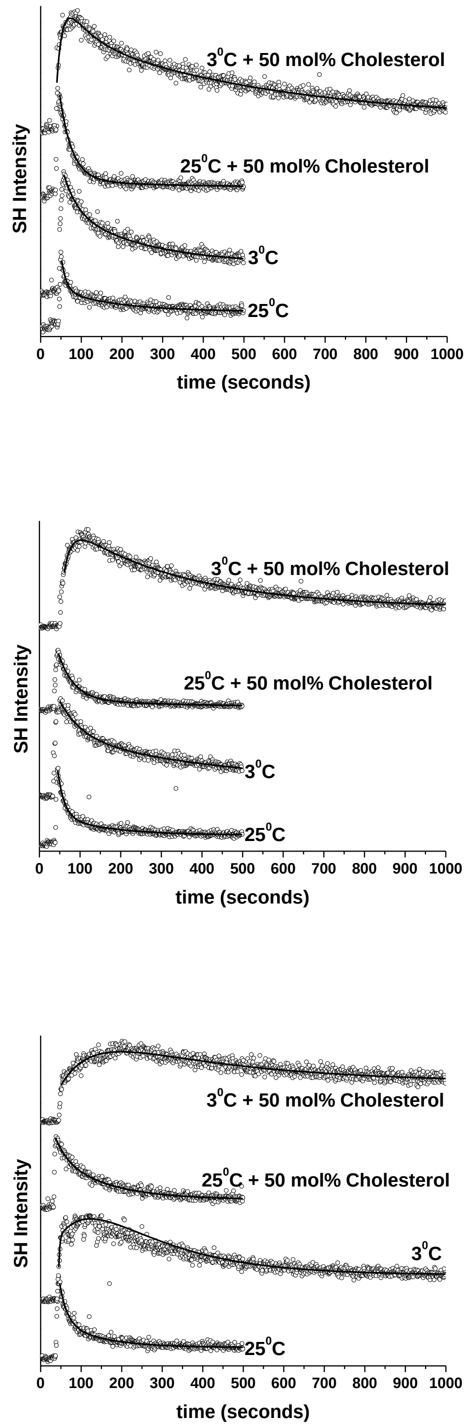

Figure 4.4: *Decay curves at room and low temperature (with and without cholesterol) of SHG signal at pH 3.0 (top), pH 4.0 (middle) and at pH 5 (Bottom). The curves are shifted vertically for clarity.*

In addition to the instantaneous rise and decay, the SH time profiles of cholesterol containing egg-PC liposomes measured at 3^0C shows the appearance of a growth at pH 3.0-5.0. All the decays are recorded at a 1000s time window to estimate the time constants as accurately as possible. While the risetime observed at pH 3 & 4 is of the order of tens of seconds, at pH 5 this increases to ~90s. In addition, the decay times also increases considerably, being multi-exponential in nature. Especially for pH 5 even at 1000s time window the accurate estimation of the slowest decay component is not possible. The details of the time constants along with their respective contributions are listed in Table 4.2.

Table 4.2: Diffusion time (in seconds) of Chlorin p_6 across PC lipid bilayer under various conditions[a]

25^0 C	**25^0 C + 50 mol% Cholesterol**	**3^0C**	**3^0 C + 50 mol% Cholesterol**
pH 3			
11 ± 1 (30%), 90 ± 8	30 ± 5 (60%), 250 ± 40	30 ± 5 (10%), 190 ± 40	10 ± 2 (growth), 55 ± 5 (38%), 500 (62%)[b]
pH 4			
19 ± 3 (25%), 120 ± 20	39 ± 7 (34%), 250 ± 30	55 ± 8 (9%), 300 ± 40	20 ± 5 (growth), 430 ± 40[b]
pH 5			
17 ± 4 (30%), 110 ± 11	29 ± 5 (10%), 130 ± 30	30 ± 10 (growth), 184, ∞[b]	90 ± 20(growth), 350, ∞[b]
pH 6			
50 ± 10	--	--	--

[a]The error bars represent standard deviation obtained from three different experiments. All time constants are in seconds. The values in parenthesis denote the pre-exponential factors.

[b]Decays are taken on a 1000s time window to extract the time constants.

4.4. Discussions

The structural changes involved in the pH dependent acid-base equilibrium of Cp_6 are shown in Scheme 4.1. As the pH is lowered, protonation of the carboxyl groups leads to an

increase in the hydrophobic character of the molecule (i.e. formation of species C-A). In absorption spectra this is reflected by a red shift concomitant with a decrease in the intensity of the soret band and broadening of the Q band (Figure 4.1). To help interpret the interaction that occurs between Cp_6 and liposomes at different pH it is essential to know the pK_a values of inter-conversion between the various (A-D) species of the drug.

The pK_a for inter-conversion between C and D has been reported to be ~7.0 [1] which is similar to the value observed for the pK_a of the side chain carboxylic groups of other porphyrins [32-33]. Therefore at physiological pH, the ~50:50 mixture of species C and D is expected to be hydrophilic as they have two and three negative charges respectively. Negatively charged liposomes used in this study would not be expected to significantly interact with the drug at physiological pH. This is consistent with the fact that addition of liposomes at pH 7.4 does not produce significant changes in the absorption spectra of the drug (Figure 4.1). However, as the pH is lowered from 7.4 to 3.0 the absorption spectra of the drug gets considerably modified in the presence of liposomes (which is still negatively charged) suggesting that successive protonation of the carboxyl groups increases the hydrophobic character of the drug. Since a decrease in pH is shown to be conducive to the formation of non centrosymmetric aggregates [34], HRS may be a suitable method to detect the formation of aggregates which in turn may give an idea about the pK_a values of interconversion between the species A B and C. With a decrease in pH the HRS signal from 10 μM Cp_6 was observed to increase in a sigmoidal fashion having an inflexion point at pH = ~4.8. It is pertinent to note that in an earlier study it was shown that at pH 3.0, Cp_6 interacts with the positively charged surfactant CTAB at CTAB concentration significantly lower than its CMC [34]. This has been attributed to electrostatic interaction between Cp_6 and CTAB which suggest that at pH 3.0 the drug is not completely protonated and

remains probably as a mixture of A and B. Further, we have observed that at pH 3.0 Cp_6 can interact electrostatically with the positively charged polymer poly-L-lysine [38]. Therefore we attribute this inflexion point to the pK_a for interconversion between the species C and B. Our results thus suggest that at pH 5.0, species B and C are dominant. A further decrease in pH will reduce the population of species C and increase the population of the species A. We note however that lack of the knowledge of the third pK_a prevents us at this stage to quantitatively assess the relative population of species A and B in the pH range 3.0-4.0.

The generation of an appreciable SH signal in the pH range of 3-5 (Figure 4.3) on addition of liposomes thus may be assumed to originate from species A, B and C. The intensity of SH signal was less at pH 6 and as the pH is increased to physiological, no distinct SH signal was observed which is consistent with the fact that interaction between the liposomes and drug (species C and D) will be a minimum around physiological pH because both are negatively charged and drug is hydrophilic at this pH. In the pH range of 3-5 the room temperature decay of SH signal can be best fitted with two exponentials which may be assumed to be dominated by the diffusion of species A and B. The neutral form of the drug (species A) is expected to diffuse through the outer lipid layer to the inner layer rapidly leading to shorter decay time and the singly deprotonated anionic species (B) of the drug are expected to diffuse slowly through a hydrophobic barrier. The observed bi-exponential decays at acidic pH thus represent the ensemble average of the diffusion rates of the two species A and B of the drug. The SH signal level does not decay to baseline at pH 6 suggesting that at this time scale Cp_6 has not distributed symmetrically between the inner and outer leaflet of the lipid bilayer. This is expected because at pH 6.0, where species C is dominant, the adsorption of the drug to the outer bilayer will decrease and its diffusion across the bilayer will be slower. However at this point it is not clear why C, a

dianionic hydrophilic species would adsorb spontaneously to the negatively charged surface of the lipid vesicle. The origin of the observed ~50s decay constant at pH 6.0 is therefore currently not understood.

Recent ^{1}H NMR experiments have shown that the rate constants for the transfer of different chlorin derivatives across a phosphatidyl choline membrane correlate strongly with the pH of the surrounding medium [11]. In particular, in acidic solution, transfer across the membrane was strongly accelerated. The protonation of ionizable groups of the chlorin derivatives is suggested to be a major determinant for the transfer rates of these molecules across the bilayer. The kinetic profiles measured at acidic pH indicated the presence of a faster (less than an hour) and a slower (100s of hours) component.

The diffusion of molecules across a lipid bilayer is also expected to be affected by the rigidity of the bilayer. Since the gel-crystalline phase transition temperature of the egg-PC liposomes is at -4^{0} C it is not feasible to attain this in aqueous medium. Therefore we used lowering of temperature of the medium and/or addition of cholesterol to the lipid bilayer to enhance the rigidity. As expected, adding cholesterol in the lipid bilayer led to an increase of the overall diffusion time. For example, addition of 50 mol% cholesterol increases both the decay times by two-three fold at pH 3, 4 and 5. Since the adsorption and diffusion of molecules across a lipid barrier is a thermal process, a lowering of the temperature of the medium should lead to an increase in the diffusion time. Accordingly at pH 3 & 4 the faster decay times shows a ~three fold increase and the slower decay times shows a ~two fold increase. Further, the amplitude of the longer decay time was found to increase significantly. However at pH 5, a dramatic change in the SH signal was observed. The SH signal now consisted of three parts: an instantaneous increase followed by a slower increase of the SH intensity which is then followed by a slower

decay. Since at this pH, species B and C are expected to be present in roughly equal amount, the instantaneous increase in the SH signal may be attributed to the adsorption of species B to the outer lipid surface. However, the cause of the observed growth in the SH signal is currently unclear. The long decay of the SH signal (whose time constant could not be correctly estimated within 1000s time window) at this pH shows that the diffusion of species B has been considerably slowed down due to temperature induced increased rigidity of the bilayer. It is thus clear that temperature has a pronounced effect on the SH decay profiles, and consequently the diffusion of the different species of Cp_6 across the PC lipid bilayer. As expected, at low temperature, incorporation of 50 mol% cholesterol in the lipid bilayer further slows down the diffusion of Cp_6. In the 1000s time window, all the decays now show a rising part the time constant of which remains similar (10-20s) at pH 3.0 and 4.0 and increases to ~90s at pH 5.0. The observed rise times at pH 3.0-4.0 may be attributed to the temperature dependent interaction of the anionic species B of Cp_6 with the lipid bilayer. In addition, the decays were observed to slow down further the effect of which is most pronounced at pH 5. All these data thus shows that dual effect of temperature and cholesterol has a profound effect on the diffusion of the various ionic species of Cp_6 across the egg-PC lipid bilayer.

We note that some of the results obtained in this study, especially the origin of the 50s decay observed at pH 6 and the origin of the slow growth in SH signal observed at pH 5 are not yet fully understood. To understand these aspects further investigations on the relative amounts of forms A, B & C present at the different pH and the relationship between the diffusion of Cp_6 and the zeta potential of liposomes are needed.

4.5. Conclusion

We have investigated the diffusion of the photosensitizer Cp_6 across the egg PC lipid bilayer at different pH by the SHG method. The HRS intensity of Cp_6 increases in a sigmoidal fashion as the pH is decreased from 7.0 to 3.0 with the inflexion point at pH ~4.8. This has been identified to the second pK_a of the drug, the first pK_a being ~7.0 as observed in a previous study. Addition of PC liposomes to a Cp_6 solution generates an instantaneous increase of the SH signal (within 1s) which then decays over a longer time (500-1000s) scale. The decay of the SH signal at acidic pH (3-5), is observed to be biphasic. The faster time constant which is of the order of tens of seconds is attributed to the diffusion of the neutral species (A, Scheme 4.1) of Cp_6 and the longer time constant is attributed to the diffusion of the charged species (B) of the drug. At pH 6, the intensity of the SH signal decreases appreciably and it is almost non observable at physiological pH. This is attributed to dominance of the negatively charged species (C & D) of the drug at this pH range which does not interact significantly with the negatively charged PC liposomes and as a consequence the SHG signal intensity is decreased considerably. We have also studied the effect of increasing the bilayer rigidity by decreasing the temperature of the system and by incorporating 50 mol% cholesterol in the lipid bilayer. We have observed that lowering of temperature has more profound effect on the diffusion rates. The dual effect of lowering temperature and incorporating 50 mol% cholesterol on the SH signal results, in addition to the instantaneous rise, a slow rise of the signal with time followed by a slower decay. The slow rise in SH signal at pH 3.0-4.0 may be attributed to the slow interaction of the ionic species B of Cp_6 with the liposomes. Further studies are needed in order to understand the pH dependent diffusion process of the drug across lipid bilayers.

4.6. References

[1] A. Datta, A. Dube, B. Jain, A. Tiwari, P.K. Gupta, Photochem. Photobiol. 75 (2002) 488.

[2] I.F. Tannock, D. Rotin, Cancer Res. 49 (1989) 4373.

[3] R. Pottier, J.C. Kennedy, J. Photochem. Photobiol. B 8 (1990) 1.

[4] L.E. Gerweck, S. Vijayappa, S. Kozin, Mol. Cancer Ther. 5 (2006) 1275.

[5] M. Sharma, A. Dube, H. Bansal, P.K. Gupta, Photochem. Photobiol. Sci. 3 (2004) 231.

[6] K. Das, B. Jain, A. Dube, P.K. Gupta, Chem. Phys. Lett. 401 (2005) 185.

[7] D.C. Buster, J.F. Hinton, F.S. Millett, D.C. Shungu, Biophys.J. 50 (1988) 145.

[8] T.X. Xiang, B.D. Anderson, Biophys. J. 72 (1997) 223.

[9] O. Cruciani, L. Mannina, A.P. Sobolev, C. Cametti, A.L. Segre, Molecules 11 (2006) 334.

[10] S.M. Mel'nikov, J.W.M. Seijen ten Hoorn, A.P.A.M. Eijkelenboom, Chem. Phys. Lipids 127 (2004) 121.

[11] M. Vermathen, P. Vermathen, U. Simonis, P. Bigler, Langmuir 24 (2008) 12521; M. Vermathen, M. Marzorat, P. Vermathen, P. Bigler, Langmuir 26 (2010) 11085.

[12] D. Cafiso, Methods Enzymol. 172 (1989) 331; D.S. Cafiso, W.L. Hubbell, Biophys. J. 44 (1983) 49.

[13] S. Kaiser, H. Hoffmann, J. Coll. Interfac. Sci. 184 (1996) 1.

[14] D. Voelker, P. Smejtek, Biophys. J. 70 (1996) 818.

[15] F. Terce, J.F. Tocanne, G. Laneelle, Eur. J. Biochem. 125 (1982) 203.

[16] J. Aubard, P. Lejoyeux, M.A. Schwaller, G. Dodin, J. Phys. Chem. 94 (1990) 1706.

[17] O. Eidelman, Z.I. Cabantchik, Biochim. Biophys. Acta 988 (1989) 310.

[18] C. Casals, E. Miguel, J. Perez-Gil, Biochem. J. 296 (1993) 585.

[19] K. Kuzelova, D. Brault, Biochemistry 33 (1994) 9447.

[20] K. Kuzelova, D. Brault, Biochemistry 34 (1995) 11245.

[21] N. Maman, D. Brault, Biochim. Biophys. Acta 1414 (1998) 31.

[22] S. Bonneau, N. Maman, D. Brault, Biochim. Biophys. Acta 1661 (2004) 87.

[23] N. Maman, S. Dhami, D. Phillips, D. Brault, Biochim. Biophys. Acta 1420 (1999) 168.

[24] K.B. Eisenthal, Chem. Rev. 106 (2006) 1462.

[25] A. Srivastava, K.B. Eisenthal, Chem. Phys. Lett. 292 (1998) 345.

[26] E.C.Y. Yan, K.B. Eisenthal, Biophys. J. 79 (2000) 898.

[27] Y. Liu, E.C.Y. Yan, K.B. Eisenthal, Biophys. J. 80 (2001) 1004.

[28] X.M. Shang, Y. Liu, E. Yan, K.B. Eisenthal, J. Phys. Chem. B 105 (2001) 12816.

[29] J. Liu, X.M. Shang, R. Pompano, K.B. Eisenthal, Faraday Discussions 129 (2005) 291.

[30] J. Liu, M. Subir, K. Nguyen, K.B. Eisenthal, J. Phys. Chem. B 112 (2008) 15263.

[31] A. Moscho, O. Orwar, D.T. Chiu, B.P. Modi, R.W. Zare, Proc. Natl. Acad. Sci. 93 (1996) 11443.

[32] B. Cunderlıkova, L. Gangeskat, J. Moan, J. Photochem. Photobiol. B Biol. 53 (1999) 81.

[33] B. Cunderlıkova, E.G. Bjorklund, E.O. Pettersen, J. Moan, Photochem. Photobiol. 74 (2001) 246.

[34] P.P. Mishra, J. Bhatnagar, A. Datta, J. Phys. Chem. B 109 (2005) 24225.

[35] E. Hendrickx, K. Clays, A. Persoons, Acc. Chem. Res. 31 (1998) 675.

[36] The HRS intensity I(2ω) is given by:

$$I(2\omega) = G(N_1 < \beta_1^2 > + N_2 < \beta_2^2 >) I^2(\omega) e^{-N_2 \alpha_2 l}$$

Where I(ω) is the incident light intensity; I(2ω) is the intensity of generated HRS signal; G is an constant which depends upon the experimental conditions, β denotes the first

order hyperpolarizability, N denotes the number density and the exponential term accounts for the loss of HRS signal at the second harmonic wavelength. The subscripts 1 & 2 refer to the solute and solvent respectively.

[37] S. Ghosh, A. Krishnan, P.K. Das, S. Ramakrishnan, J. Am. Chem. Soc. 125 (2003) 1602.

[38] R.K. Saini, P.K. Gupta, K. Das, J. Mol. Struc. 1024 (2012) 13.

Chapter – 5

A comparative study on the effect of Curcumin and Chlorin p_6 on the diffusion of two organic cations across a negatively charged lipid bilayer probed by second harmonic spectroscopy

5.1. Introduction

The efficacy of any drug depends strongly upon its interactions with biological membranes. Therefore, studies on drug-lipid interaction are vital to understand and explain the pharmacokinetic properties of drugs. Because of the complexity of the cell membrane structure most of these studies are carried out on simplified artificial membrane systems, which mimic the natural bilayer lipid membrane [1]. Drug lipid interactions can alter the main biophysical properties of membranes such as membrane potential, fluidity and permeability [2-15]. These interactions are expected to depend on the chemical structure and hydrophilicity/hydrophobicity of the drug molecule. Second harmonic (SH) spectroscopy has been used to monitor the real time diffusion of organic ions across a bilayer as this method is surface specific [16-22]. Therefore SH spectroscopy can be used to investigate drug induced changes in lipid bilayer permeability of organic ions. We have earlier showed that the presence of the medicinal pigment Curcumin in a bilayer markedly reduces the diffusion times of a hemicyanine dye LDS-698 [21]. In this report we have compared the effect of Curcumin and Chlorin p_6 (Cp_6), a chlorophyll derivative on the diffusion of two organic cations, Malachite Green (MG) and LDS-698 (LDS). Following earlier

studies, the pH of the medium was kept acidic (5.0) for MG and neutral (7.4) for LDS [16-21]. It is pertinent to note that while Curcumin is hydrophobic at both pH 5.0 and 7.4, Cp_6 is hydrophobic at pH 5.0 and hydrophilic at pH 7.4. Therefore an additional motivation of the present work is to investigate whether pH plays a role in drug induced changes in lipid bilayer permeability. The chemical structures of the molecules used in this study are provided in Scheme 5.1.

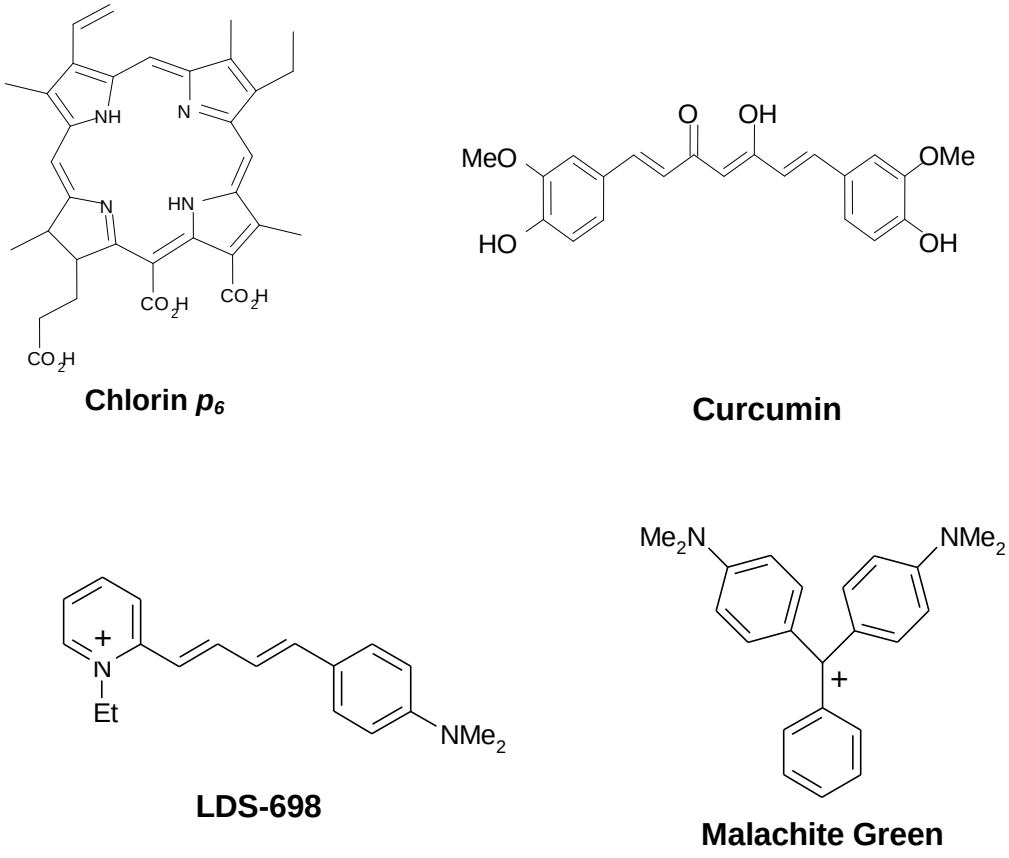

Scheme 5.1*: Chemical structures of MG, LDS, Cp$_6$ and Curcumin.*

5.2. Materials & Methods

LDS-698 (from Exciton) was a gift from Prof. N. Sarkar and was used as received. Cp_6 and Curcumin were purified before use as described in earlier chapters. MG oxalate salt (Sigma product No. M9015) was dissolved in acidic water and then precipitated by making the solution basic. The solid was collected after centrifugation and then re-crystallized from water-alcohol mixture.

SH measurements were performed using the 800 nm quasi-CW output of a Ti-Saphhire (Coherent Mira) laser pumped by a green (532 nm, Coherent Verdi 5W) laser. The average laser power used in the experiments was 600 mW and the pulse width at this wavelength was ~150 fs. The polarization of the laser was fixed in vertical plane by using a quarter wave-plate. The laser beam was focused into the sample by a convex lens having a focal length of 10 cm. The generated SH light was detected using an Edinburgh Instruments LifeSpec single photon counting system. A band pass filter was placed before the monochromator to reject the fundamental. The wavelength resolution of the monochromator was 2 nm. The SH light (at 400 nm) was detected at right angles with respect to the fundamental (800 nm) by a PMT using single photon counting technique. The SH signal were collected every second. The sample in the cuvette was constantly stirred during the measurement using a magnetic stirrer. Sample temperature was controlled by a Neslab circulating water chiller. SH experiments were done as follows: First the signal from 2 mL of buffer containing LDS-698 (pH 7.4) or MG (pH 5.0) or the drugs (at pH 5.0 & 7.4) was recorded followed by addition of 20 μL of liposome solution at 50s time point. The final concentration of lipid was 20 μM. To investigate the effect of drug-liposome interaction on membrane permeability of MG and LDS micro-liter aliquots from a concentrated stock solution of the drugs were added to the liposome solution and incubated for at

least 30 minutes for attaining equilibrium between the drug and the liposome. The liposomal drug solution (20 μL) was then added to 2 mL buffer solution (final lipid concentration: 20 μM) containing either LDS-698 or MG dye.

The observed SH signal was then fitted exponentially as: $I_{SH}(t) = \sum a_i \exp(-t/\tau_i) + A_0$; where $I_{SH}(t)$ denotes the time dependent SH intensity; a_i and τ_i are the pre-exponential and time constants associated with the i^{th} component respectively and A_0 is long time value of $I_{SH}(t)$. $I_{SH}(t)$ data for the maximum cases can be adequately represented by a sum of two exponentials.

5.3. Results

5.3.1. Absorption and emission spectra of the drugs in the presence of POPG liposomes

The absorption and emission spectra of the drugs in the presence of POPG liposomes are shown in Figure 5.1. In aqueous environment the absorption and especially the emission spectra of Curcumin shows a significant change in the presence of POPG liposomes suggesting that there is a strong interaction between the hydrophobic drug and liposome. This is consistent with previous reports supporting the lipophilic nature of the drug [25-26]. However for Cp_6 the observed changes in the absorption and emission spectra in the presence of POPG liposomes are dependent on the pH of the medium. The spectroscopic properties of Cp_6 show almost no change at pH 7.4 suggesting that drug-liposome interaction at this pH to be a minimum. As reported in a previous study [23], the interaction between Cp_6 and liposome is stronger at pH 5.0 due to partial protonation of the carboxylic acid group which makes the drug hydrophobic. As a result the absorption spectra of Cp_6 show significant changes around the 660 nm region and the emission spectra changes markedly in the presence of POPG liposomes at pH 5.0.

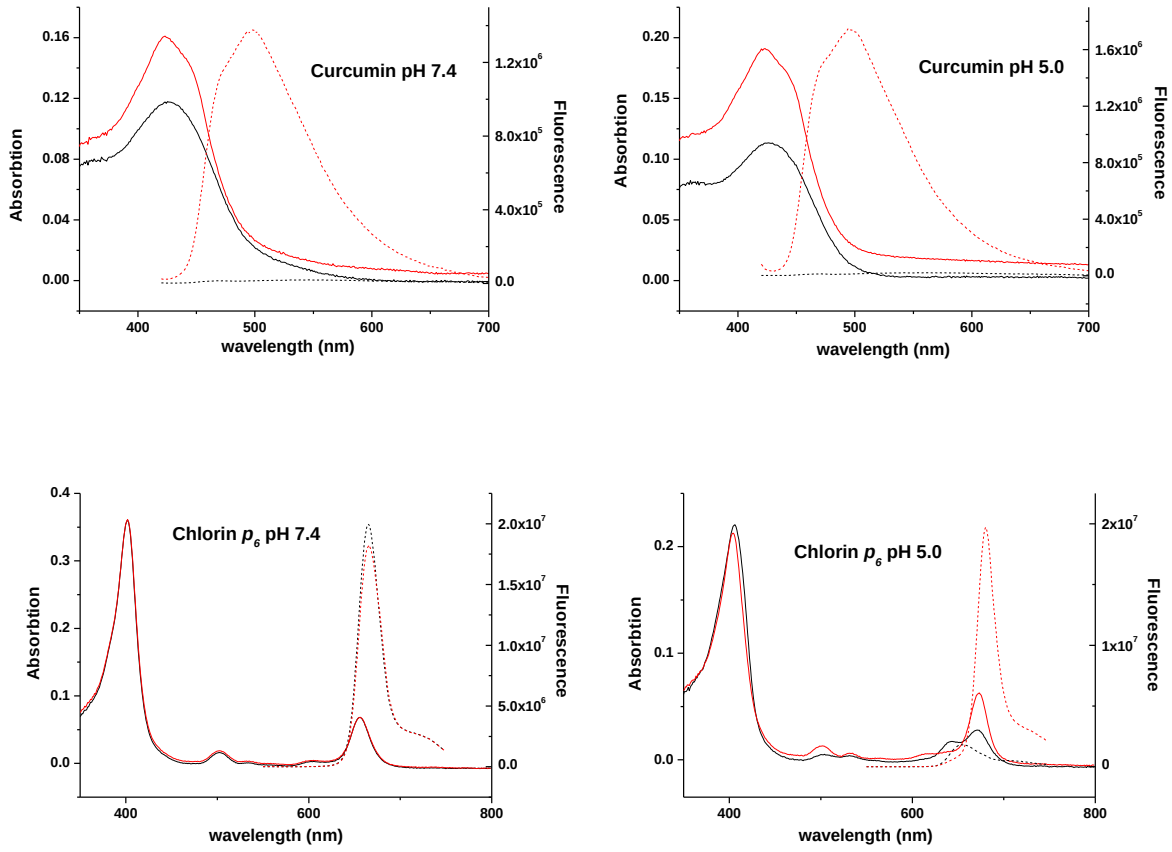

***Figure 5.1**: Absorption (solid) and emission (dashed) spectra of Curcumin and Cp$_6$ at pH 5.0 (right panel) and at pH 7.4 (left panel) in presence (red) and in absence (black) of POPG liposomes.*

5.3.2. SH signal from the drugs in the presence and absence of liposomes

The SH signal from Curcumin in the presence of POPG liposomes was not measurable with our experimental conditions. The increase of the SH signal of Cp_6 after addition of liposomes is dependent on the pH and near physiological pH it is too weak to be detected by our experimental setup. Consistent with our previous observations [22] Cp_6 gave a measurable SH signal in presence of liposomes when the pH of the medium was 5.0 (Figure 5.2). As expected

increasing the rigidity of the bilayer by decreasing the temperature makes the diffusion of Cp_6 slower. The diffusion time constant of Cp_6 increases by ~8 times when the temperature is lowered from 25 ^{0}C to 2 ^{0}C (Figure 5.2).

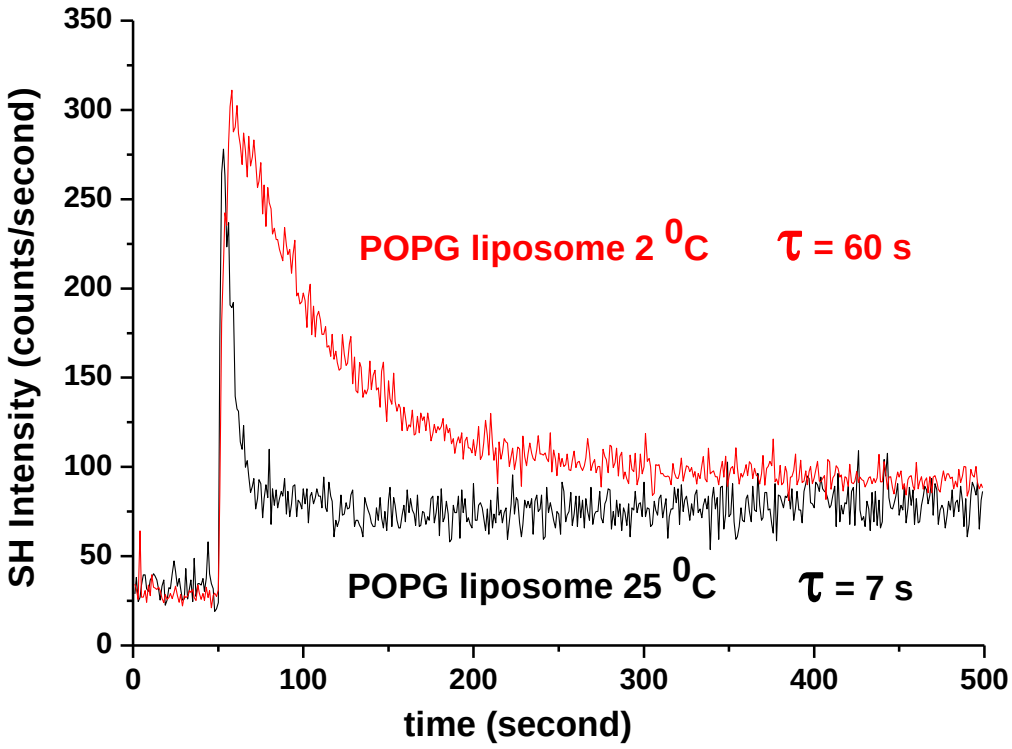

Figure 5.2: *SH intensity profile of Cp_6 (4 µM) before and after addition of POPG liposomes at 2^{0}C (red) and 25 ^{0}C (black). The diffusion time constants after exponential fitting are also shown.*

5.3.3. Diffusion of MG and LDS across POPG liposomes: Effect of Curcumin and Cp_6

The SH signal of Cp_6 in presence of POPG liposomes levels off within 100 to 300 seconds at pH 5.0. Therefore to investigate the effect of Cp_6 on the diffusion of LDS and MG we have incubated the drug with the liposomes for at least 30 minutes to ensure that SH signal from the drug is a minimum. Identical incubation times were also followed for Curcumin to ensure identical experimental conditions. Figure 5.3 shows the SH signal from 6 μM LDS (at pH 7.4) and 6 μM MG (at pH 5.0) before and after addition of POPG liposomes. The instantaneous increase in the SH signal of MG and LDS-698 (following liposome addition) is attributed to electrostatic adsorption of MG and LDS-698 on the outer lipid bilayer. Figure 5.3 also shows the SH signal from LDS and MG before and after addition of POPG liposomes containing either Curcumin or Cp_6 (drug concentration = 4 μM). The presence of the drugs (especially Curcumin) affects the time profile of the SH intensity of MG and LDS. The diffusion time constants of MG and LDS-698 obtained from the exponential fitting of their SH intensity decays are shown in Table 5.1. The time profiles of SH intensity of MG and LDS with increasing concentrations of Curcumin and Cp_6 are provided in Figures 5.4. The corresponding diffusion time constants after exponential fitting are provided in Table 5.2. Finally in Figure 5.5 the observed variations in the average diffusion time constants of LDS and MG with increasing drug concentration are compared. The normalized (i.e. with respect to no drug condition) values of the time constants are plotted in Figure 5.5.

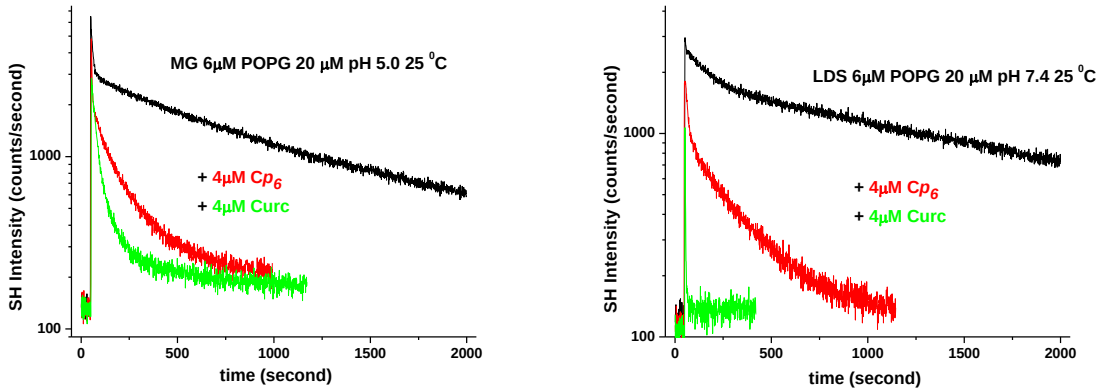

Figure 5.3*: SH intensity profile of MG (left) and LDS-698 (right) before and after addition of POPG liposomes under different conditions at 25 ^{0}C. The black curves denote only liposomes; red and green curves denote liposomes containing 4 μM of Cp$_6$ and Curcumin respectively.*

Table 5.1: Diffusion time constants (in seconds) of MG and LDS in the presence of Curcumin and C*p*$_6$ obtained from exponential fitting of the decay of SH intensity[a]

System	a_1	τ_1	a_2	τ_2	τ_{av}
LDS 6 uM	0.35	110	0.60	1952	1223
+ 4 uM C*p*$_6$	0.57	16	0.37	257	105
+ 4 uM Curc	0.87	2	0.04	9	2.0
MG 6 uM	0.56	11	0.37	813	307
+ 4 uM C*p*$_6$	0.68	4	0.28	141	43
+ 4 uM Curc	0.80	27	0.13	155	43

[a]The errors in the observed time constants are estimated to be about 10% based on experiments performed on three different liposomes samples.

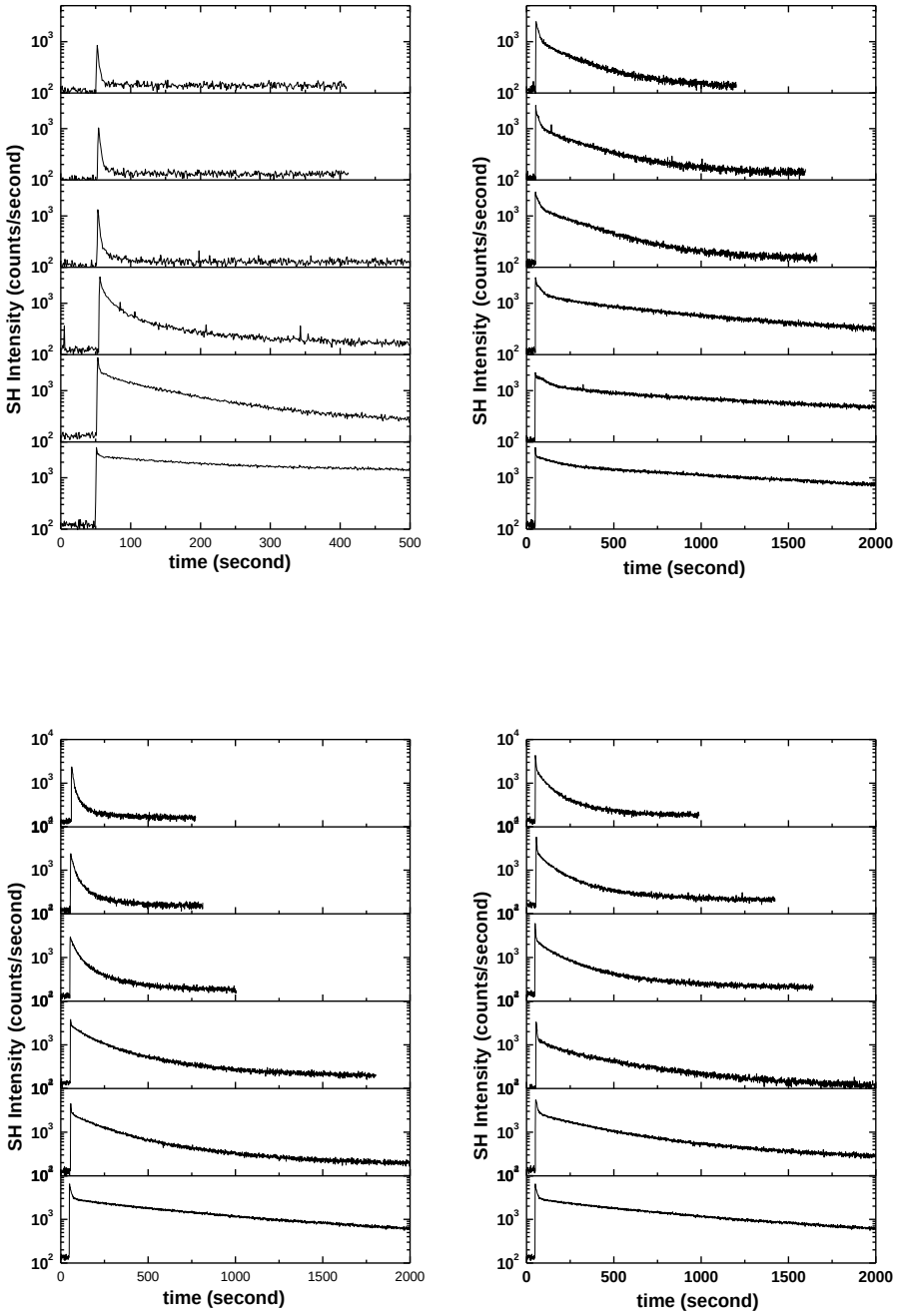

Figure 5.4*: Effect of drug concentration on the SH time profiles of 6 uM LDS (Left top: Curcumin; Right top: Cp_6) and 6 uM MG (Left bottom: Curcumin; Right bottom: Cp_6). For each panel, the concentration of the drug increases from bottom to top.*

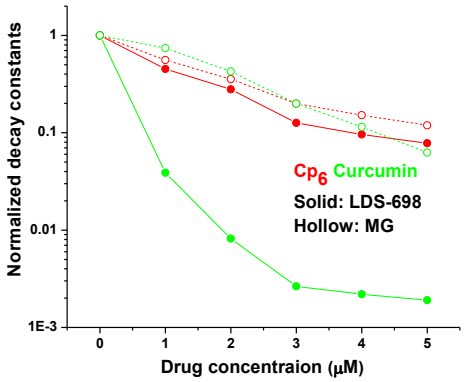

Figure 5.5*: Effect of increasing drug concentration on the diffusion time constants of MG (6 μM; hollow symbols) and LDS-698 (6 μM; solid symbols). The values plotted are normalized with respect to the diffusion time constant of the cations in the presence of POPG liposomes containing no drug.*

Table 5.2: Average diffusion time constants (in seconds) of MG and LDS with increasing drug concentrations[a]

Drug concentration (μM)	LDS + Cp6	LDS + Curcumin	MG + Cp6	MG + Curcumin
0	1220	1220	310	310
1	550	47	173	230
2	340	10	110	132
3	154	3	62	62
4	117	3	47	36
5	95	2	37	19

[a]The errors in the observed time constants are estimated to be about 10% based on experiments performed on three different liposomes samples.

5.3. Discussion

The main objectives of this study are: i) to compare the effect of Curcumin and Cp_6 on the diffusion of MG and LDS and ii) investigate the role of pH in drug induced changes in membrane permeability. It is expected that drug induced alterations, if any, in the decays of the SH intensity of the dyes (MG & LDS) should depend primarily on the binding efficiency between the drug and the liposomes. The quantum of reduction in the average diffusion times of the organic cations by the drugs were observed to depend upon the cation type. Consistent with earlier observation [21], Curcumin is able to markedly reduce the average diffusion time constant of LDS by ~600 times but when the diffusing cation is MG the reduction is a modest ~7 times (Table 5.1). The observed results suggest that pH might play an important role. In comparison to Curcumin, Cp_6 causes the average diffusion time constant of LDS and MG to reduce by ~12 and ~7 times respectively (Table 5.1). Considering the fact that absorption and emission spectra of Cp_6 did not change much after addition of liposomes at pH 7.4 (Figure 5.1), a significant reduction in the average diffusion time of LDS in the presence of POPG liposomes and 4 μM Cp_6 is interesting. This indicates definite interactions between the negatively charged drug and negatively charged liposomes. This interaction, not detected by static spectroscopy is enough to significantly alter the average diffusion time of LDS. Since the drug (especially Curcumin) induced changes in the permeability of the bilayer were observed to depend on pH as well as cation type, we have compared the relative changes in the average diffusion time constants of the cations (LDS & MG) with increasing drug concentration at pH 5.0 and 7.4. To eliminate the contribution arising from the intrinsic effect of the cation the diffusion time constants were normalized with respect to no drug condition. Figure 5.5 clearly shows that pH is playing a role

in the drug induced permeability of the lipid bilayer. While a substantial pH effect is observed for Curcumin, for Cp_6, a modest pH effect was observed.

Several studies have indicated that Curcumin affects the bilayer organization, by interacting with the polar head group region of the lipid [12-15]. The ground state pK_a values for the phenolic protons of Curcumin are estimated to be 10.5 and 10 and that for the enolic proton was estimated to be 8.4 [24]. Fluorescence quenching studies of liposomal Curcumin revealed that distribution of Curcumin in the bilayer is dependent on the pH of the medium. At acidic pH, where the neutral form of the drug is a majority it is preferentially located in the hydrophobic part of the bilayer, while at basic pH, where the anionic form of the drug is a majority it is located near the polar head group region of the bilayer [26]. Therefore it is reasonable to assume that interaction of the drug with the polar head group region of the bilayer will be stronger at pH 7.4 which will in turn affect bilayer permeability significantly higher than at pH 5.0.

Results obtained from our earlier study on the pH dependent binding of Cp_6 with POPC bilayer [22] also suggested that Cp_6 at acidic pH resides in the hydrophobic region of the bilayer whereas at neutral pH it resides close to the hydrophilic region of the bilayer. Therefore it is also reasonable to assume that increased bilayer permeability induced by Cp_6 at pH 7.4 is caused by its interaction with the polar head groups of the lipid molecules due to its preferential location near the bilayer interface.

Therefore a reasonable explanation of the observed pH effect on the bilayer permeability caused by Curcumin and Cp_6 can be attributed to their increased presence at the lipid bilayer interface at pH 7.4 which in turn maximizes their interaction with the polar head groups of the bilayr thereby affecting the bilayer organization.

5.4. Conclusion:

The results presented in this study shows that SH spectroscopy can be a useful investigative tool to probe membrane permeability caused by drug-liposome interaction. Alteration in drug induced membrane permeability depends upon the interaction of the drug with the polar head groups of the lipid molecules. Drugs like Curcumin and Cp_6, whose bilayer localization depends upon the pH of the medium can significantly alter membrane permeability against organic cations.

5.5. References

[1] C. Peetla, A. Stine, V. Labhasetwar, Mol. Pharm. 6 (2009) 1264.

[2] A. Grancelli, A. Morros, M.E. Cabanas, O. Domenech, S. Merino, J.L. Vazquez, M.T. Montero, M. Vinas, J. Hernandez-Borrell, Langmuir 18 (2002) 9177.

[3] A. Berquand, N. Fa, Y.F. Dufrene, M.P. Mingeot-Leclercq, Pharm. Res. 22 (2005) 465.

[4] F. Barcelo, J. Prades, S.S. Funari, J. Frau, R. Alemany, P.V. Escriba, Mol. Membr. Biol. 21 (2004) 261.

[5] H.Y. Cheng, C.S. Randall, W.W. Holl, P.P. Constantinides, T.L. Yue, G.Z. Feuerstein, Biochim. Biophys. Acta, Biomembr. 1284 (1996**)** 20.

[6] Y. Corvis, W. Barzyk, G. Brezesinski, N. Mrabet, M. Badis, S. Hecht, E. Rogalska, Langmuir 22 (2006) 7701.

[7] A.V. Agasosler, L.M. Tungodden, D. Cejka, E. Bakstad, L.K. Sydnes, H. Holmsen, Biochem. Pharmacol. 61 (2001) 817.

[8] A.A. Hidalgo, W. Caetano, M. Tabak, O.N. Oliveira, Biophys. Chem. 109 (2004) 85.

[9] S.S. Feng, K. Gong, J. Chew, Langmuir 18 (2002) 4061.

[10] A. Preetha, N. Huilgol, R. Banerjee, Colloids Surf. B 53 (2006) 179.

[11] A. Preetha, N. Huilgol, R. Banerjee, J. Membr. Biol. 219 (2007) 83.

[12] W.C. Hung, F.Y. Chen, C.C. Lee, Y. Sun, M.T. Lee, H.W. Huang, Biophys. J. 94 (2008) 4331.

[13] Y. Sun, C.C. Lee, W.C. Hung, F.Y. Chen, M.T. Lee, H.W. Huang, Biophys. J. 95 (2008) 2318.

[14] J. Barry, M. Fritz, J.R. Brender, P.E. Smith, D.K. Lee, A. Ramamoorthy, J. Am. Chem. Soc. 131 (2009) 4490.

[15] A. Perez-Lara, A. Ausili, F.J. Aranda, A. Godos, A. Torrecillas, S. Corbalan-Garcia, J.C. Gomez-Fernandez, J. Phys. Chem. B 114 (2010) 9778.

[16] A. Srivastava, K.B. Eisenthal, Chem. Phys. Lett. 292 (1998) 345.

[17] E.C.Y. Yan, K.B. Eisenthal, Biophys. J. 79 (2000) 898.

[18] Y. Liu, E.C.Y. Yan, K.B. Eisenthal, Biophys. J. 80 (2001) 1004.

[19] J. Liu, X.M. Shang, R. Pompano, K.B. Eisenthal, Faraday Discuss. 129 (2005) 291.

[20] J. Liu, M. Subir, K. Nguyen, K.B. Eisenthal, J. Phys. Chem. B 112 (2008) 15263.

[21] G.K. Varshney, R.K. Saini, P.K. Gupta, K. Das, Langmuir 29 (2013) 2912.

[22] R.K. Saini, P.K. Gupta, K. Das, J. Phys. Chem B 116 (2012) 4199.

[23] K. Das, B. Jain, A. Dube, P.K. Gupta, Chem. Phys. Lett. 401 (2005) 185.

[24] M. Bernabe-Pineda, M.T. Ramirez-Silva, M. Romero-Romob, E. Gonzalez-Vergara, A. Rojas-Hernandez, Spectrochimica Acta Part A 60 (2004) 1091.

[25] G. Began, E. Sudharshan, K. Udaya Sankar, A.G. Appu Rao, J. Agric. Food Chem. 47 (1999) 4992.

[26] A. Kunwar, A. Barik, R. Pandey, K.I. Priyadarsini, Biochim. Biophys.Acta 1760 (2006) 1513.

Chapter – 6

Conclusions:-

The first part of this thesis work has been devoted to spectroscopic characterization of photoexcited Curcumin in toluene-polar solvent mixtures investigated with steady state and picoseconds time resolved fluorescence spectroscopy.

The results obtained shows that ESHT reactions of Curcumin excited state depend critically upon the H-bonding property of the polar solvent. Consequently the solvation times of the pigment in toluene-methanol become slower (20-40 times) with respect to that in neat methanol. Dipolar solvation and IHB reorganization are coupled and therefore also depends critically on the H-bonding property of the polar solvent. Polar solvents having either HBD or both HBA and HBD were able to cause the spectral relaxation of the pigment in the binary mixture significantly slower. The observed results indicate that the rate limiting step in the excited state dynamics of the pigment in toluene-polar solvent mixtures might be the formation and reorganization of the intermolecular H-bonding between the keto group of the pigment and the H-bond donating property of the polar solvent. However as noted in Chapter-3, a significant part of the solvation dynamics (~30%) could not be observed due to limited time resolution (~40 ps) of the TCSPC setup. Therefore fluorescence upconversion experiments with 150-200 femtosecond time resolution can provide with more information about the IHB reorganization process of the pigment in the excited state. In addition time resolved (with femtosecond time resolution) infrared spectroscopic investigations which can probe the C=O and O-H stretching vibrations of the pigment are expected to provide further information about the IHB reorganization.

The second part of this thesis work involves investigating the interaction of Cp_6 and Curcumin with lipid bilayer by SH spectroscopy.

The diffusion characteristic of the photosensitizer Cp_6 across an egg lecithin membrane was observed to depend upon the pH of the medium. However, some of the results, especially the origin of the 50s decay observed at pH 6 and the origin of the slow growth in SH signal observed at pH 5 are not yet fully understood. To understand these aspects further investigations on the relative amounts of different ionic species of the drug present at the different pH and the relationship between the diffusion of Cp_6 and the surface charge of liposomes are needed.

Finally the results obtained on the effect of liposomal Curcumin and liposomal Cp_6 on the diffusion kinetics of two organic cations shows a substantial pH effect. Based on the results obtained from earlier studies this was attributed to the increased interaction between the drug and the polar head groups of the lipid at pH 7.4 where the drug resides closer to the lipid-water interface. In order to understand the interaction of the drug with the polar head groups of the lipid molecules more studies are required. Since both drugs are fluorescent, fluorescent based techniques like resonance energy transfer are expected to give a better idea about the localization of the drug in the bilayer region. Additionally other techniques like FTIR, NMR etc can also provide information on this aspect.